DRAFT

CAL/APT PROGRAM: TEST RESULTS FROM ACCELERATED PAVEMENT TEST ON PAVEMENT STRUCTURE CONTAINING AGGREGATE BASE-SECTION 503RF

Report Prepared for

CALIFORNIA DEPARTMENT OF TRANSPORTATION

by

John Harvey, David Hung, Jorge Prozzi, Leonie Louw,
Irwin Guada, Clark Scheffy

Pavement Research Center
Institute of Transportation Studies
University of California, Berkeley

DISCLAIMER

The contents of this report reflect the views of the authors who are responsible for the information and the accuracy of the data presented herein. The contents do not necessarily reflect the official views of policies of the California Department of Transportation or the Federal Highway Administration. The report does not constitute a standard, specification, or regulation.

FINANCIAL DISCLOSURE STATEMENT

This research has been funded by the Division of New Technology and Research of the State of California Department of Transportation (contract No. RTA-65W485). The total contract amount for the five year period (1 July 1994 through 30 June 1999) is $5,751,159. This report presents the results of the fourth HVS test completed in September 1996 on a pavement section containing untreated aggregate base. The report provides an analysis of the test results and conclusions which contain implications for Caltrans pavement design and pavement construction practices.

IMPLEMENTATION STATEMENT

Results of this HVS test, like that on the previously tested sections—500RF, 501RF, and 502RF, demonstrate the importance of mix compaction on pavement performance (both fatigue and permanent deformation) and show that the improved pavement performance which results from improved compaction can result in large, quantifiable savings to the State.

As in the previous sections, a weak bond was observed between the asphalt-concrete lifts in the sections which was found to significantly degrade pavement performance. The recommendations contained in the earlier reports relative to the use of a tack coat are confirmed by the results of this test as well.

ACKNOWLEDGMENTS

Financial support for this project was provided by the State of California Department of Transportation as part of the CAL/APT Project. Mr. Wesley Lum of the Division of New Technology and Research is the CAL/APT Project Manager and Mr. William Nokes, Office of Project Planning and Design, served as the Contract Monitor during the period of the test for the University of California, Berkeley contact.

TABLE OF CONTENTS

LIST OF FIGURES

LIST OF TABLES

EXECUTIVE SUMMARY

This report is the fourth in a series which describe the results of tests and their interpretation on full-scale pavements constructed at the Richmond Field Station (RFS) which have been designed and constructed according to Caltrans procedures. It describes the results of the Heavy Vehicle Simulator (HVS) test on the *fourth* of *four* pavement test sections, an asphalt-concrete section containing an untreated aggregate base designated Section 503RF. The tests on these four test sections have been performed as part of Goal 1 of the CAL/APT Strategic Plan *(1)*.

One objective of the test program is to obtain data to quantitatively verify existing Caltrans pavement design methodologies for asphalt treated permeable base (ATPB) pavements and conventional aggregate base pavements with regard to failure under trafficking at moderate temperatures (Goal 1), while preparing a uniform platform on which overlays (Goal 3) will be constructed to be trafficked. Other objectives are:

- to quantify the effective elastic moduli of the various pavement layers, based on an ad-hoc use of layered elastic analysis;
- to quantify the stress dependence of the pavement layers;
- to determine the failure mechanisms of the various layers; and
- to determine and compare the fatigue lives of the two types of pavement structure.

HVS loading on this pavement section began in March 1996 and was completed in September 1996 after the application of about 1.91×10^6 load repetitions. At the end of the 14

test, cracking had reached a level which, according to Caltrans pavement management criteria, resembled a newer pavement that had failed by alligator cracking.

Chapter 2 describes the test program for Section 503RF. Design thicknesses for the pavement components for a Traffic Index of 9.0 (1.0 million ESALs) were: aggregate subbase—229 mm (0.75 ft); aggregate base—274 mm (0.90 ft); and asphalt concrete—137 mm (0.45 ft). Actual thicknesses at the loading site were: aggregate subbase—305 mm (1.00 ft); aggregate base—274 mm (0.90 ft); and asphalt concrete—147 mm (0.48 ft).

Table 2.1 summarizes the data collection program for Section 501RF. Loading, applied by dual bias-ply tires inflated to a pressure of 690 kPa (100 psi), consisted of 150,000 repetitions of a 40 kN (9,000 lb) load followed by 50,000 repetitions of a 80 kN (18,000 lb) and then by about 1.71 million repetitions of a 100 kN (22,500 lb) load. At the termination of loading, fatigue cracking was visible throughout the test section. Lateral wander of the wheels over the one meter (3.3 ft) width of the section was the same as for the other three test sections (500RF, 501RF, 502CT).

Chapter 3 summarizes the data obtained during the course of loading. Pavement response measurements were obtained using Multi-Depth Deflectometers (MDDs), the Road Surface Deflectometer (RSD), the laser profilometer, and a straight edge. Fatigue crack development was monitored using photographs and analyzed using a digital image analysis procedure. Thermocouples were used to measure the air temperature and pavement temperatures at various depths in the asphalt concrete. To maintain a reasonably consistent temperature of about 20°C, a temperature control cabinet (“cold box”) was installed.

As with Sections 500RF and 501RF, cracking appears to have occurred in only the top lift of the aggregate concrete layer. Moreover, it was observed, from a limited coring program after the HVS testing was completed, that there appeared to be little or no bond between the two lifts used to achieve the constructed thickness of the aggregate concrete layer and no bonding occurred under the HVS trafficking at 20°C. In addition, measurements indicate that the lower asphalt concrete lift was compacted to an average air-voids content of 4.4 percent and the upper lift had similar compaction, i.e. to an average air-voids content of about 4.8 percent.

The 1.91 million repetitions applied to Test Section 501RF corresponds to about 81 million ESALs (based on the Caltrans load equivalency factor of 4.2). Chapter 4 provides a detailed analysis of the test results using multilayered elastic analysis to explain the observed behavior.

Results of the analysis reported in Chapter 4 indicate a reasonable correspondence between the Caltrans design estimate of approximately 1,000,000 ESALs and the HVS test measurement of approximately 81,000,000 ESALs. An impediment to reconciling these two estimates has been the inability to accurately quantify effects of the layer interface condition. The following findings of this aspect of the study are considered to have been reasonably well demonstrated and to represent appropriate hypotheses for future inquiry and validation:

1. Fatigue life measurements under full-scale accelerated loading are typically expected to exceed design estimates because design estimates must incorporate a safety factor to minimize the risk of premature failure while accommodating, at the same time, expected variability in testing, in construction, in traffic, and in mix design. As it was shown for Test

Section 501RF, which has the same structural design as Test Section 503RF, for a design reliability level of 90 percent, the computed ratio of simulated HVS ESALs to design ESALs estimated using the fatigue analysis and design system was approximately 3.7.

2. The mix fatigue analysis and design system proved to be an effective tool for explaining fatigue performance of the HVS pavement. The relatively good agreement between the simulation estimate and actual HVS measurement suggests that the analysis and design system may prove useful for structural design as well as for mix design.

3. According to Asphalt Institute's subgrade strain criteria, severe rutting associated with permanent deformations in the unbound layers in the HVS pavement would not be expected. Testing of HVS Section 503RF generally confirmed this.

4. The analyses reported herein corroborate prior work showing the importance of good compaction of the asphalt concrete surface to superior fatigue performance. Good compaction of the mix also reduces the amount of rutting contributed by the unbound pavement layers.

5. The improved fatigue performance of Section 503RF as compared to that of Section 501RF was due primarily to the increased thickness and higher degree of compaction of the asphalt concrete in Section 503RF.

6. Loss of bond at the interface between asphalt-concrete lifts can cause a significant reduction in fatigue life and an increase in rutting resulting from increased stresses in the unbound layers.

7. Different mixes, even with similar binders, can result in significantly different fatigue performance. The importance and effectiveness of laboratory fatigue testing and

simulation to quantitatively estimate differences in fatigue performance in situ were demonstrated by analyses presented in this chapter.

Chapter 5 contains the conclusions which are as follows:

1. The fatigue analysis and design system developed during the SHRP program and refined within the CAL/APT program has been used to explain the difference between the design estimate for Section 503RF of approximately one million ESALs and the HVS measurement of approximately 81 million ESALs. Although some of the discrepancy remains unaccounted for (possibly as a result of difficulties in modeling the bonding between the two lifts of asphalt concrete), the overall agreement helps to validate both the analysis and design system as a mechanism for structural design and provides some indication of the limits of validity of the current Caltrans design methodology.

2. As with Sections 500RF and 501RF, results of this HVS test suggest that the Asphalt Institute's subgrade strain criteria to control rutting resulting from permanent deformations in the unbound layers is a reasonable design parameter. Accordingly, these criteria are suitable for use in mechanistic/empirical analyses of rutting to supplement routine Caltrans design procedures in special investigations.

3. Results of the 503RF test confirm those of the 501RF that suggest that the Caltrans structural design procedure may not be sufficiently conservative for pavements with aggregate base, typical compaction, and certain asphalt concrete mixes. The analysis and design system used herein and being refined, in part, through the CAL/APT program, should provide an improved methodology for structural pavement design permitting a higher level of reliability to

be obtained in pavements of this type. The results indicate that thicker asphalt concrete layers and better asphalt concrete compaction can significantly improve pavement performance.

4. The recommendations regarding mix compaction and tack coat application resulting from the Sections 500RF and 501RF tests are supported by the results obtained from Section 503RF.

CHAPTER 1

INTRODUCTION

This report is one of a series of reports which describe the results of Accelerated Pavement Testing with the Heavy Vehicle Simulator (HVS) on full-scale pavements at the Richmond Field Station (RFS) of the University of California at Berkeley (UCB) designed and constructed according to Caltrans procedures. It contains a summary and interpretation of the results from the HVS test on the third of four pavement test sections: an asphalt-concrete section containing a conventional aggregate base, designated section 503RF. Tests on these four test sections have been performed as part of Goal 1 of the CAL/APT Strategic Plan (*1*).

The first report in this series, entitled: *Initial CAL/APT Program: Site Information, Test Pavements Construction, Pavement Materials Characterizations, Initial CAL/HVS Test Results, and Performance Estimates* contains detailed information on the construction of the test pavements, as well as results of tests to define the properties of the various components of the four test pavements (*2*). The second and third reports in this series, entitled: *CAL/APT Program: Test Results From Accelerated Pavement Test on Pavement Structure Containing Asphalt Treated Permeable Base (ATPB)—Section 500RF* and *CAL/APT Program: Test Results From Accelerated Pavement Test on Pavement Structure Containing Untreated Aggregate Base—Section 501RF* contain detailed information of the drained ATPB Section 500RF *(3)* and undrained aggregate base Section 501RF *(4)*, respectively. To minimize the length of this report, information utilized herein and contained in the above noted reports will only be referenced. A separate report has been prepared describing the performance of ATPB under saturated conditions in laboratory repeated load tests, performance estimates of pavements

containing saturated ATPB through simulations, and a review of Caltrans experience with ATPB *(5)*.

The information and findings presented herein support the recommendations regarding changes in Caltrans construction and construction control procedures presented in References *3* and *4*.

1.1 OBJECTIVES

As noted in earlier reports, the primary objective of the four Goal 1 test pavements is to develop data to quantitatively verify existing design methodologies for asphalt treated permeable base (ATPB) pavements and conventional aggregate base pavements with regard to failure under trafficking at moderate temperatures. Other objectives include:

- quantification of the effective elastic moduli of the various pavement layers, based on an ad-hoc use of layered elastic analysis;
- quantification of the stress dependence of the pavement layer materials;
- determination of the failure mechanisms of the various layers; and
- determination and comparison of the fatigue performance of the two types of pavement structures.

This report, together with the reports on each of the four sections, associated special reports, and a final report will complete the test plan objectives and the work defined for Goal 1 of the Strategic Plan *(1)*.

1.2 PURPOSE AND SCOPE

This report presents the results of tests in Section 503RF together with their analyses relative to observed performance of the section in fatigue. The sequence of HVS testing of the four test pavements was: 1) 500RF (drained ATPB section); 2) 501RF (undrained aggregate base section); 3) 502CT (drained ATPB section); and 4) 503RF (undrained aggregate base section).

1.3 ORGANIZATION OF REPORT

Chapter 2 contains a complete description of the test program performed on Section 503RF, including the loading sequence, instrumentation, and data collection scheme. Chapter 3 presents a summary and discussion of the data collected during the test including pavement performance and temperatures. In Chapter 4, the actual pavement performance is compared with the fatigue life predicted for the test section by the Caltrans thickness design procedure. Analyses are presented that evaluate the effects of construction variables and mix characteristics on fatigue performance and in turn, enable the results of the HVS testing to be extrapolated to actual Caltrans in-service pavements. Chapter 5 contains a summary of the results together with conclusions based on the results.

CHAPTER 2

TEST PROGRAM

2.1 TEST SECTION LAYOUT

Four test sections were constructed as part of Goal 1 of the CAL/APT Strategic Plan: two sections containing an asphalt treated permeable base (ATPB) (Sections 500RF and 502CT), and two with a conventional aggregate base (Sections 501RF and 503RF). The layout of the test sections is described in the report on Section 500RF *(3)*; a schematic of this layout is shown in Figure 2.1.

The pavement structure (Figure 2.2) was designed following Caltrans procedures *(6)*. It consists of a dense-graded asphalt concrete surface, an untreated aggregate base and subbase (both classified as AASHTO A-1-a materials) and a clay subgrade (AASHTO classification A-7-6). A summary of the construction control data for this section is contained in Reference *2*.

The design thicknesses of the different pavement layers for sections 503RF and 501RF are: aggregate subbase—229 mm; aggregate base—274 mm; and asphalt concrete—137 mm. However, the actual thicknesses of the aggregate subbase vary across the sections because of a 2 percent transverse slope on the entire test pavement. As-built thicknesses of the aggregate subbase and asphalt concrete layers estimated from a few cores are 305 mm and 162 mm, respectively. Exact layer thicknesses of each of the HVS test sites will be determined from measurements in test pits after the overlay testing is completed [Goal 3 of the CAL/APT Strategic Plan *(1)*]. Construction measurements and data from several cores obtained next to Section 503RF indicate that the aggregate base thickness is approximately equal to the design thickness.

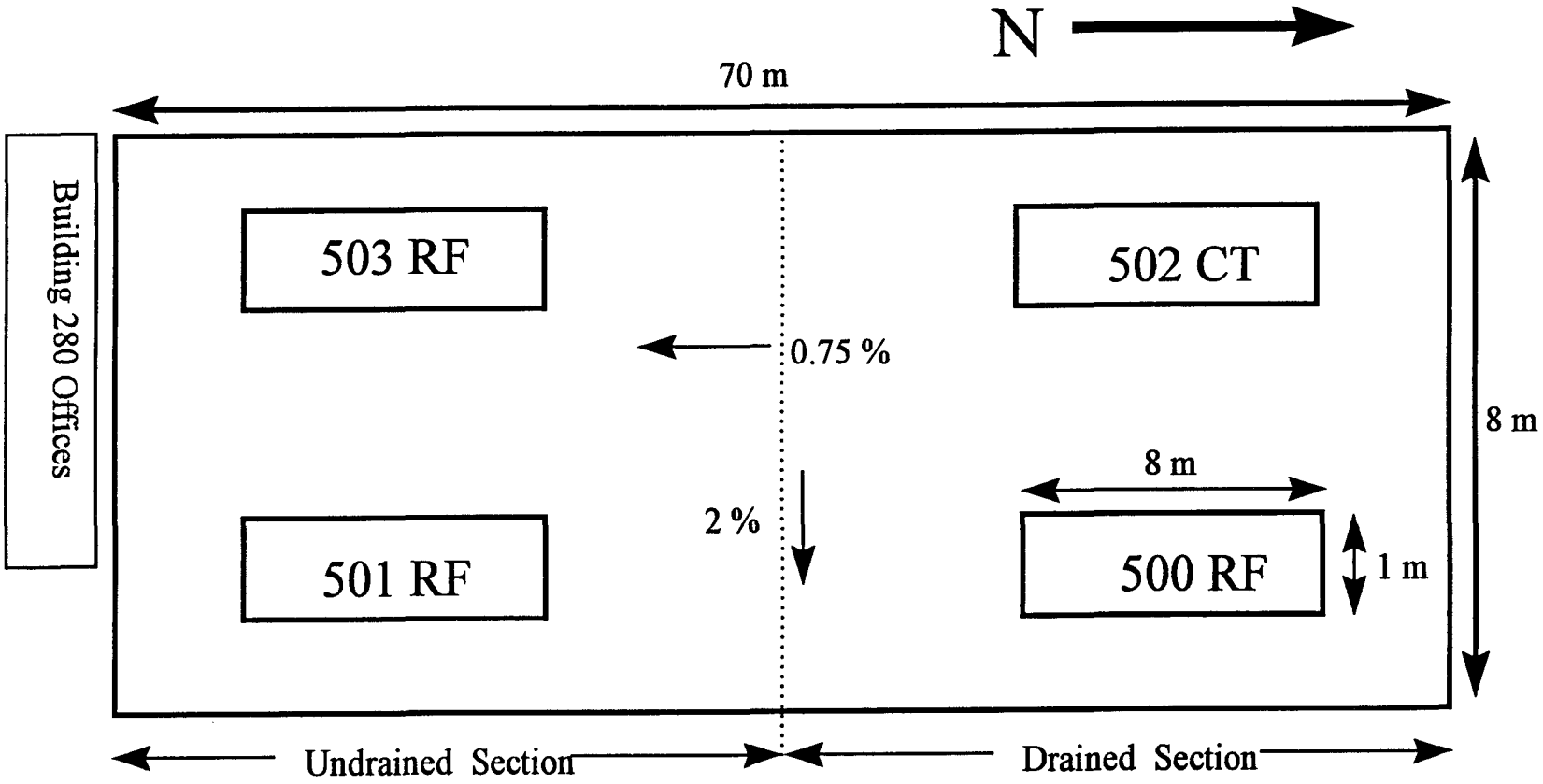

Figure 2.1 Layout of Goal 1 test sections

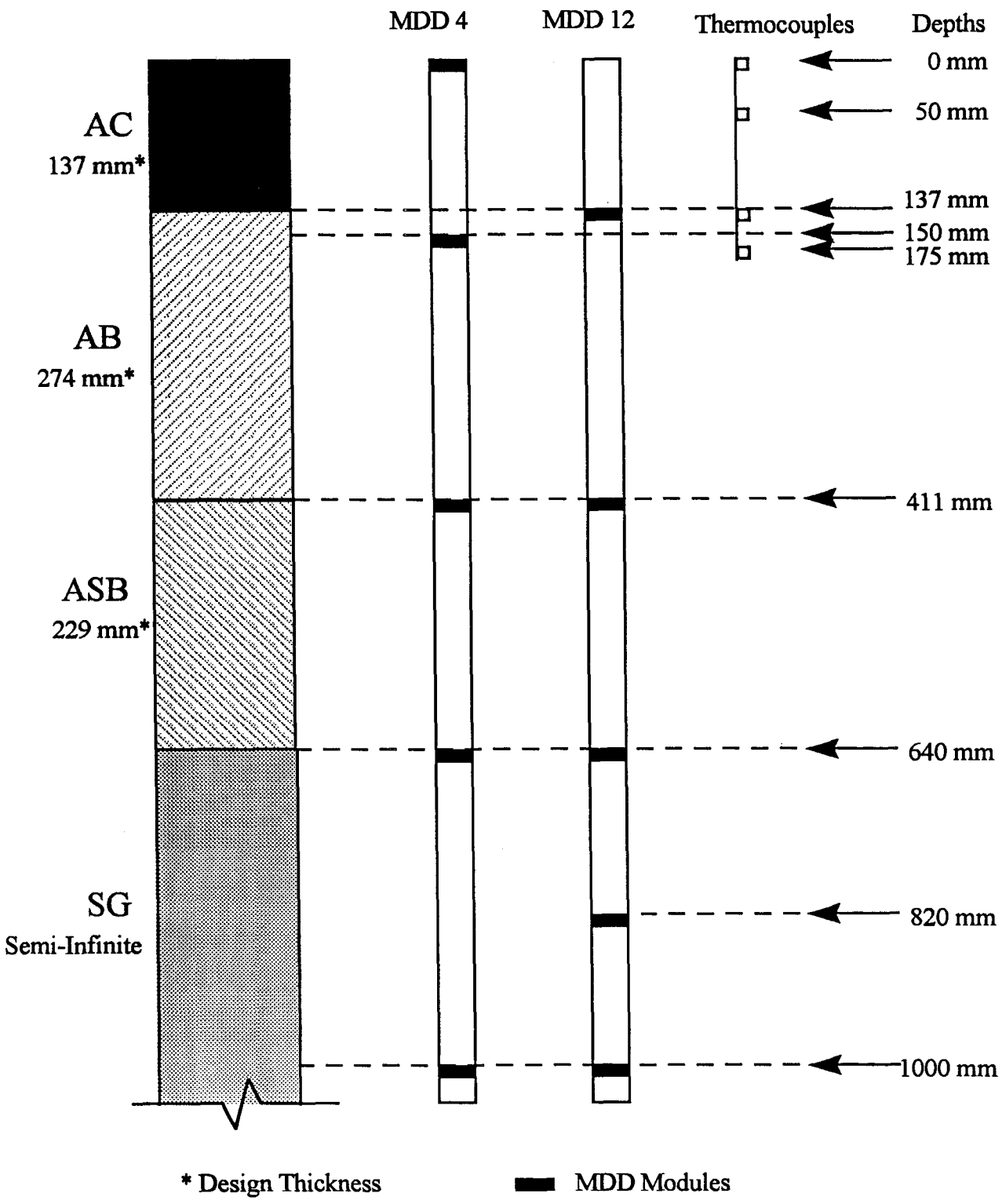

Figure 2.2 503RF pavement structure with MDD and thermocouple positioning

2.2 TEST PROGRAM

2.2.1 Loading Program

HVS trafficking of the test section was initiated in March 1996 and completed in September 1996 after the application of more than 1.91×10^6 load repetitions. At this point cracking had reached a level which, according to Caltrans pavement management criteria, resembled a newer pavement that had failed by alligator cracking. The HVS test program followed for Section 503RF, is summarized in Table 2.1. This table shows the data collection schedule during the course of the test. The loading applied to Section 503RF is similar to that applied to Sections 500RF *(3)* and 501RF *(4)*. As seen in Table 2.1, a dual-wheel load of 40 kN was used to traffic the section for the first 150,000 repetitions to prevent excessive initial deformation of the newly constructed asphalt concrete. After that, the load of the dual-wheel was increased to 80 kN for 50,000 repetitions. After 200,000 repetitions the trafficking load was increased to 100 kN; this load was maintained for the remainder of the test to accelerate pavement cracking.[1]

Since the objective of the test was to evaluate the fatigue performance of the pavement, the pavement was loaded and monitored until failure by alligator cracking at 1,908,480 repetitions. The HVS was equipped with bias-ply truck tires inflated to a pressure of 690 kPa. Lateral wander over the 1 m width of the test section was programmed to simulate traffic wander on a typical highway lane *(6)*.

---

[1] Due to the overloading of the 100 kN trafficking loads and the accelerated nature of the loads, the effect of beginning the test with the 100 kN load would be to cause excessive and unrealistic damage to the pavement, especially the fresh AC layer. For this reason, the load is first applied as 40 kN, which is more representative of real traffic, and later as 80 kN to settle the pavement.

Table 2.1 Data collection program for Test Section 503RF

Repetitions	Trafficking Load kN	Rut Profiles	MDD				RSD											
							Centerline				200 mm Left[a]				200 mm Right[a]			
			Test Wheel Load, kN				Test Wheel Load, kN				Test Wheel Load, kN				Test Wheel Load, kN			
			40	60	80	100	40	60	80	100	40	80	60	100	40	80	60	100
10	40	X	X				X				X				X			
10,000 to 50,000 (10,000 incr)	40	X	X				X				X				X			
100,000	40	X	X				X				X				X			
125,000	40	X	X				X				X				X			
150,000	40 to 80	X	X	X	X		X		X		X		X		X		X	
175,000	80	X	X		X		X		X		X		X		X		X	
200,000	80 to 100	X	X	X	X	X	X		X	X	X		X	X	X		X	X
225,000	100	X	X			X	X			X								
250,000	100	X	X			X	X			X								
300,000 to 800,000 (50,000 incr)	100	X	X			X	X			X	X			X	X			X
Crack Appearance (400,000)	100	X	X		X	X	X		X	X	X		X	X	X		X	X
800,000 to final (50,000 incr)	100	X	X			X	X			X								
800,000 to final (100,000 incr)	100	X	X			X												
850,000 to final (100,000 incr)	100	X	X			X	X			X								
Final (1,908,480)	100	X	X	X		X	X	X	X	X	X	X	X	X	X	X	X	X

[a] Looking in direction of increasing longitudinal reference points (0-16)

2.2.2 Measurements

To evaluate pavement response during HVS testing of Section 503RF, measurements were obtained using the following instruments:

- Multi-Depth Deflectometer (MDD);
- Road Surface Deflectometer (RSD);
- Laser Profilometer, and
- straight edge.

Fatigue crack development was monitored using photographs. Thermocouples were used to measure air and pavement temperatures at various depths in the asphalt concrete. Detailed descriptions of the instrumentation and the various measuring equipment are included in Reference *3*.

Surface deflection measurements with the RSD were obtained at the reference points along the centerline of the section and at locations 200 mm on either side of the centerline, as shown in Figure 2.2. The latter measurements, taken slightly off the centerline where the wander pattern results in fewer load applications, assist in characterizing the full test section. Measurements of surface rut depth using the laser profilometer permit the determination of:

- the location and magnitude of the maximum rut depth;
- the average rut depth which occurred throughout the test section, and
- the rate of rutting developement.

Permanent deformations occurring in the layers during the course of loading as well as in-depth elastic deflections during loading are measured using the MDDs at the two consecutive locations shown in Figure 2.2 and at the depths shown in Figure 2.3. Surface deflections measured at MDD4 provide a check on RSD deflections measured at the same point.

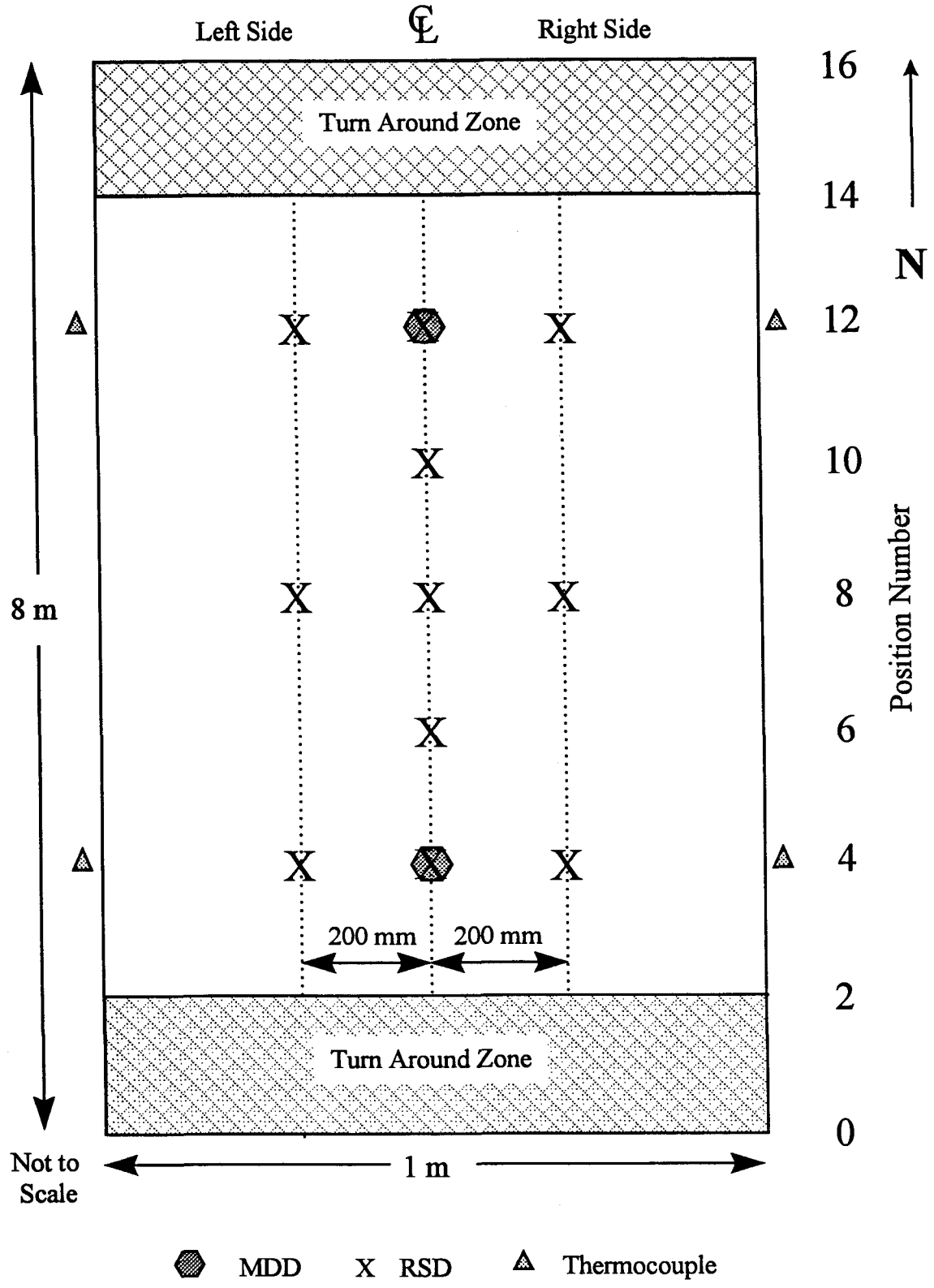

Figure 2.3 Plan view of test section and location of instruments for data collection

All pavement temperature measurements using thermocouples (locations shown in Figures 2.2 and 2.3) were obtained at one-hour intervals during HVS operation. Air temperatures near the test section were recorded at the same intervals, as well as at the time of data collection.

Visual observation of surface distress was directed to the identification and demarcation of surface cracks as well as the measurement of their lengths. It should be noted that at the conclusion of testing of the overlaid section 503RF (Goal 3), a trench will be dug to allow visual inspection and measurement of the thicknesses of all the layers, and to obtain material for laboratory testing. This visual inspection will provide essential information for data interpretation and clarify any inconsistencies generated during the test.

Depths at which the Multi Depth Deflectometers (MDDs) and thermocouples were placed are shown in Figure 2.2, while their locations on the surface of the test section are shown in Figure 2.3. Positions at which deflections were measured with the Road Surface Deflectometer (RSD) are also shown in Figure 2.3. Intervals between measurements (Table 2.1), in terms of load repetitions, were selected to enable adequate characterization of the pavement as damage developed.

2.3 ENVIRONMENTAL CONDITIONS

As with Section 501RF, the pavement surface temperature was maintained at $20 \pm 4°C$ to minimize rutting in the asphalt concrete and, at the same time, to accelerate fatigue damage from load repetitions. The temperature control chamber, developed earlier *(4)*, was used; as will be seen in Chapter 3, the chamber provided the requisite temperature control.

The pavement surface receives no direct rainfall because the test sections are built in the indoor facility at the Richmond Field Station. However, the pavement test sections in this

facility are subject to subsurface water infiltration since they are built on the natural subgrade. Water can access the pavement due to lateral movement (of water) from outside the building, as well as from the ground water table. Initially, during the rainy season of 1994-95 and before construction of the first test pavements, excessive water penetrated into the building from the west side. A drainage system was installed around the outside of the building to mitigate the influence of this water on the test pavements. The drainage system is described in detail in Reference *2*.

CHAPTER 3

DATA SUMMARY: TEMPERATURES, PERMANENT DEFORMATIONS, ELASTIC DEFLECTIONS, CRACKING

This chapter provides a summary of the data obtained as well as a brief discussion of the results. Interpretation of the data in terms of pavement performance is discussed in Chapter 4.

3.1 TEMPERATURES

Pavement temperatures were controlled using the temperature control box constructed prior to the test on Section 501RF *(4)*. Both air and pavement temperatures were monitored and recorded regularly during the entire loading period for Section 503RF as noted in Chapter 2. For evaluation of fatigue cracking, both the temperature at the bottom of the asphalt concrete (approximately 160 mm for this test) and temperature gradient are the controlling temperature parameters *(8)*.

Air temperatures inside the temperature control chamber ranged from 16°C to 25°C during the entire testing period of Section 503RF. The target air temperature was 20°C±4°C, the temperature range expected to promote fatigue cracking and minimize rutting of the asphalt concrete layer. The target was only exceeded for a few days in April 1996 when the average daily temperature reached 25°C. The daily average air temperatures, calculated from the hourly temperatures recorded during HVS operation, are graphically presented in Figure 3.1. The air temperatures were slightly higher than those obtained during testing of Section 501RF *(4)*.

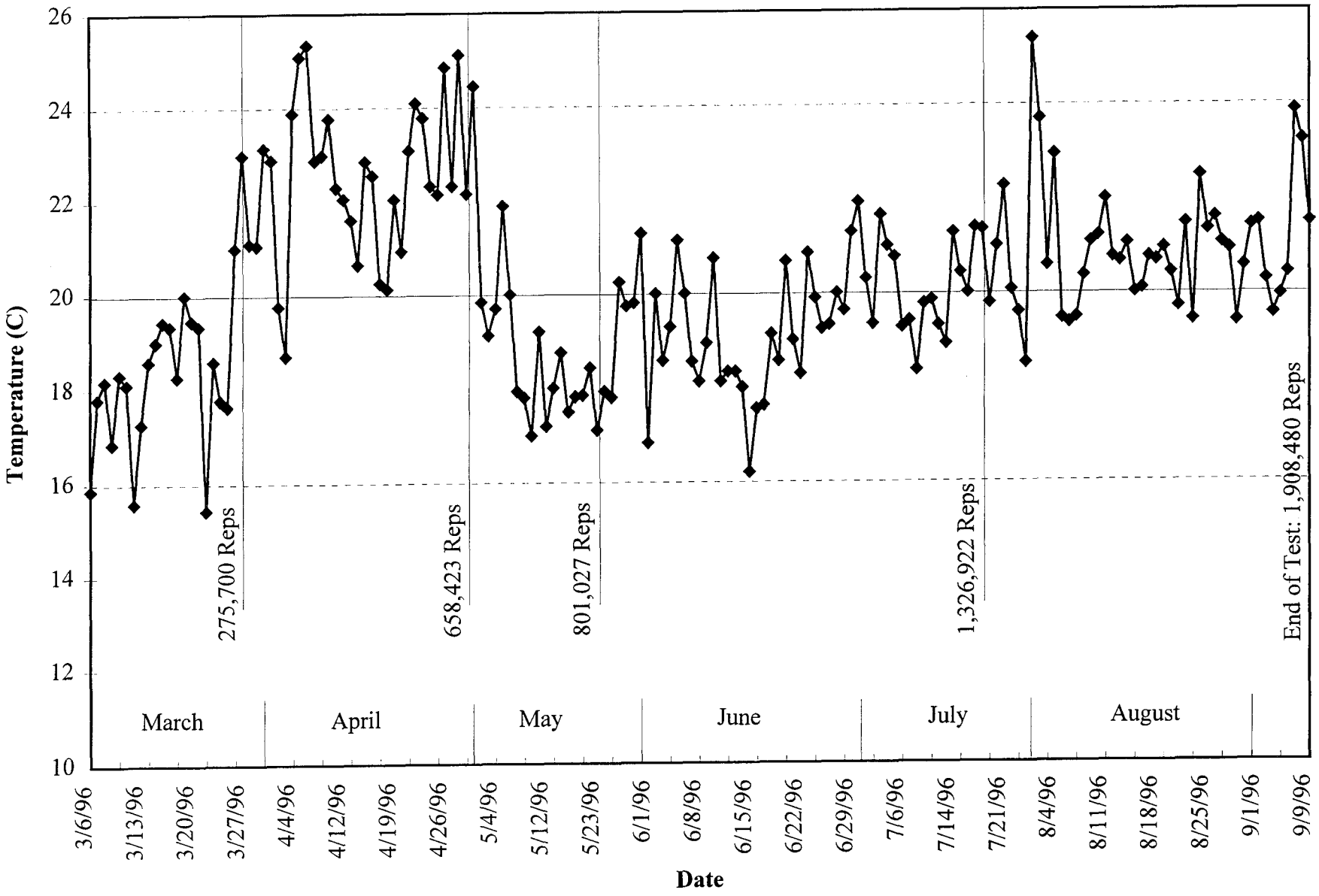

Figure 3.1 Daily average air temperatures, Section 503RF

To illustrate temperature variation during the day, air temperature data were divided into four 6-hour intervals. In the first interval, all the temperatures collected at the end of hour 0100 to the end of hour 0600 were averaged. The other periods, 0700 to 1200 hours, 1300 to 1800 hours, and 1900 to 2400 hours, were averaged in the same manner. Average air temperatures for each of the intervals for the entire test period are shown in Table 3.1; it will be noted that average air temperatures over the four time periods exhibited only a small variation remaining within the range $20 \pm 1°C$.

Table 3.1 Average temperatures (°C) over 6-hour intervals for the air, pavement surface, and at various depths in the asphalt concrete

TIME PERIOD	Air Temp (°C)		Surface Temp (°C)		In-depth temperatures (°C)					
					50 mm		137 mm		175 mm	
	Avg	Std Dev	Avg	Std Dev	Avg	Std Dev	Avg	Std Dev	Avg	Std Dev
0100-0600	19.9	2.3	20.2	1.7	20.5	1.6	20.7	1.5	20.8	1.5
0700-1200	20.0	2.5	20.1	1.6	20.2	1.6	20.4	1.5	20.5	1.5
1300-1800	20.9	2.7	20.3	1.7	20.4	1.5	20.5	1.4	20.5	1.4
1900-2400	20.5	2.4	20.4	1.6	20.6	1.5	20.7	1.4	20.8	1.3
Maximum[a] Difference	1.0		0.4		0.4		0.3		0.3	

[a] difference between minimum and maximum 6-hour interval averages

The "maximum difference" data in Table 3.1 show that pavement temperatures fluctuated less than the air temperatures throughout the day. The maximum variation in the average pavement temperature was only about 0.4°C at a depth of 50 mm, while the average air temperature experienced a larger maximum variation—1.0°C.

Daily averages of the surface and in-depth temperatures are shown in Figure 3.2. These temperatures have warming and cooling trends similar to those of the daily average air temperatures. Average pavement surface temperatures were close to the average air temperatures as illustrated in Figure 3.2 and Table 3.1.

Table 3.2 presents the average temperatures for five periods during the test, which exhibited the following temperature trends: warming, constant, cooling, warming, and constant.

Table 3.2 Average daily temperatures during five periods

Temperature Trends		Warming	Constant	Cooling	Warming	Constant
Dates (period length)		3/6–3/27 (21 days)	3/28–4/30 (33 days)	5/1–5/23 (22 days)	5/24–7/18 (55 days)	7/19–9/9 (52 days)
Repetitions at End of Period		275,700	658,423	807,143	1,326,922	1,908,480
Location		**Average Temp (°C)**				
	Air	18.3	22.3	19.0	19.7	20.9
	Surface	18.8	22.1	18.9	19.9	20.6
	50 mm	18.9	22.1	19.2	20.1	20.8
	137 mm	18.8	22.0	19.5	20.3	21.0
	175 mm	18.7	21.9	19.7	20.5	21.1

While a more detailed comparison of pavement temperatures will be provided in the summary report for the Goal 1 tests, it should be noted that the average daily pavement temperature at a depth of 137 mm was slightly higher for Section 503RF than for Section 501RF, i.e. 20.6°C versus 19.0°C.

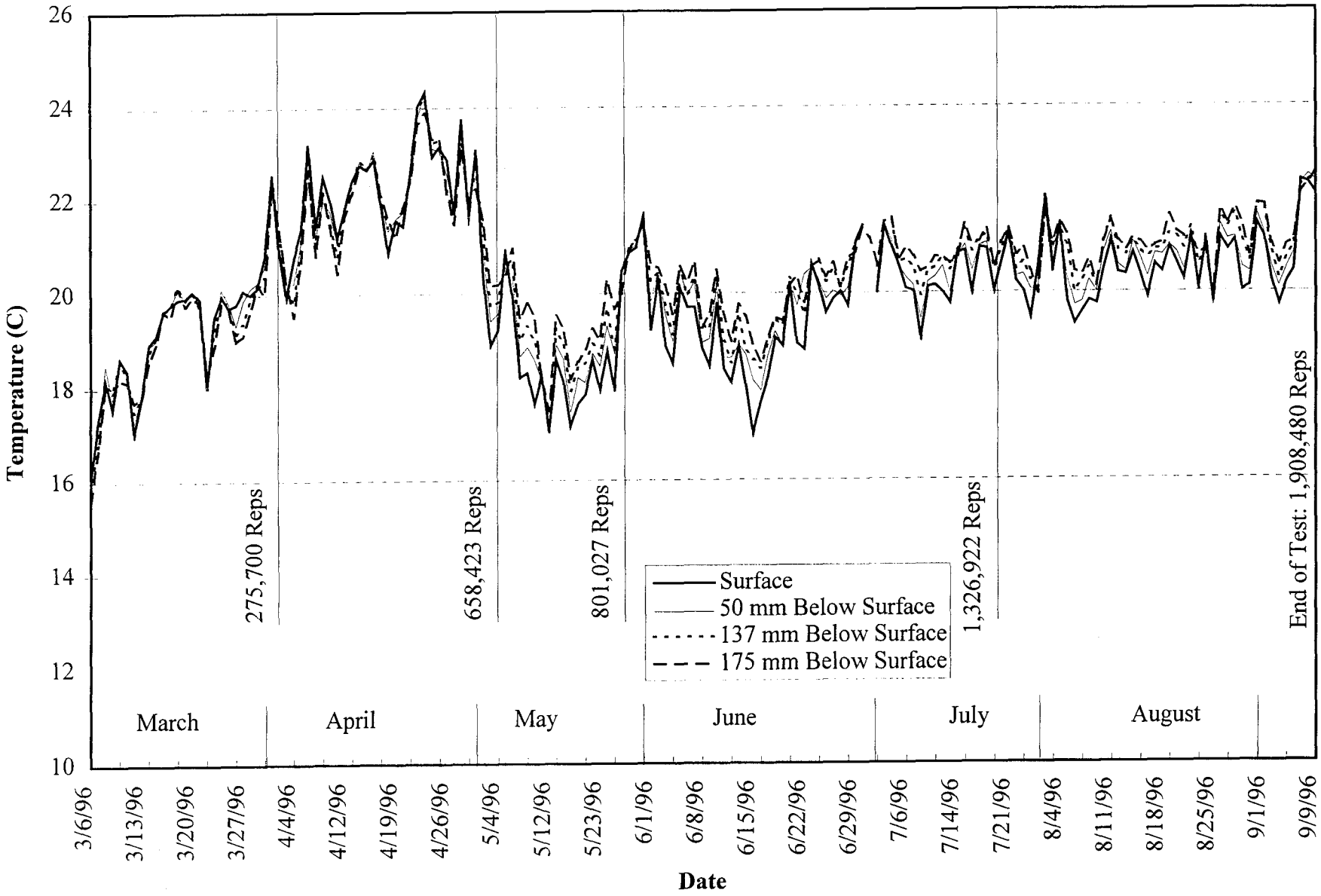

Figure 3.2 Daily average temperatures at pavement surface and at various depths in the asphalt concrete, Section 503RF

3.2 RAINFALL AND WATER CONTENTS OF UNTREATED MATERIALS

The trafficking of Section 503RF occurred predominantly during California's dry season. The average rainfall was about 28 mm per month. Figure 3.3 shows the monthly rainfall from July 1994 to November 1996 as recorded by the National Weather Service at Richmond, California (near the Richmond Field Station).

Water contents of the unbound materials were measured after construction of the four sections associated with Goal 1 in March/April 1995 and prior to the construction of the overlays (Goal 3) in February 1997, Table 3.3. Both sets of moisture samples were collected at about the same period, two years apart. Since the testing of Section 503RF took place during the later part of the two year period, Figure 3.3, it would seem reasonable to assume that the water contents of the untreated materials during the test would be close to those shown for February 1997 in Table 3.3.

Table 3.3 Water contents of materials in unbound layers

LOCATION	IN-SITU WATER CONTENT	
	March/April 1995[a]	February 1997[b]
aggregate base	4.2-6.0	4.6-4.9
aggregate subbase	4.0-7.9	5.3-6.0
subgrade	13.6-23.9	14.4-16.3

[a] moisture tests conducted on twelve samples per layer
[b] moisture tests conducted on four samples per layer

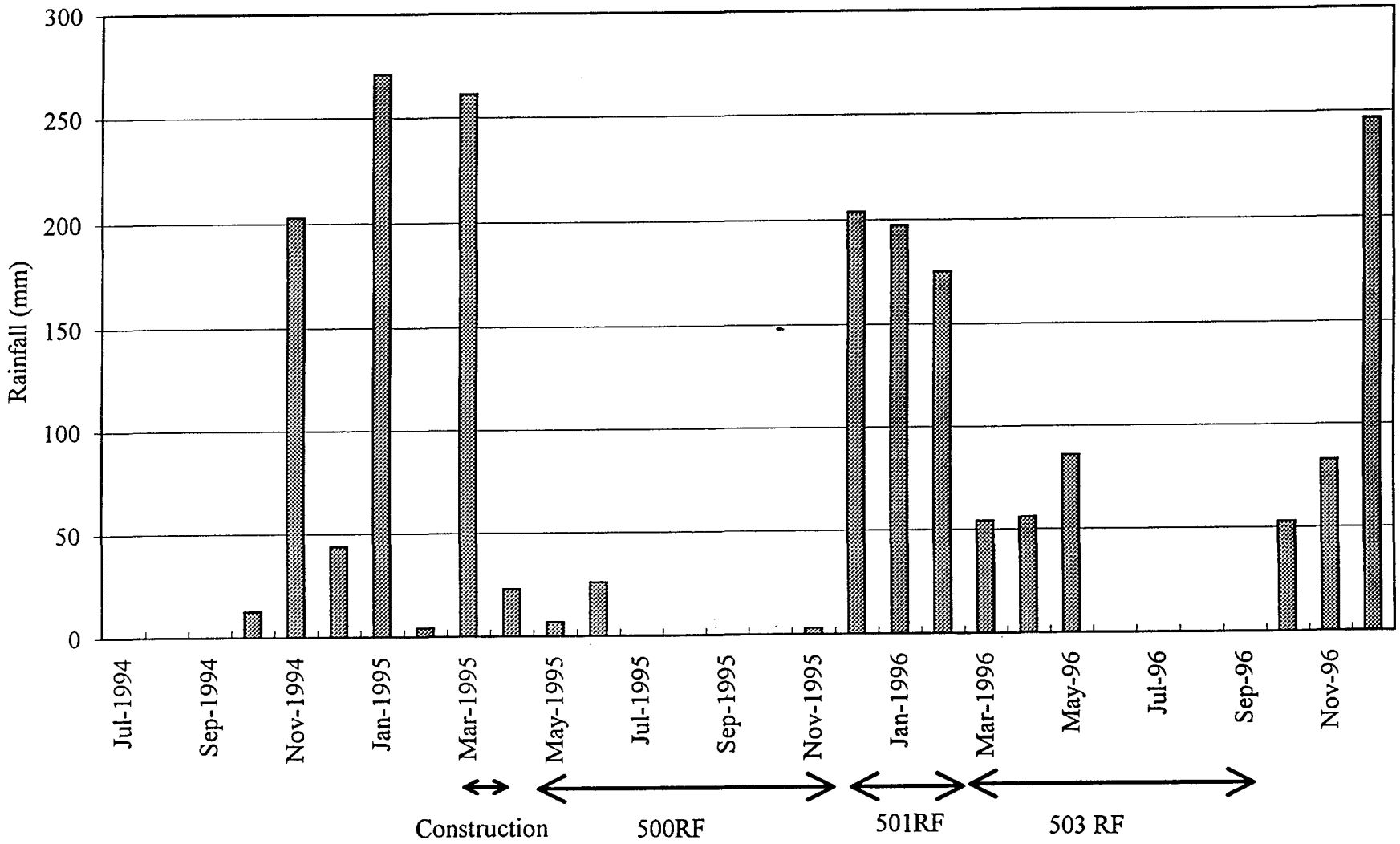

Figure 3.3 Monthly rainfall data in Richmond (National Weather Service)

3.3 PERMANENT DEFORMATION

Permanent deformation (rutting) response at the pavement surface was monitored with the Laser Profilometer and a straight edge. Two Multi-Depth Deflectometers (MDDs) were also used to determine the permanent deformation at the surface and at various depths within the pavement. Results of the surface and in-depth permanent deformation measurements are discussed in this section.

3.3.1 Permanent surface deformation (rutting)

Asphalt pavements deform under the action of traffic due to shear and densification of the pavement layer materials which are subjected to dynamic stresses produced by the traffic loads. When a new pavement (or test section) is open to traffic, it typically undergoes both additional compaction and shear deformation which results in the development of surface permanent deformation or rutting. With the HVS, the rate at which that rutting occurs is usually greater initially and typically diminishes as trafficking progresses until reaching a steady state. If the load level is subsequently increased, the pavement will undergo again another phase of rapid rutting development until a new steady phase for that new load level is reached. This initial phase is referred to as the "embedment" phase herein.

Figure 3.4 shows the development of permanent deformation with load repetitions as determined from the laser profilometer for Section 503RF. Two sets of data are presented:

1. average rut depth; and
2. average maximum rut depth.

These terms are described in Reference *3*. In this figure, the 40 kN and 80 kN embedding phases can be seen. Cracking which appeared on the surface at 400,000 repetitions did not play a significant role in the development of surface deformation.

The Laser Profilometer provides sufficient information to evaluate the permanent deformation of the entire test section surface at regular intervals of load repetitions, as illustrated in Figures 3.5 through 3.9. Figure 3.5 illustrates the pavement surface after 15,000 repetitions and shows a minimal amount of rutting. Figures 3.6 to 3.9 show the rutting progression at the surface from 200,000 up to 1.91 million wheel load applications.

At the conclusion of trafficking (1.91×10^6 repetitions), the average rut depth was approximately 7.9 mm while the average maximum rut depth had reached 10.8 mm. Surface rutting was fairly uniform over all the test section; however, a slightly larger rut depth was experienced at Point 12 (where MDD12 was installed) and at both sections ends where the HVS wheels reverse. This is expected since at both ends the speed of the wheels is slower and loading times are therefore longer. In addition, the pavement is subjected to surface shear forces at those locations resulting from braking and accelerating forces which also contribute to rutting development.

The data from the straight edge and laser profilometer measurements are in reasonable agreement, Figure 3.10. The slight differences between the two methods result because the laser profilometer is more sensitive to tiny changes and pits in the surface texture of the pavement and is more accurate.

Figure 3.4 provides the information to permit determination of the rate of rut development at various stages in the test. To do this, data subjectively were divided into phases which were determined from changes in the loading, as well as from observed changes in the rate of development of permanent deformation. These phases are summarized in Table 3.4, with the calculated rate of rutting expressed in millimeters of rut per million load applications (mm/MiLA).

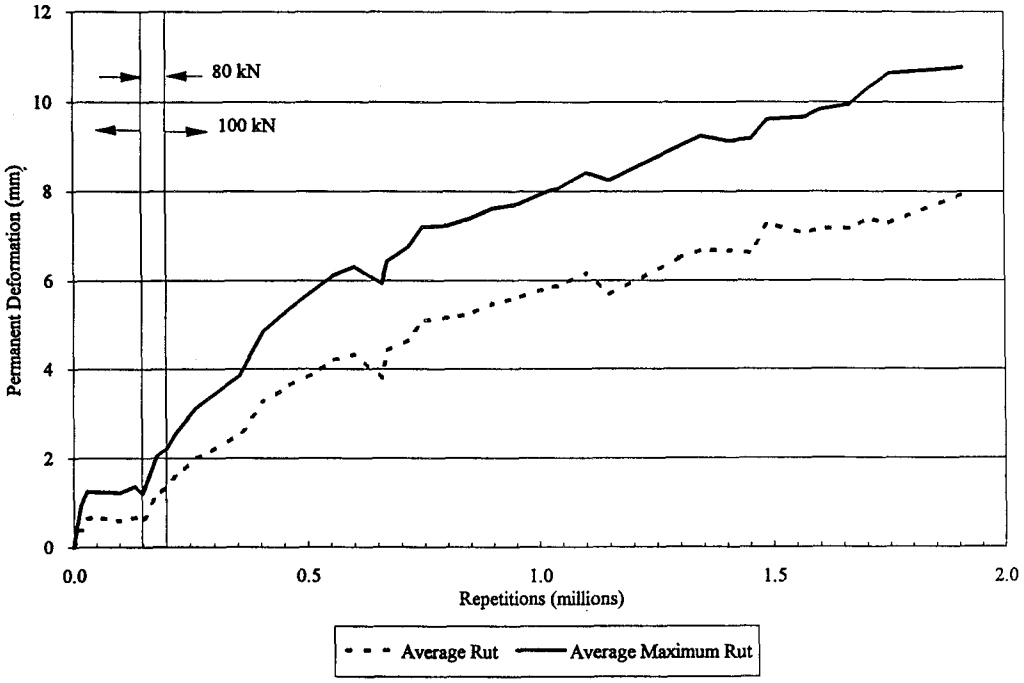

Figure 3.4 Permanent deformation determined from laser profilometer

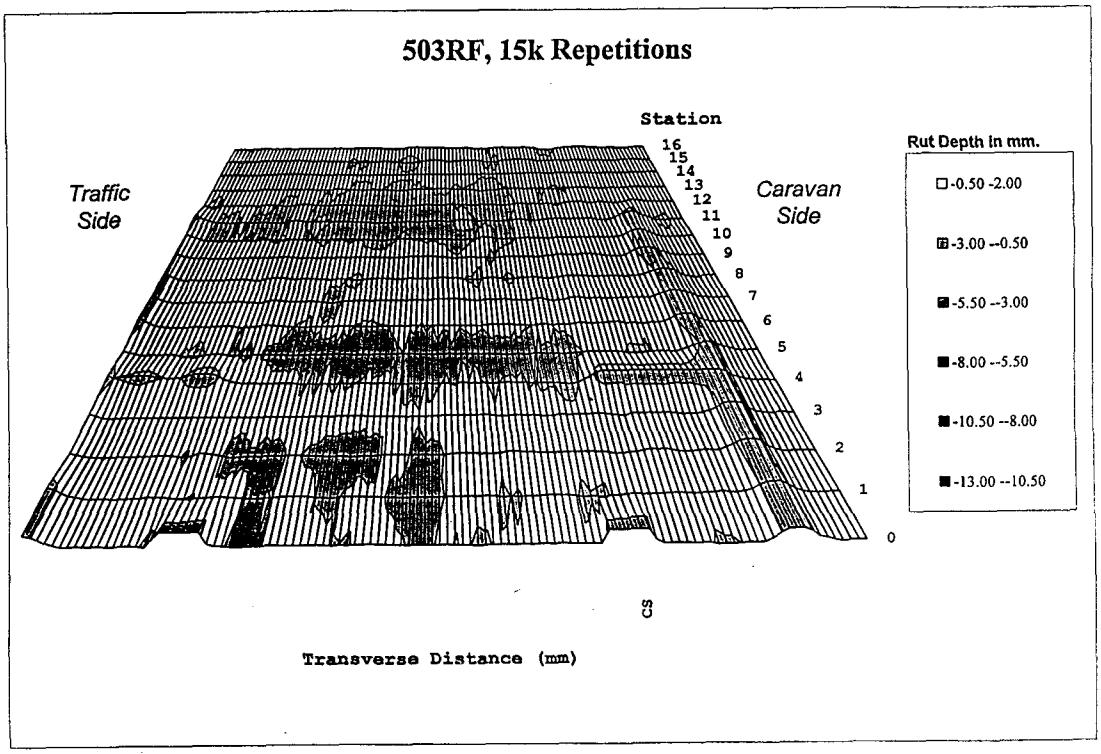

Figure 3.5 Permanent deformation at 15,000 repetitions

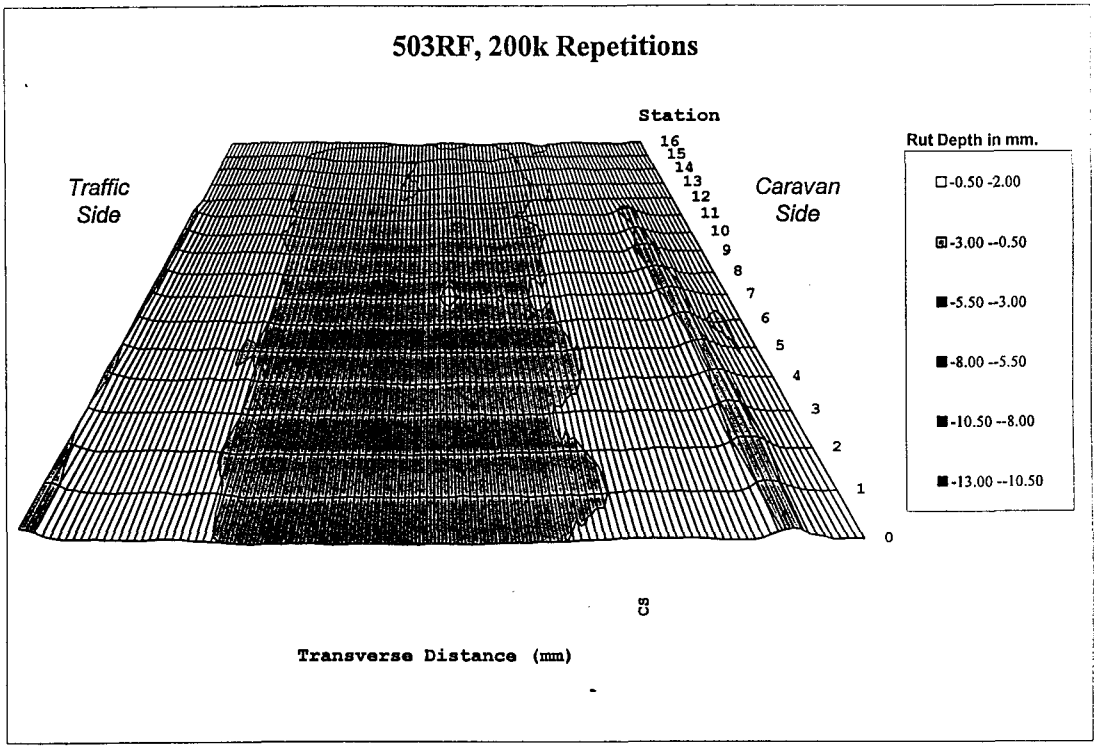

Figure 3.6 Permanent deformation at 200,000 repetitions

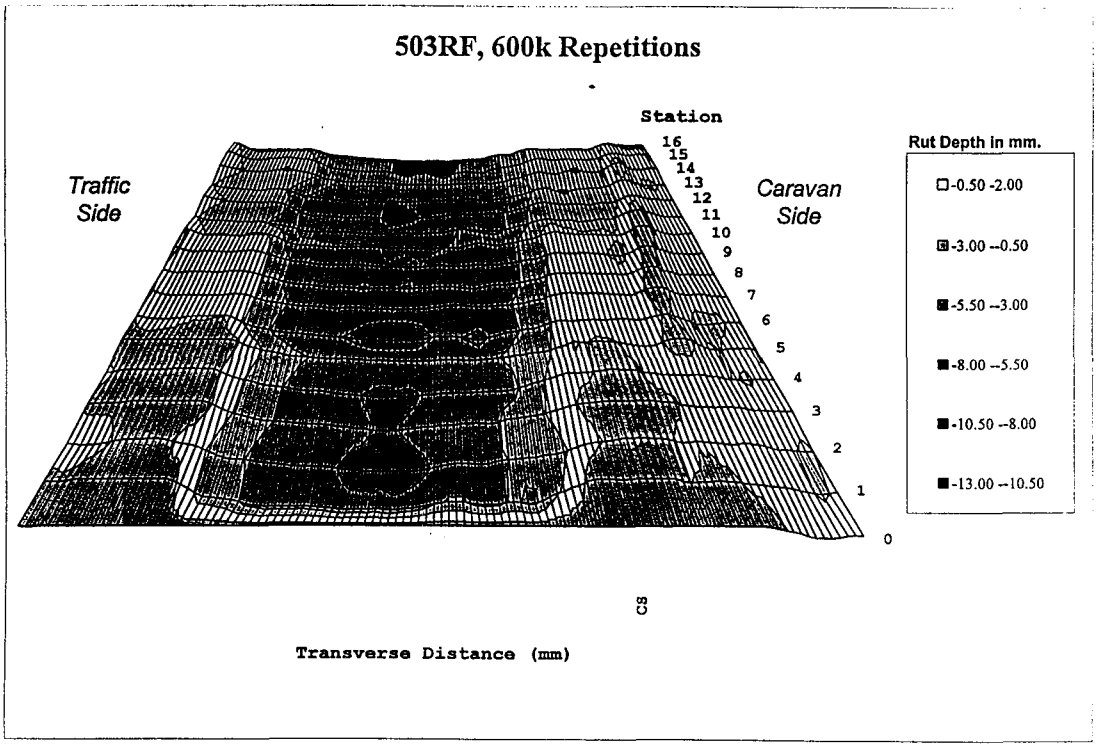

Figure 3.7 Permanent deformation at 600,000 repetitions

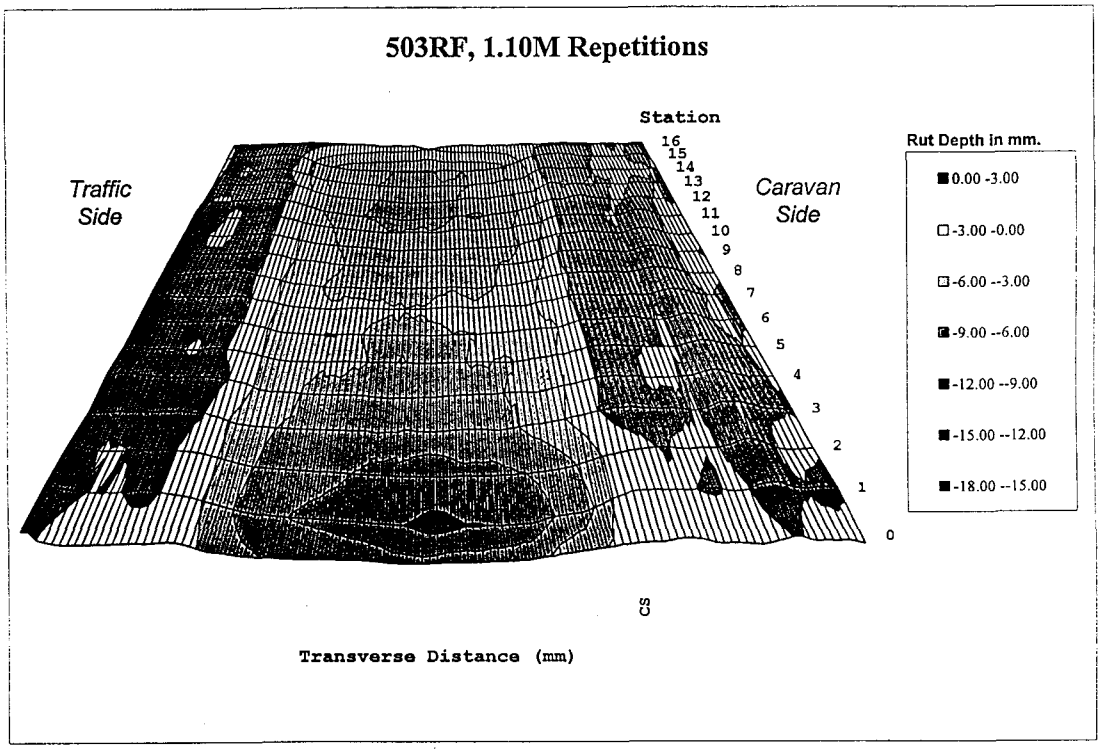

Figure 3.8 Permanent deformation at 1.1 million repetitions

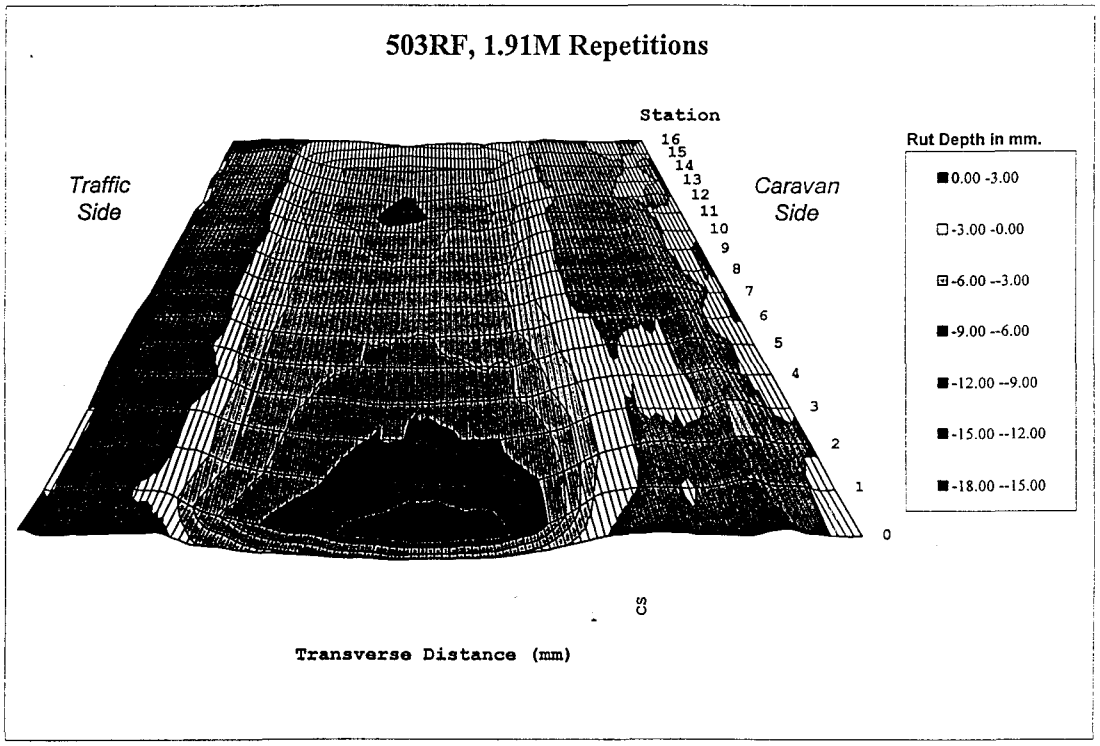

Figure 3.9 Permanent deformation at 1.91 million repetitions

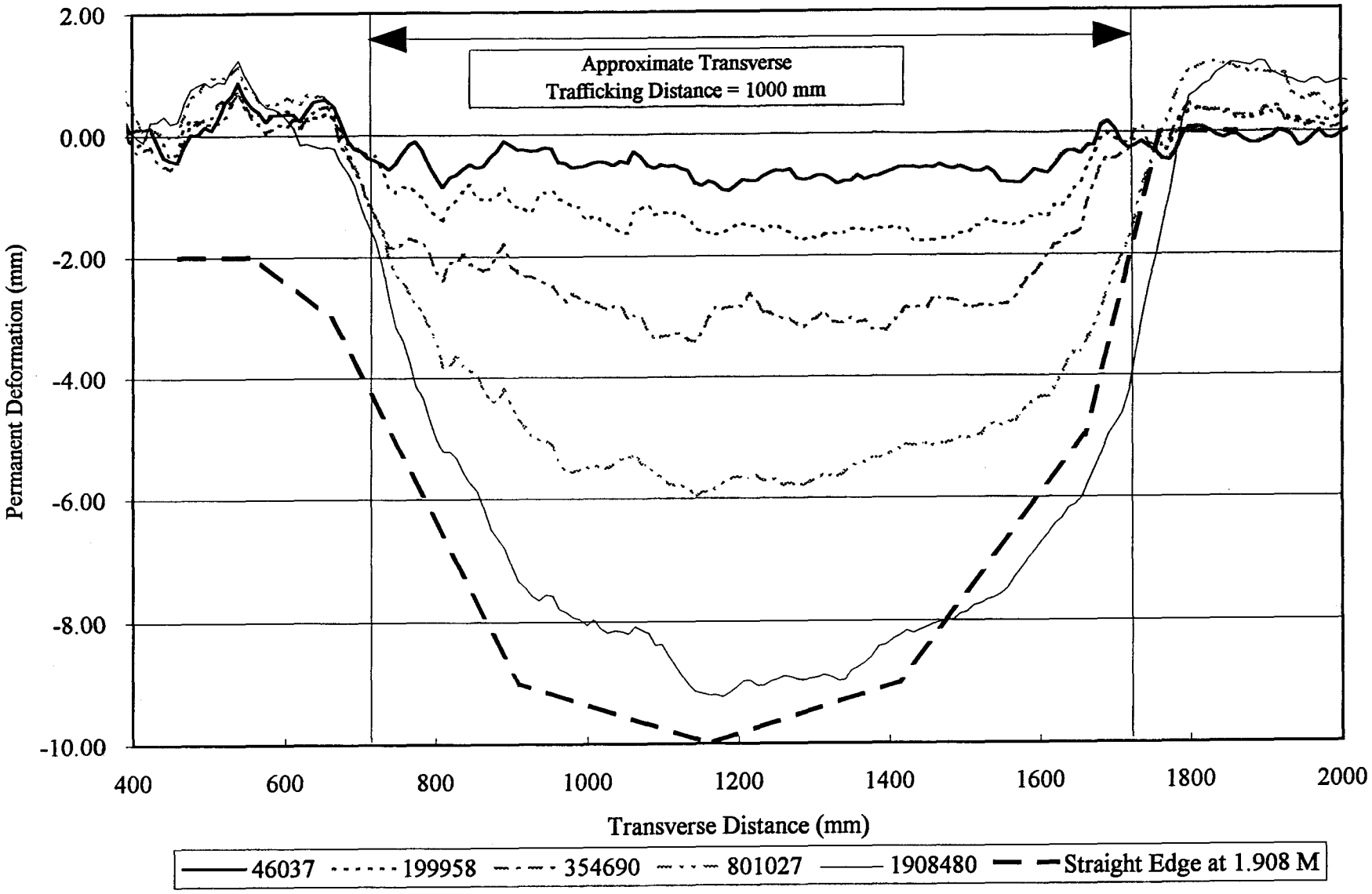

Figure 3.10 Profilometer cross section and straight edge measurements

The first phase, 0 to 50,000 repetitions, is an embedding phase in which the asphalt pavement undergoes post-construction compaction as the result of the 40 kN traffic loading. Figure 3.4 shows that the embedding phase appears completed at approximately 50,000 load repetitions at 40 kN. The test plan required that the 40 kN load be maintained to 150,000 repetitions to ensure that this initial embedding phase was complete so that the pavement would be able to withstand the higher wheel loads (80 kN and 100 kN) without excessive damage to the asphalt concrete due to the accelerated loading. At 150,000 repetitions the load was increased to 80 kN and a rapid increase in rutting rate was observed (Figure 3.4). The load was further increased to 100 kN at 219,972 repetitions and the rut depth rate again increased significantly.

As with other tests, each time the load was increased, a new embedding phase was observed; 150,000 to 200,000 repetitions represented the embedding phase resulting from the increase in load from 40 kN to 80 kN. The next embedding phase, when the load was increased at about 200,000 repetitions to 100 kN, lasted to approximately 400,000 repetitions, at which time cracking appeared at the surface. However, the appearance of surface cracks did not lead to an increase in rut rate as seen in Figure 3.4. After 400,000 repetitions (the end of the final embedding phase), the rut rate remained steady until the test end.

During the embedding phases for the 40 kN and 80 kN only approximately 25 percent of the final average rut depth occurred. At 400,000 repetitions, the approximate time at which cracking was detected, approximately 41 percent of the final average rut depth was obtained. During the remaining 1.5 million repetitions, the average rut depth increased at a constant rate of about 3.1 mm/million 100 kN repetitions. This rate is slightly lower than that obtained during the loading of Section 501RF, i.e. 3.3 to 5.4 mm/MILA.

Table 3.4 Rutting rates during HVS loading on Section 503RF

Phase	Repetitions ($\times 10^3$)	Load (kN)	Condition	Average Rut (mm)	Maximum Rut (mm)	Average Rut Rate (mm/MiLA)[a]
I	0–50	40	Embedding	0.69	1.2	13.8
II	50–150	40	Steady-State	0.69	1.2	0
III	150–200	80	Embedding	1.35	2.2	13.2
IV	200–400	100	Embedding	3.26	4.9	9.6
V	400–1908	100	Steady-State	7.94	10.8	3.1
[a] MiLA = Million Load Application						

3.3.2 In-depth permanent deformations

With the aid of the MDD modules it is possible to measure the accumulation of vertical permanent deformation at various depths in the pavement during the course of the HVS test. By subtracting the permanent deformations measured at two consecutive depths, for MDDs at Points 4 and 12 as seen in Figure 3.11, it is possible to estimate the deformation occurring in each layer. Table 3.5 contains the results of these analyses.

Table 3.5 Vertical permanent deformation in each layer as measured by MDD modules

Layer	Thickness (mm)	Vertical Permanent Deformation at MDDs (mm)	Percentage of Total Deformation (percent)
Dense-Graded Asphalt Concrete	137	5.5	47.5
Aggregate Base	274	3.9	33.6
Aggregate Subbase	307	2.0	17.3
Subgrade	semi infinite	0.2	1.7
Total		11.6	100

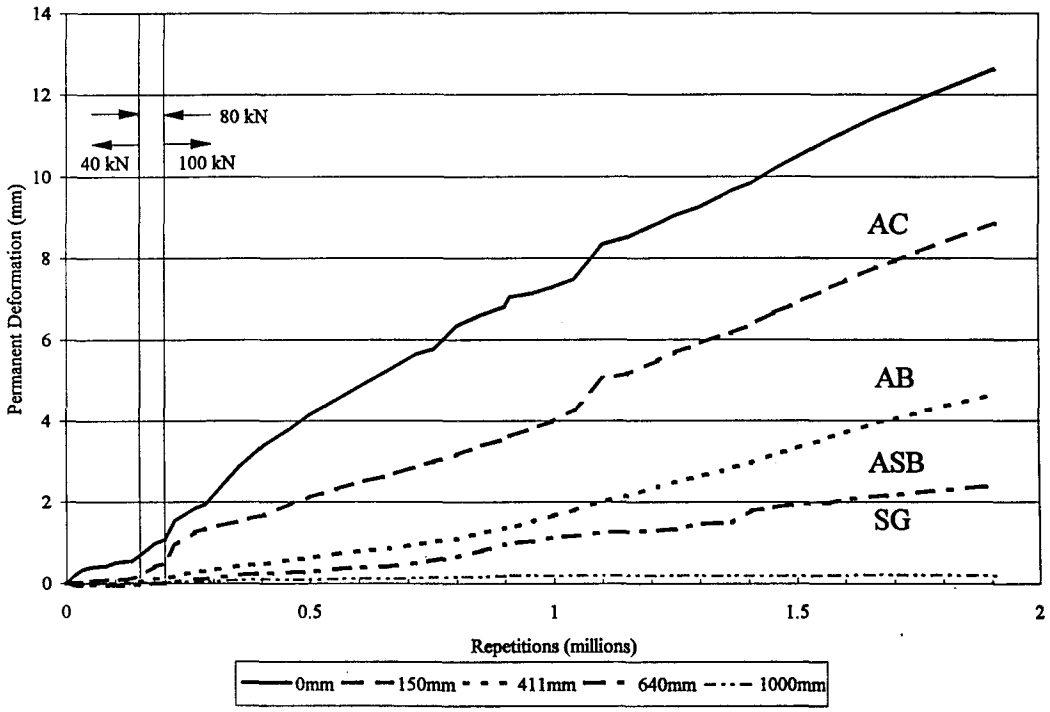

a. Vertical permanent deformation of various layers at Point 4

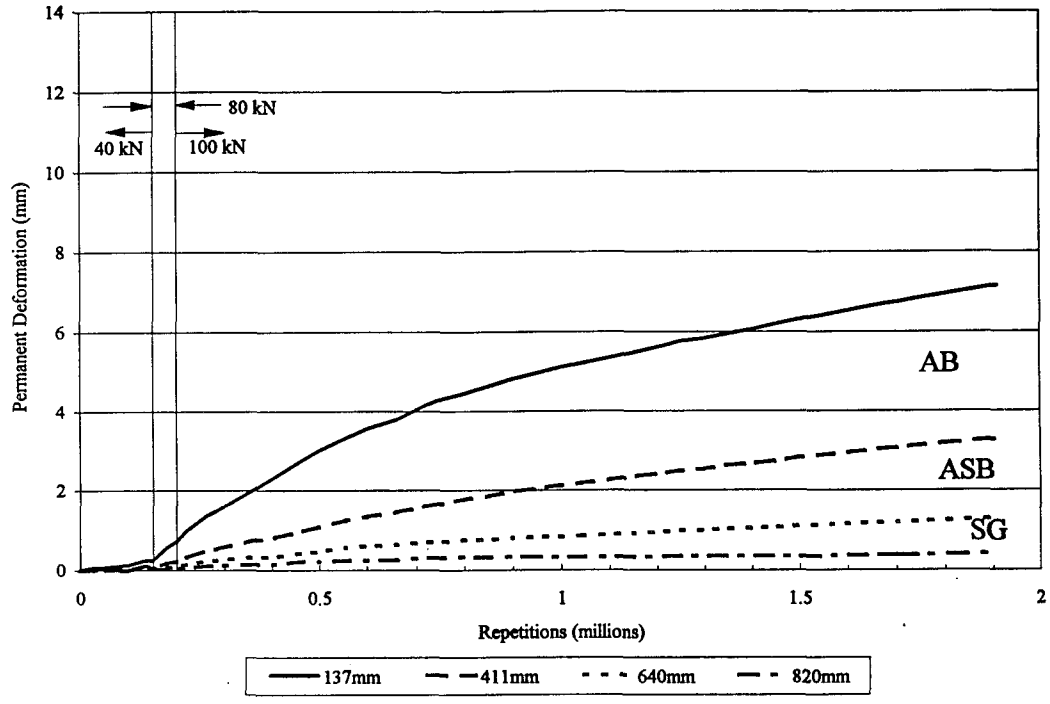

b. Vertical permanent deformation of various layers at Point 12

Figure 3.11 Permanent deformations measured at MDD locations

Comparison of the rut depth (vertical permanent deformation) measured by the surface module of the MDD at Point 4 and by the surface profilometer at the same location show close agreement as seen in Figure 3.12. Compatibility of these different measures of permanent deformation provide confidence in the permanent deformation data to be presented in the next two sections.

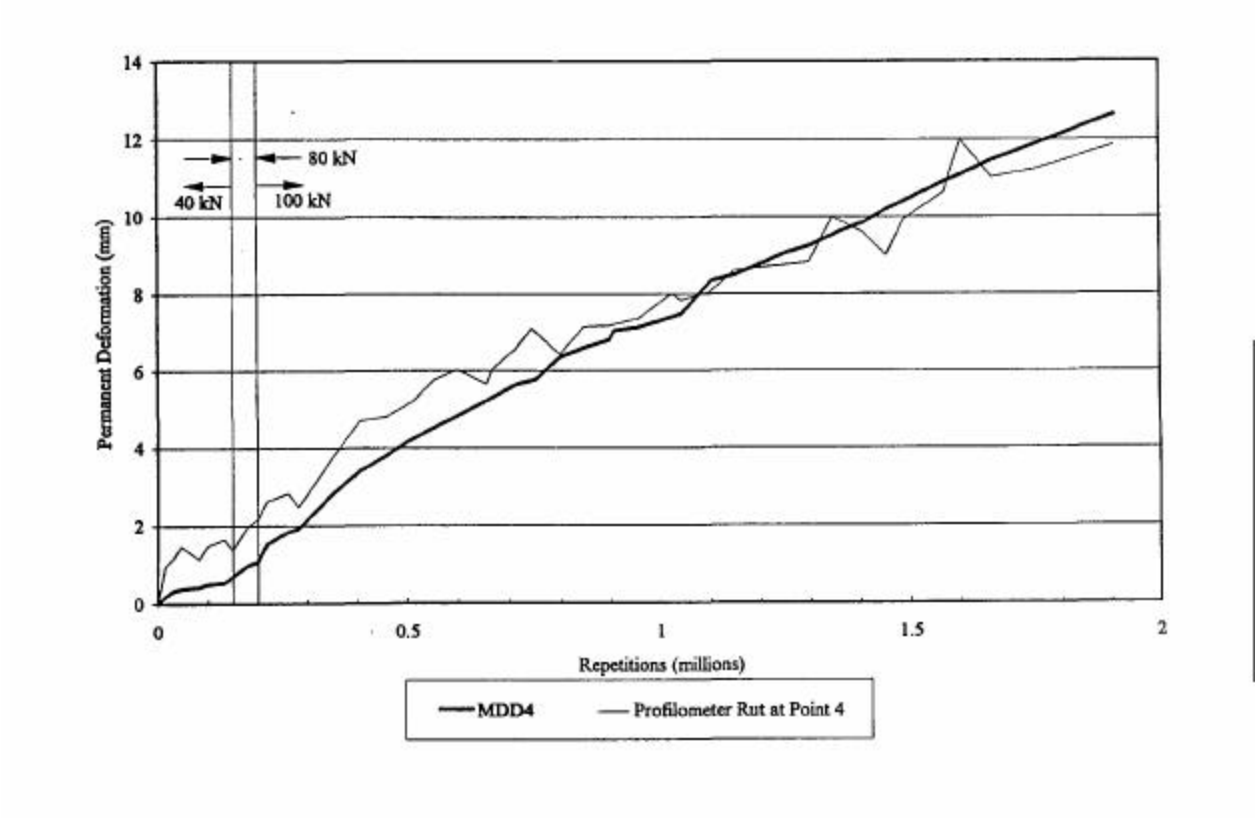

Figure 3.12 Permanent deformation comparison of MDD at Point 4 and the laser profilometer

3.3.2.1 Asphalt concrete. Table 3.6 shows that the asphalt concrete layer contributed almost half (47.4 percent) of the observed surface permanent deformation. From an examination of Figures 3.5 through 3.10, little upheaval is observed adjacent to the ruts, which is similar to that which occurred Section 501RF, the other undrained pavement test

Table 3.6 Air-voids contents in the asphalt concrete

	Specimen[a]	Air-Voids Top Lift, percent	Air-Voids Bottom Lift, percent
Outside Trafficked Area	1	4.8	5.3
	2	4.6	3.7
	3	4.9	4.1
	Average 1, 2 & 3	4.8	4.4
Inside Trafficked Area	4	4.7	3.5
	5	6.0	3.2
	Average of 4 & 5	5.4	3.4
[a] Position of specimen indicated in Figure 3.12			

To estimate what proportions of the measured rutting were attributable to volume decrease and to shear distortion, five cores 100 mm in diameter were extracted so that their air-voids contents could be measured. Three cores were obtained from about .6 m outside the trafficked area in the same lane and the other two from inside the test section at Points 1 and 15.5 within the areas where the wheel changes direction as shown in Figure 3.13. Results of the air-voids determinations on these cores are summarized in Table 3.6.

The change in air-voids content during trafficking was minimal in both the top and bottom lifts as seen in Table 3.6. These data suggest that the majority of rutting is due to shear deformation rather than volume decrease because of traffic densification *(7)*.

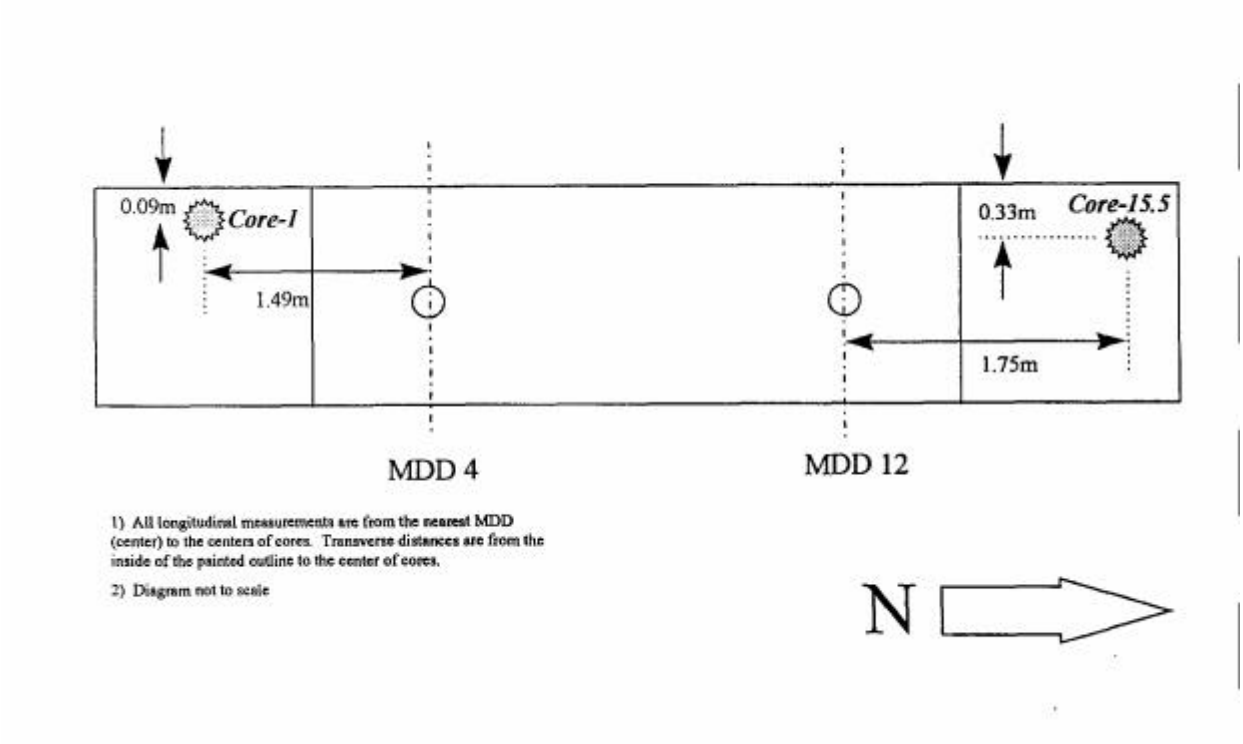

Figure 3.13 Core locations

3.3.2.1 Unbound layers. From the information presented in Table 3.5, it will be noted that one third of the total permanent deformation measured at the surface occurred in the aggregate base. To verify these results, a trench will be dug after completion of the Goal 3 overlay tests.

The proportion of permanent deformation in the aggregate base layer is similar to that obtained for the corresponding layer in Section 501RF *(4)*, the other undrained section, i.e. 33 percent versus 26 percent.

The remainder of the rut depth at the surface resulted from permanent deformations occurring in the subbase and subgrade materials, a total of about 19 percent. On Section 501RF, permanent deformations in the subbase and subgrade were responsible for about 22 percent of the total rut depth measured at the surface, an amount comparable to Section

503RF. These results reinforce earlier observations that the Caltrans design procedure provides an adequate pavement thickness to minimize permanent deformation in the subgrade, even under the 100 kN loading used for the majority of the testing for Section 503RF.

3.4 ELASTIC (RECOVERABLE) DEFLECTIONS

Elastic (recoverable) deflections provide an indication of the overall stiffness of the pavement structure and, therefore, a measure of the load carrying capacity. As the stiffness of a structure decreases, its ability to support load decreases due to damage in the pavement materials with the result that for a given load and tire pressure, deflection increases. During HVS testing elastic deflections are measured with two instruments: the MDD and the RSD. The RSD measures surface deflection basins whereas the MDD measures the surface deflections at Point 4 and the in-depth deflections at two locations, Points 4 and 12 (MDD4 and MDD12 as shown in Figure 2.2 and 2.3).

3.4.1 Surface deflections

In this section of the report, surface deflections as measured by the RSD and the MDD at Point 4 are summarized. Since pavement temperature did not vary significantly during the test, the influence of temperature on deflections was neglected.

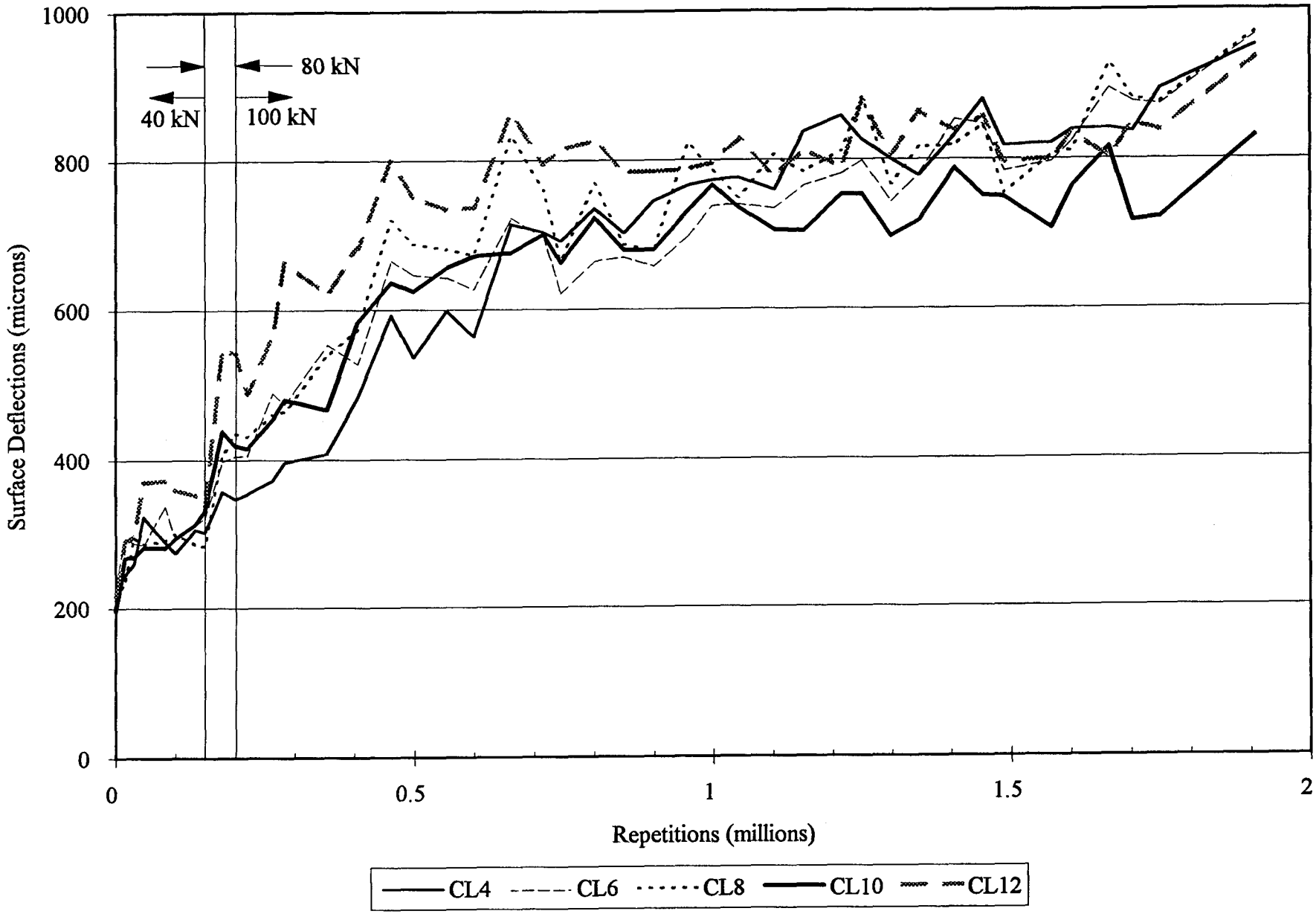

Figure 3.14 Road surface deflections—40 kN test load

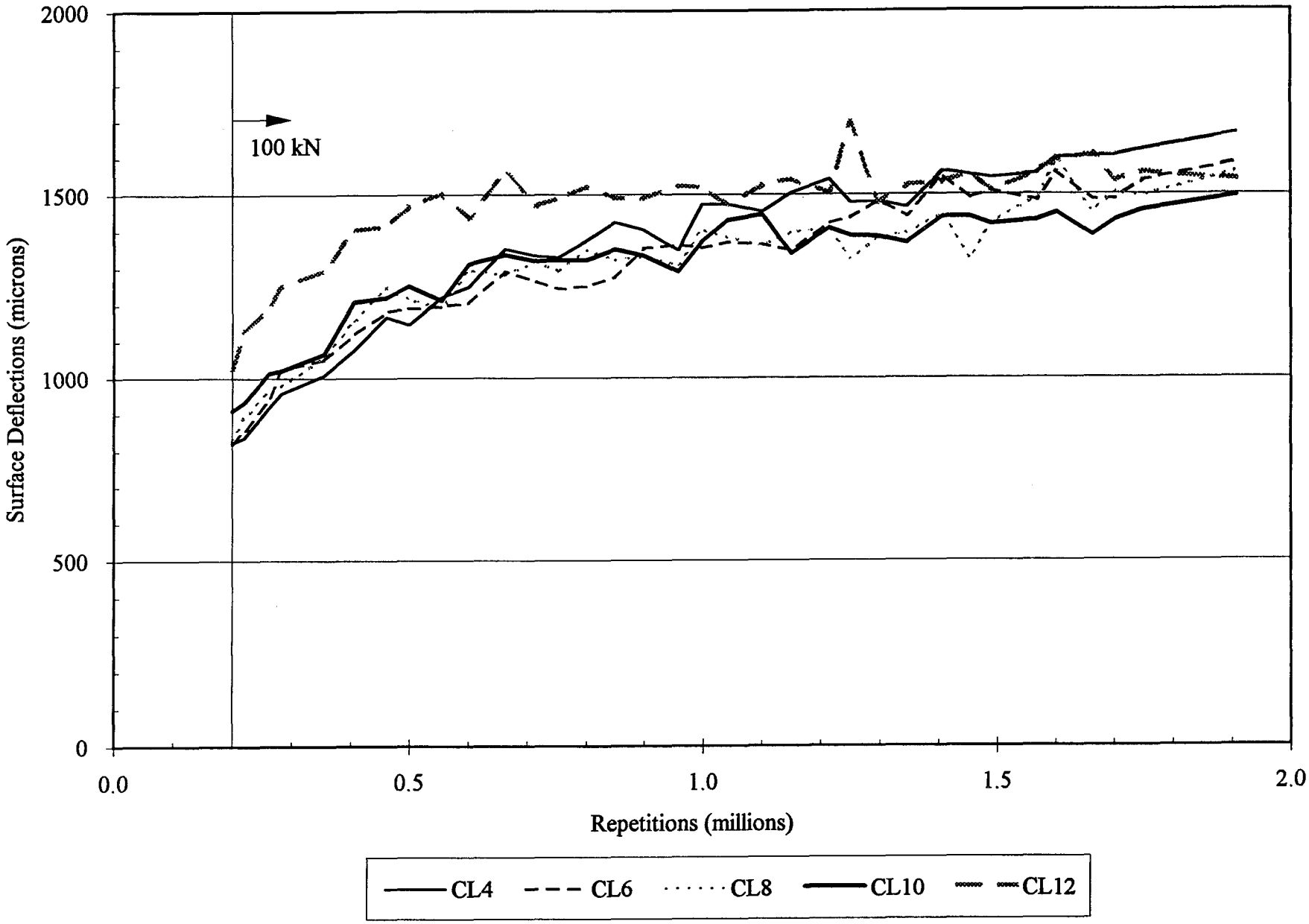

Figure 3.15 Road surface deflections—100 kN test load

3.4.1.1 RSD surface deflection results. Figures 3.14 and 3.15 show the individual RSD deflections for centerline measuring Points 4, 6, 8, 10, and 12 under 40 kN and 100 kN dual-wheel loads respectively. These deflections are all within a narrow band which means that the section exhibited uniform structural behavior. The variation between the centerline deflections at Points 4, 6, 8, and 10 is approximately 20 percent throughout the whole testing period.

Unlike Section 501RF *(4)*, Section 503RF showed no marked increase in surface deflection after cracks appeared at the surface at about 400,000 repetitions. The 40 kN surface deflections increased from an initial value of 218 microns (at 10 load applications) to930 microns upon completion of the test (1.91 million load applications), a 327 percent increase. The 100 kN surface deflections increased from approximately 900 microns (at 200,000 repetitions) to 1,500 microns at the end of the test, an increase of approximately 67 percent. The surface deflection data show a marked increase after the increase of the trafficking load to 100 kN. A summary of the average of all 40 kN RSD deflection data measured on the test section before HVS loading commenced and after 1.91×10^6 load applications is contained in Table 3.7.

Table 3.7 Average of 40 kN RSD Deflections

Deflection (microns)	**Before HVS testing**	**After 1.91×10^6 HVS load applications**
Average	218	931
Standard deviation	12	52

The average RSD deflections are illustrated in Figures 3.16 and 3.17 for 40 kN and 100 kN loads respectively. Phases with similar trends in the rate of increase in elastic deflection are indicated on these figures by Roman numerals. Deflections in phases I, II, III occurred as the load was increased from 40 kN to 80 kN to 100 kN, respectively, and indicate increased damage rates as loading was increased. Point C (approximately 400,000 repetitions) indicates crack appearance on the surface of the pavement. The rate of deflection increase appears to slow substantially after the appearance of cracks at the surface, as indicated in Phase IV (500,000 to 1,910,000 repetitions).

The RSD measurements at the center line and 200 mm on either site of the the center line plotted in Figures 3.16 and 3.17 also indicate that damage was fairly uniform laterally across the section.

Figures 3.18 and 3.19 provide comparisons between Sections 503RF and 501RF of surface deflections versus load repetitions for the 40 kN and 100 kN test loads, respectively. It will be noted that the deflection relationships for the two tests show about the same magnitudes and trends with load repetitions.

3.4.1.2 MDD surface deflection results. Figures 3.20 and 3.21 summarize the surface deflections measured at MDD Point 4 using the 40 kN and 100 kN loads respectively. Also shown in these figures are the results of the RSD deflections measured at these points at the same time. A good agreement between the measurements by the two devices is evident. These data emphasize the usefulness of the RSD data in defining the uniformity or lack thereof in the performance throughout the 1 m by 8 m test sections, and as an independent check of MDD measurements.

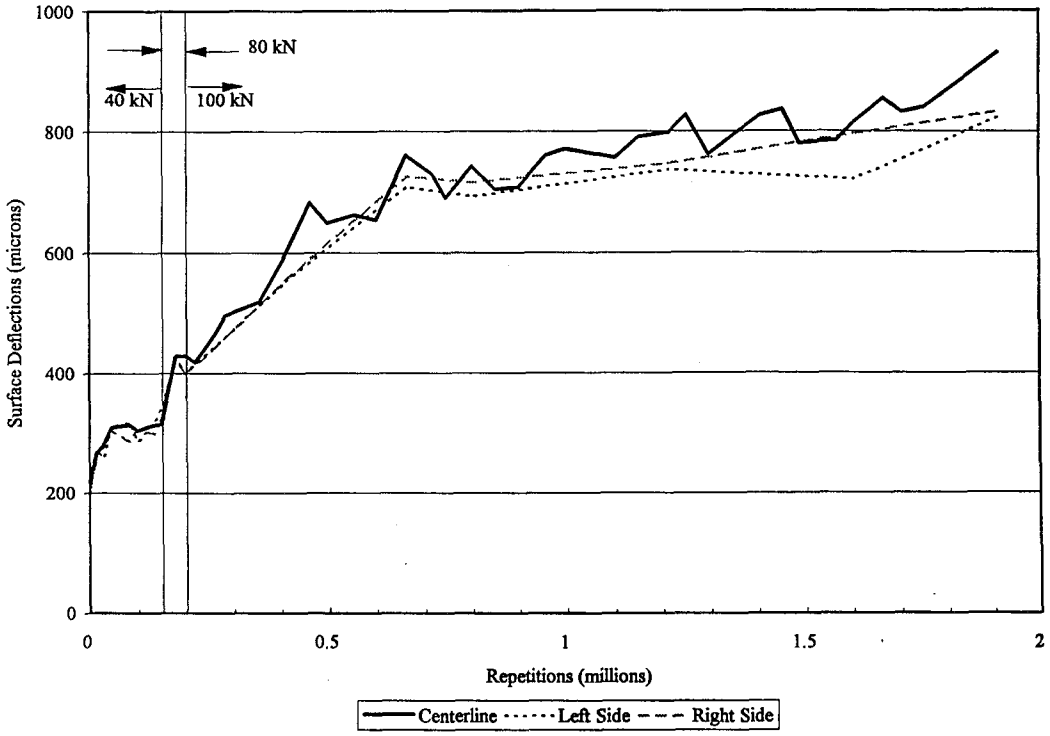

Figure 3.16 Average road surface deflections—40 kN test load

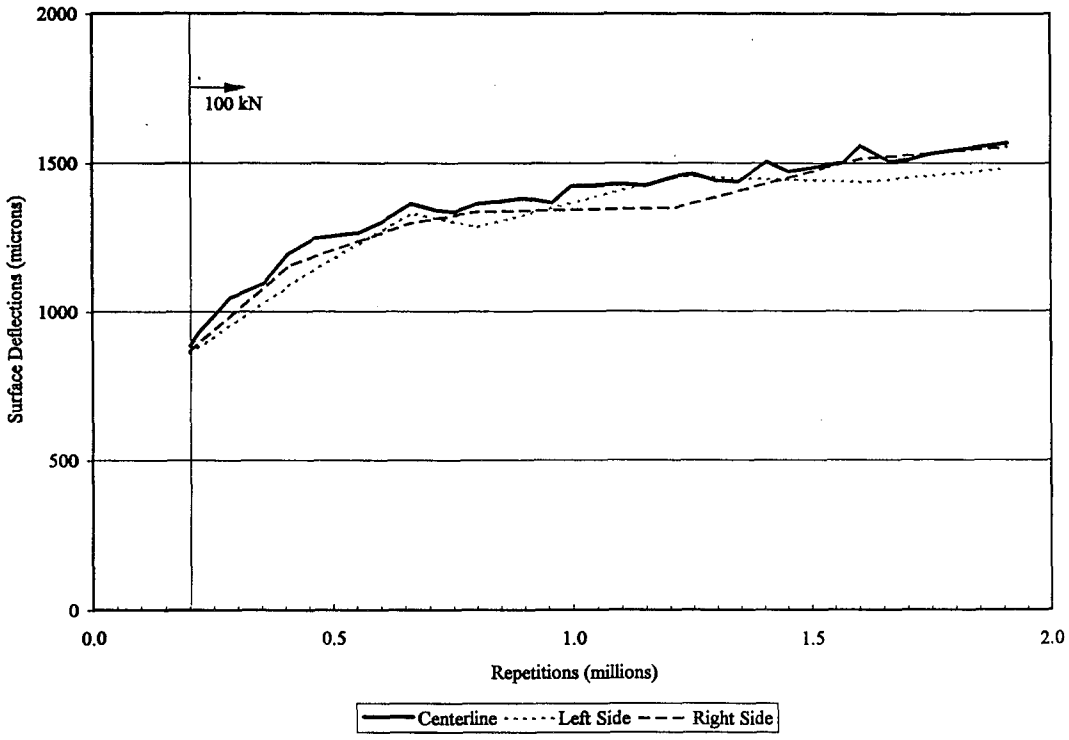

Figure 3.17 Average road surface deflections—100 kN test load

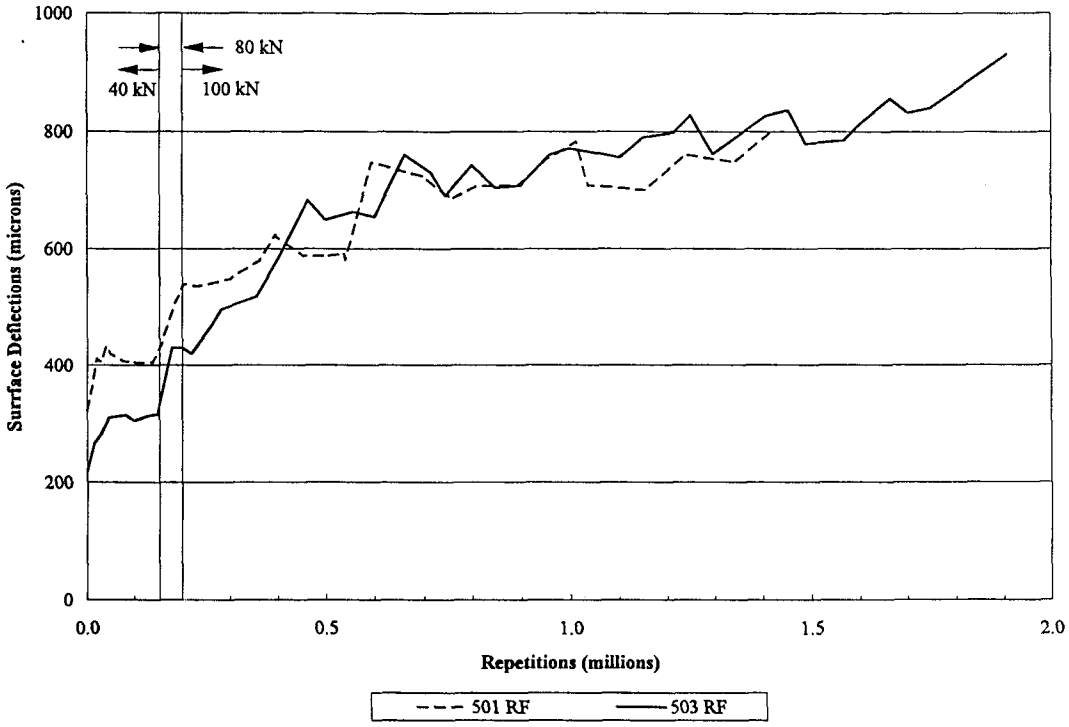

Figure 3.18 Comparison of RSD surface deflections for Sections 501RF and 503RF—40 kN test load

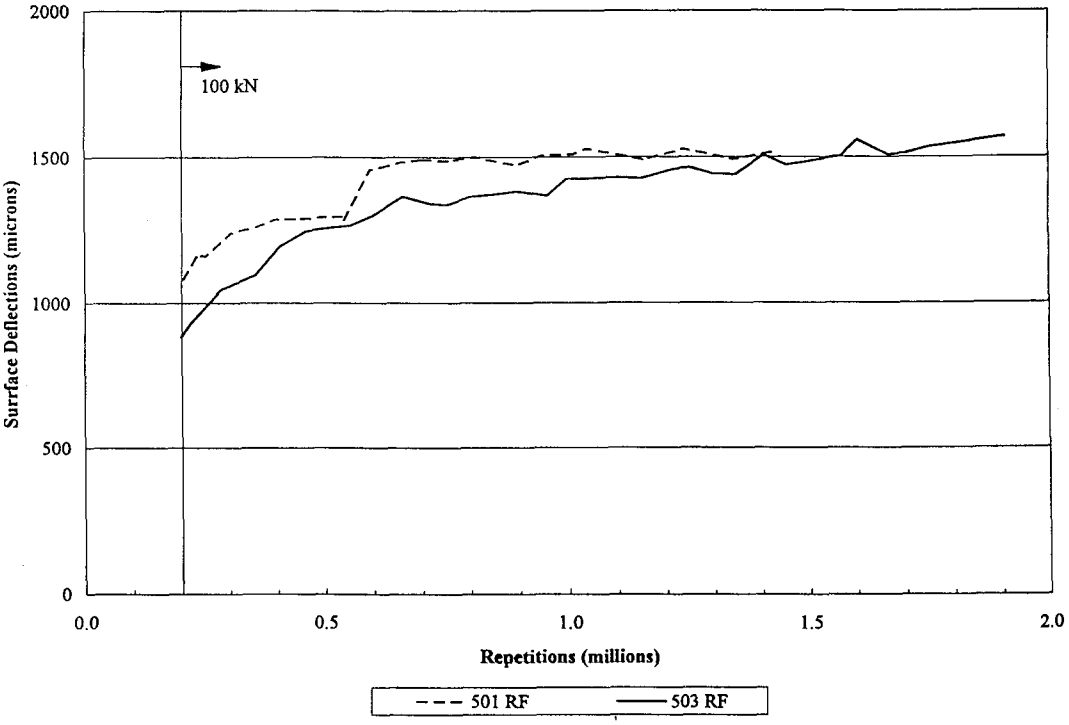

Figure 3.19 Comparison of RSD surface deflections for Sections 501RF and 503RF—100kN load

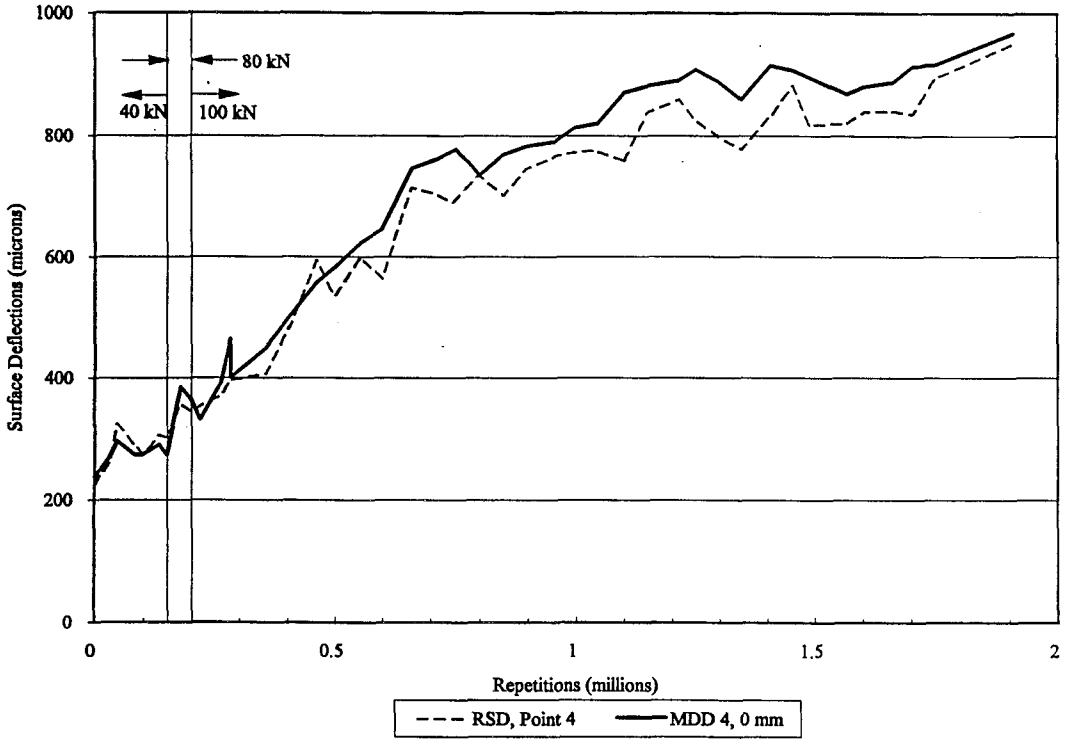

Figure 3.20 Comparison of elastic deflections determined by the RSD and by the MDD at Point 4 with a 40 kN load

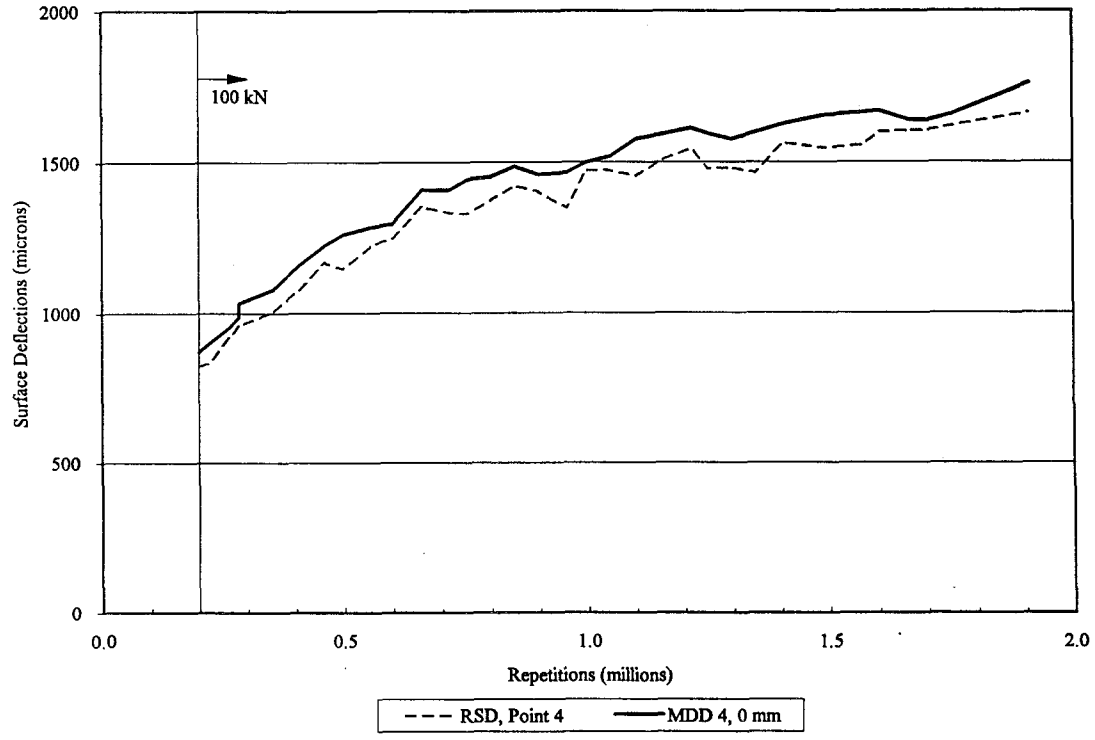

Figure 3.21 Comparison of elastic deflections determined by the RSD and by the MDD at Point 4 with a 100 kN load

3.4.2 In-depth elastic deformations

Figures 3.22 through 3.25 summarize the in-depth deflections measured at various stages of trafficking under the 40 kN and 100 kN dual-wheel loads. Averages of all 40 kN and 100 kN MDD elastic deflection data measured on Section 503RF before HVS loading commenced and after 1.91 million load applications are summarized in Table 3.8 and Table 3.9 for the 40 kN and 100 kN test loads respectively. As noted earlier, the 100 kN test load deflections were measured only after the HVS had reached 200,000 load repetitions, at which point the traffic load was increased to 100 kN (Table 2.1). The data contained in these tables represent the average of 3 deflection measurements per measuring point.

Tables 3.8 and 3.9 suggest that the damage which took place in the asphalt concrete layer (as manifested by surface cracking) is responsible for the increase in surface deflection. Due to the decrease in stiffness in the surface layer resulting from cracking, the deflections in the other layers also increased. From Tables 3.8 and 3.9 it is also possible to determine the proportion of the total surface deflection contributed by each layer. Results of this analysis are presented in Tables 3.10 and 3.11 for 40 kN and 100 kN test loads respectively.

As will be seen in Tables 3.10 and 3.11, the proportion of total elastic deflection occurring in the aggregate base decreased slightly as the asphalt concrete was damaged. This decrease can be attributed, at least in part, to the stiffening in the granular layer resulting from increased stresses in that layer as a result of decreased asphalt concrete stiffness. It will also be noted that the proportion of elastic deformation occurring in the subbase and subgrade increased slightly due to the probable increase in stresses at these levels as well.

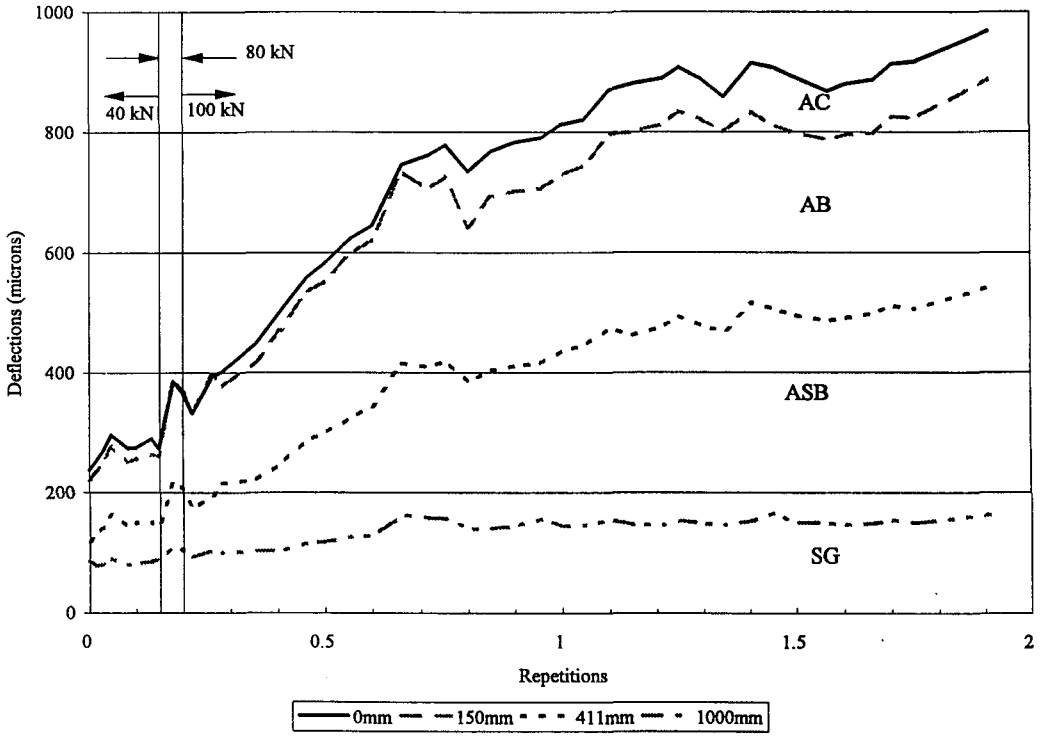

Figure 3.22 Deflections measured by the MDD at Point 4 versus load repetitions at various depths below pavement surface, 40 kN test load

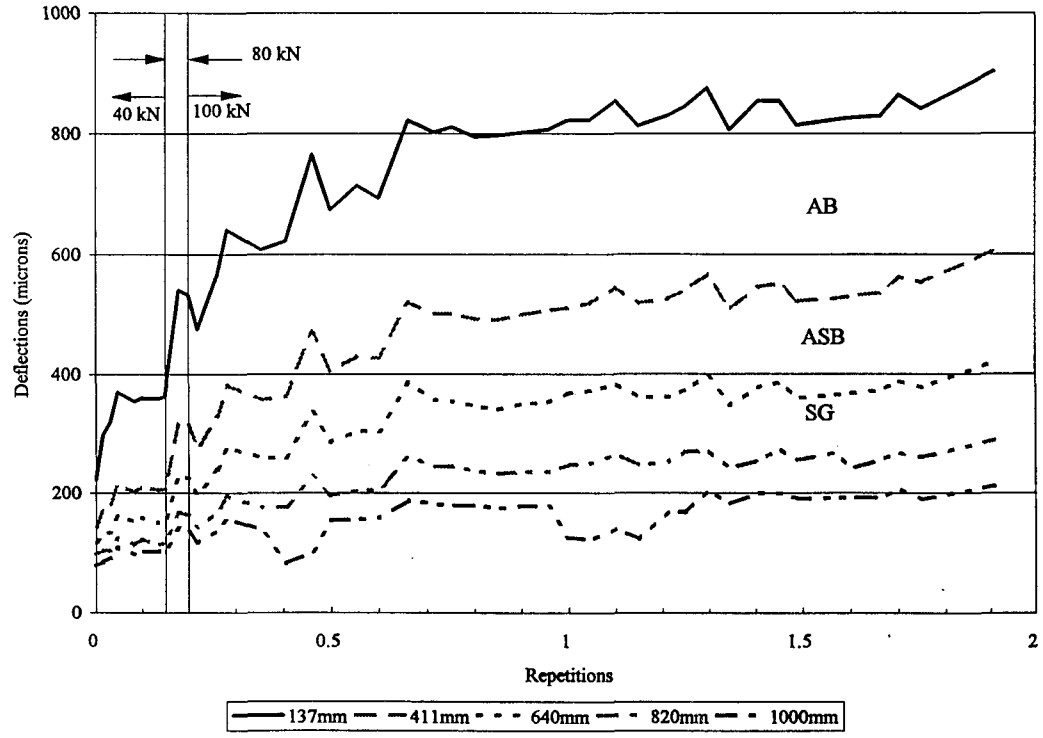

Figure 3.23 Deflections measured by the MDD at Point 12 versus load repetitions at various depths below pavement surface, 40 kN test load

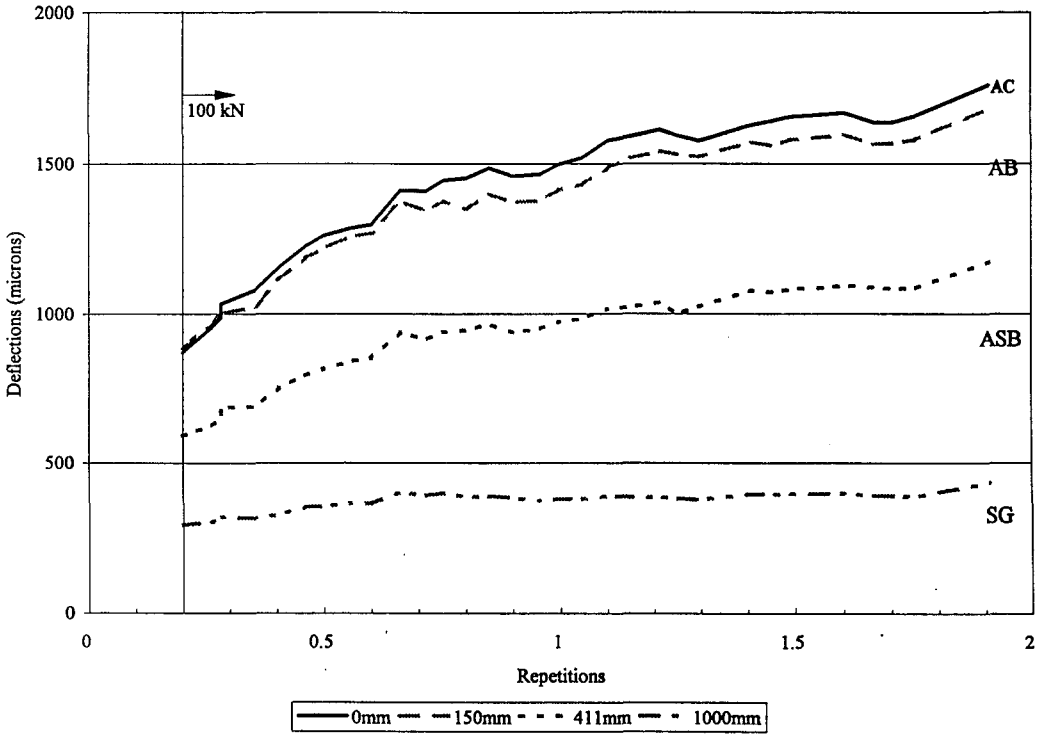

Figure 3.24 Deflections measured by the MDD at Point 4 versus load repetitions at various depths below pavement surface, 100 kN test load

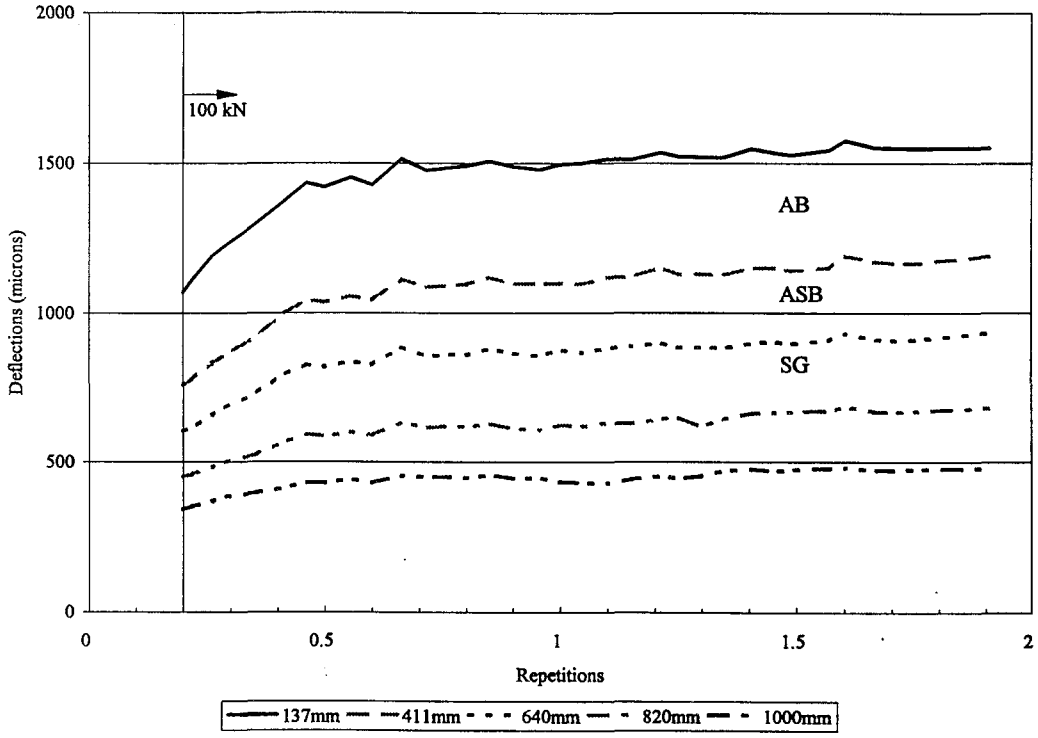

Figure 3.25 Deflections measured by the MDD at Point 12 versus load repetitions at various depths below pavement surface, 100 kN test load

Table 3.8 Summary of 40kN MDD elastic deflections

Level (mm)	Pavement layer	Elastic in-depth deflections (microns): Test Load = 40kN			
		MDD at Point 4		MDD at Point 12	
		Before HVS loading	After 1.91×10^6 load applications	Before HVS loading	After 1.91×10^6 load applications
0	asphalt concrete	238	968	230[a]	975[a]
137	asphalt concrete	228[a]	905[a]	222	905
150	aggregate base	223	889	[a]	[a]
411	aggregate subbase	119	542	142	606
640	subgrade	90	400[b]	117	420
820	subgrade	[a]	[a]	96	289
1000	subgrade	87	164	78	212

[a] MDD modules were not placed at these locations (see Figure 2.3); estimated value
[b] MDD module failed; estimated value

Table 3.9 Summary of 100kN MDD elastic deflections

Level (mm)	Layer	Elastic in-depth deflections (microns): Test Load = 100kN			
		MDD at Point 4		MDD at Point 12	
		After 200,000 load repetitions	After 1.91×10^6 load repetitions	After 200,000 load repetitions	After 1.91×10^6 load repetitions
0	asphalt concrete	871	1761	1085[a]	1620[a]
137	asphalt concrete	857[a]	1700[a]	1068	1551
150	aggregate base	-	1681	[a]	[a]
411	aggregate subbase	592	1173	757	1191
640	subgrade	448	558	603	934
820	subgrade	[a]	[a]	450	682
1000	subgrade	291	434	341	500[b]

[a] MDD modules were not placed at these locations (see Figure 2.3); estimated value
[b] estimated value

Table 3.10 Percentage elastic deflection per layer, 40 kN test load

Pavement Layer	Percentage of total elastic deflection			
	MDD at Point 4		MDD at Point 12	
	Before HVS loading	After 1.91 M load applications	Before HVS loading	After 1.91 M load applications
asphalt concrete	4.2	6.5	3.5[a]	7.2[a]
aggregate base	43.7	37.5	34.8	30.7
aggregate subbase	12.2	14.7[a]	10.9	19.1
subgrade	37.8	41.3[a]	50.8	43.1

[a] MDD modules were not placed at these locations (see Figure 2.2)
Note: Calculated from Table 3.8

Table 3.11 Percentage elastic deflection per layer, 100 kN test load

Pavement Layer	Percentage elastic deflection			
	MDD at Point 4		MDD at Point 12	
	After 200,000 load applications	After 1.91×10^6 load applications	After 200,000 load applications	After 1.91×10^6 load applications
asphalt concrete	1.6[a]	3.5	1.6[a]	4.3[a]
aggregate base	30.4[a]	29.9	28.7	22.2
aggregate subbase	16.5	34.9	14.2	15.9
subgrade	51.4	31.7	55.6[a]	57.6[a]

[a] MDD modules were not placed at these locations (see Figure 2.2)
Note: Calculated from Table 3.9

3.5 VISUAL INSPECTIONS

Since fatigue distress in an asphalt concrete pavement manifests itself in the form of surface cracks, crack monitoring was an essential part of data collection for Section 503RF. As with Sections 500RF *(3)* and 501RF *(4)*, crack monitoring included visual inspection of the test section, direct measurement of crack length and photographic documentation of the cracking progress. In addition to these methods, a new system of digital image analysis was used to further evaluate the cracking progress in asphalt pavements.

This section discusses the extent and severity of surface cracking and details the methodology used to obtain this information with a description of the digital image analysis procedure used for the first time with test section 501RF. Reference *4* contains a detailed description of the methodology for crack analysis and assessment.

3.5.1 Visual inspection of cracks

The first surface cracks were observed at approximately 400,000 repetitions and regular inspection of crack development was continued to the end of the test. To obtain crack length data, the pavement was illuminated with high-power lights followed by the marking of the cracks with lumber crayon in order to make them easily visible. The total length of the cracks was then calculated using the digital method described in Reference *4*. The observed average crack length obtained by this method as a function of load repetitions is shown in Figure 3.26.

As with the other sections, Section 503RF exhibited only hairline cracks which were at times difficult to detect visually. This minimal deterioration of the hairline cracks observed at the pavement surface can likely be attributed, as noted in References *3* and *4*, to two factors:

1. lack of rainfall and dust on the surface of the test pavement, and
2. lack of cracking in the bottom lift of asphalt concrete.

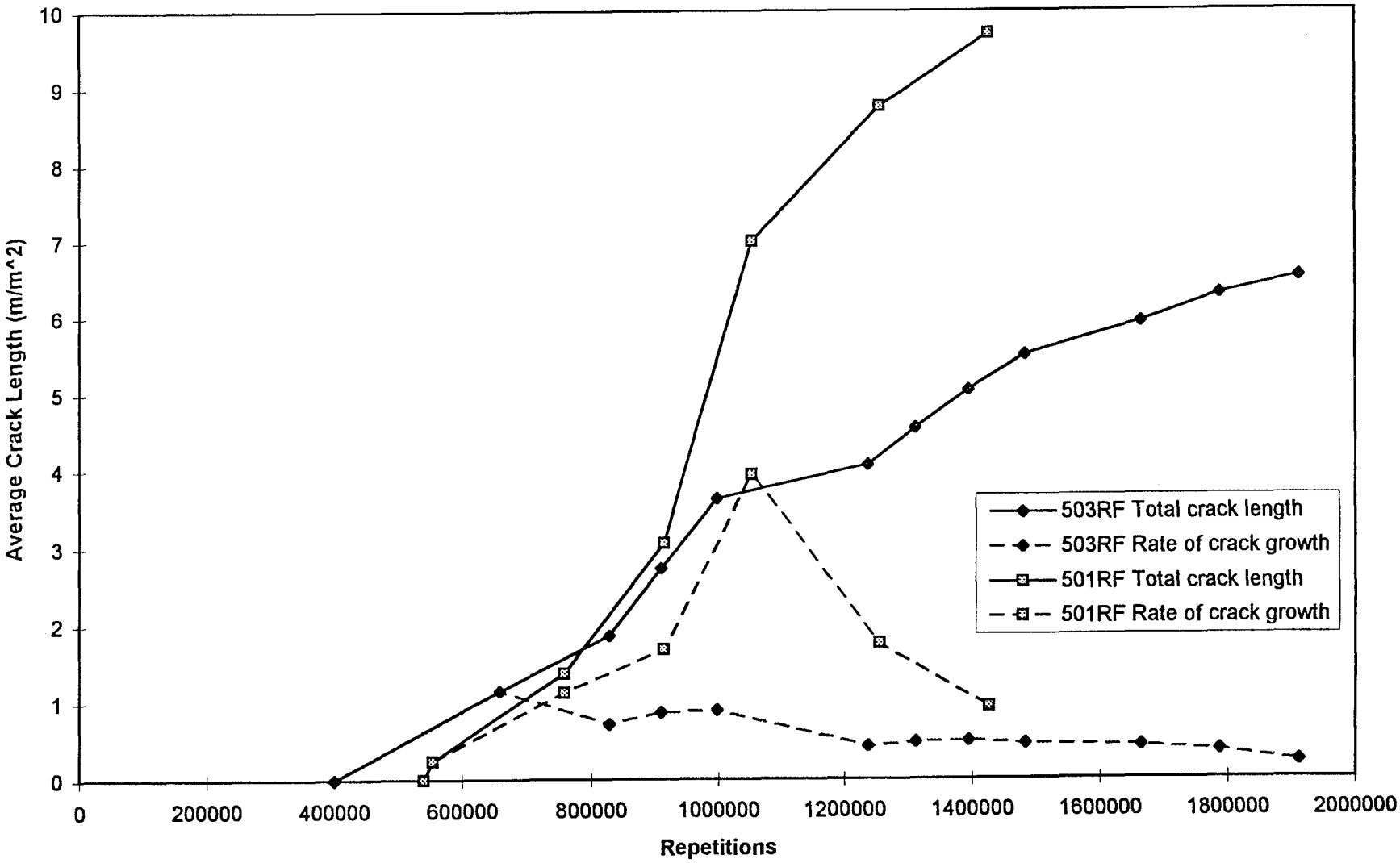

Figure 3.26 Crack length and rate of crack growth versus load repetitions

3.5.2 Assessment of cracking on Section 503RF

From Figure 3.26 it can be seen that the pavement cracked much like the other sections. The first type of cracks that was observed on the surface of Section 503RF were transverse cracks. In the field, however, cracks may initiate as longitudinal or transverse cracks. For Section 503RF, longitudinal cracking occurred at approximately one million repetitions. The influence of the overloading and speed of the wheel on crack orientation is under investigation and will be reported later.

Soon after cracks were first detected at approximately 400,000 repetitions, a period of rapid crack growth ensued followed by a tapering off at about 1.0 million repetitions. Charts of cracks and crack length by section, shown in Figures 3.27 through 3.30 and Figures 3.31 through 3.34 respectively, indicate the severity of the cracking experienced on Section 503RF during the test. The highly cracked condition at the end of the test (1.91m reps) is also shown. It can be assumed that further trafficking of this section would have lead to additional longitudinal cracking which would connect the already established transverse cracks and resulting in further alligator cracking.

Figure 3.31 shows the crack length as a distribution function. This figure illustrates that some alligator cracking developed at the traffic side of the test pavement near Points 4 and 5. This region is also a region of slightly higher permanent deformation. Referring back to the initial site report *(2)* this phenomenon can be explained by the fact that the initial surface deflections were slightly higher there than in the remaining test section. Assuming the HVS wheel load was distributed evenly along the length of the test section, the data show that this region is weaker than the rest of the test section and therefore is less fatigue and permanent deformation resistant.

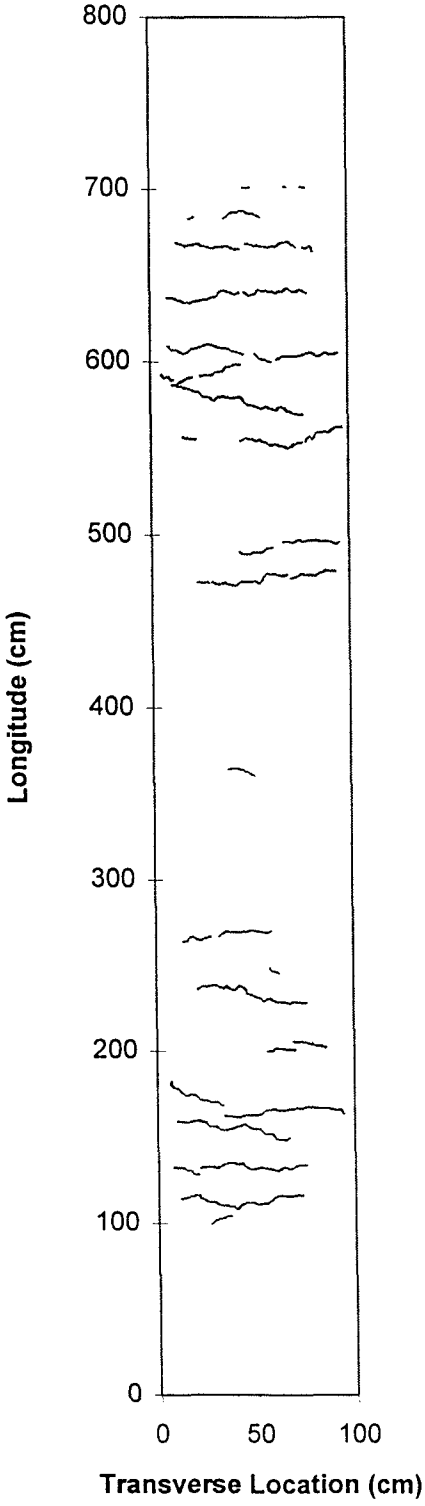

Figure 3.27 Schematic of cracking pattern at 828,000 repetitions

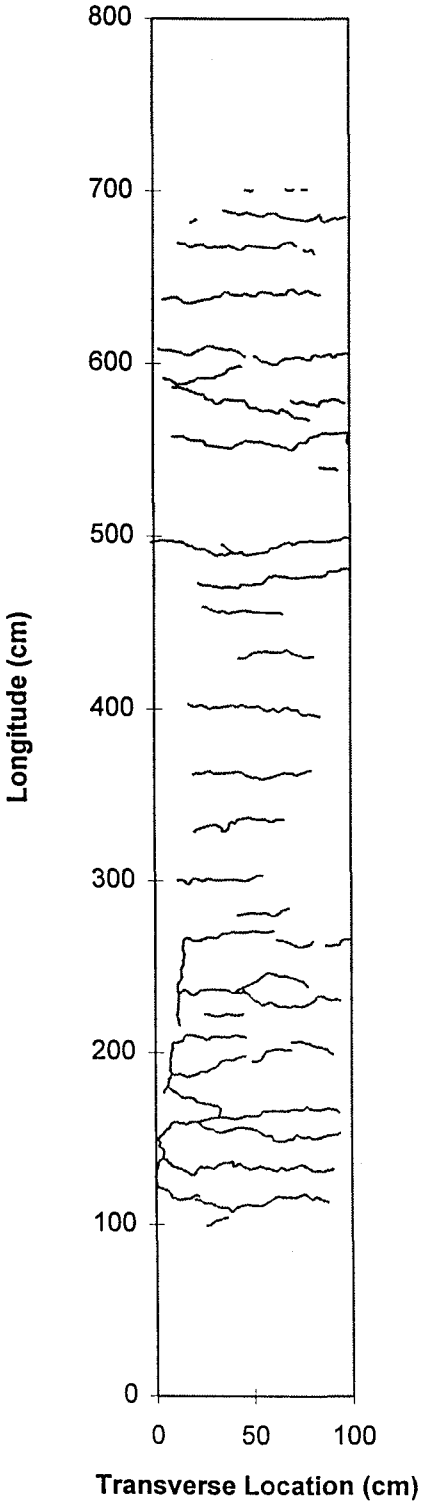

Figure 3.28 Schematic of cracking pattern at 998,000 repetitions

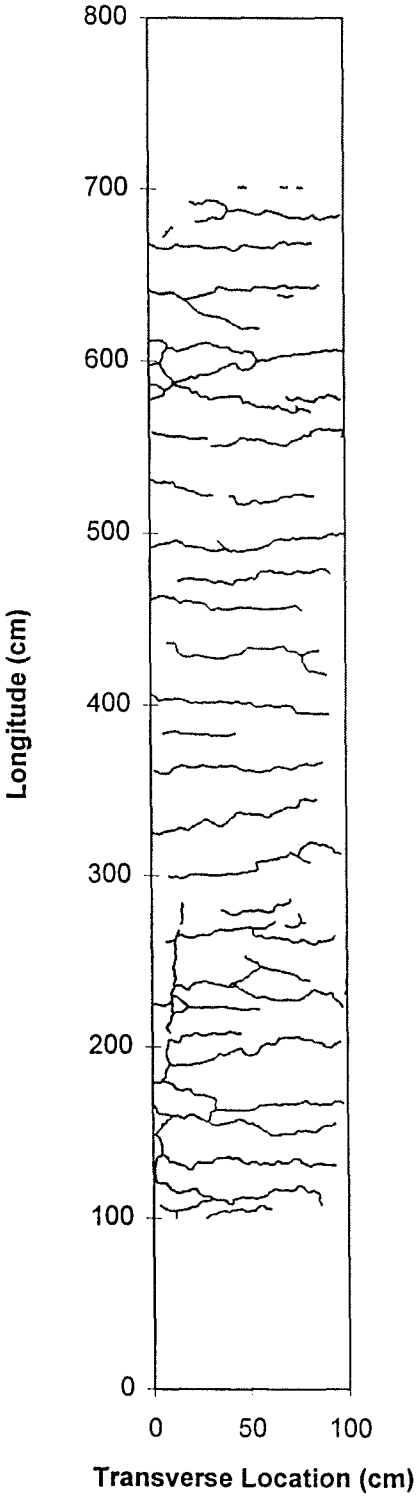

Figure 3.29 Schematic of cracking pattern at 1,390,000 repetitions

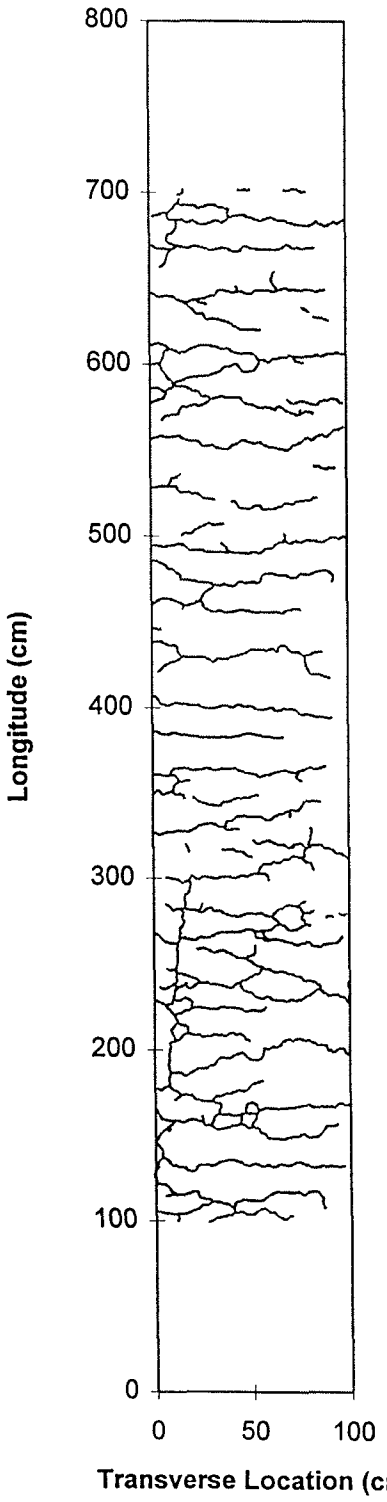

Figure 3.30 Schematic of cracking pattern at 1,910,000 repetitions

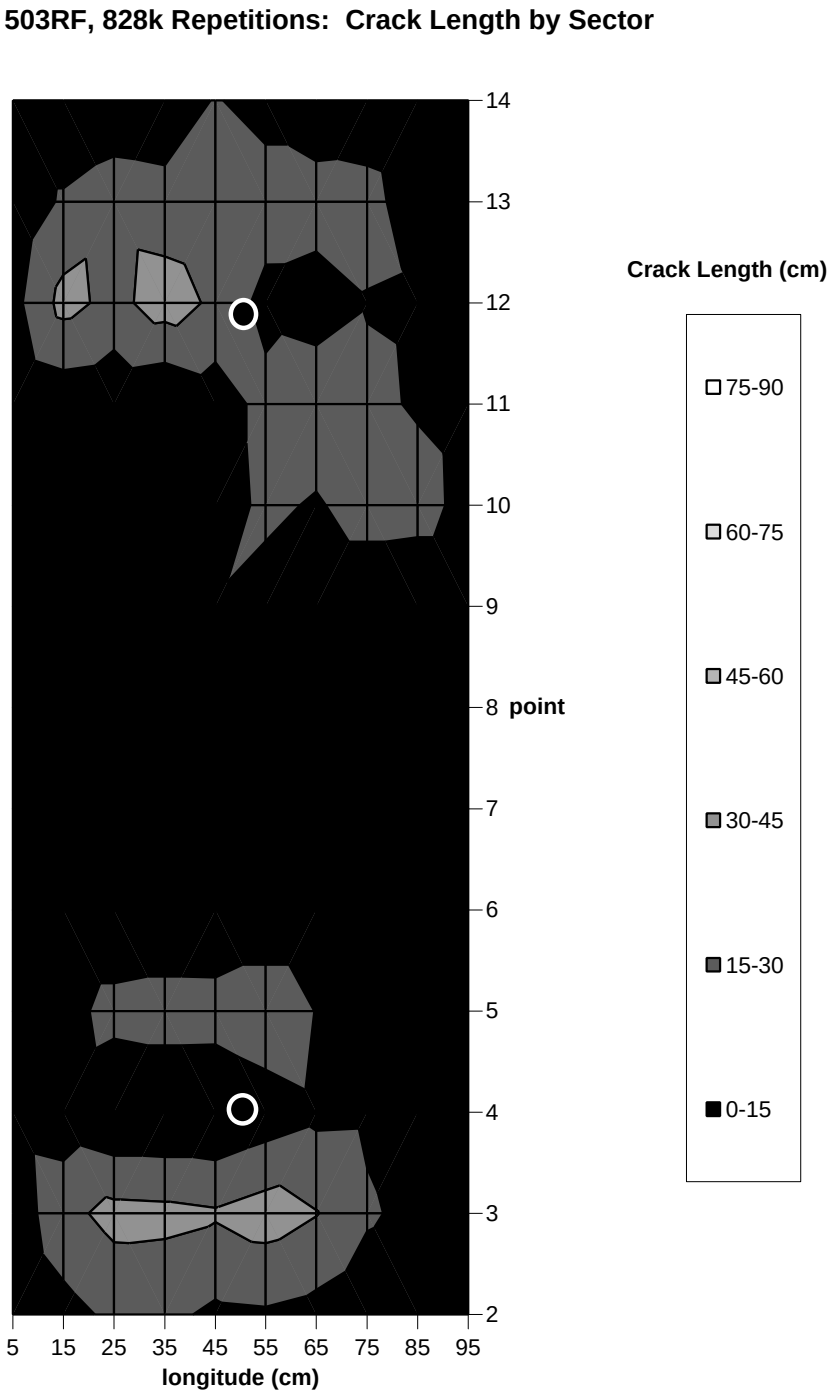

Figure 3.31 Crack length by sector at 828,000 repetitions

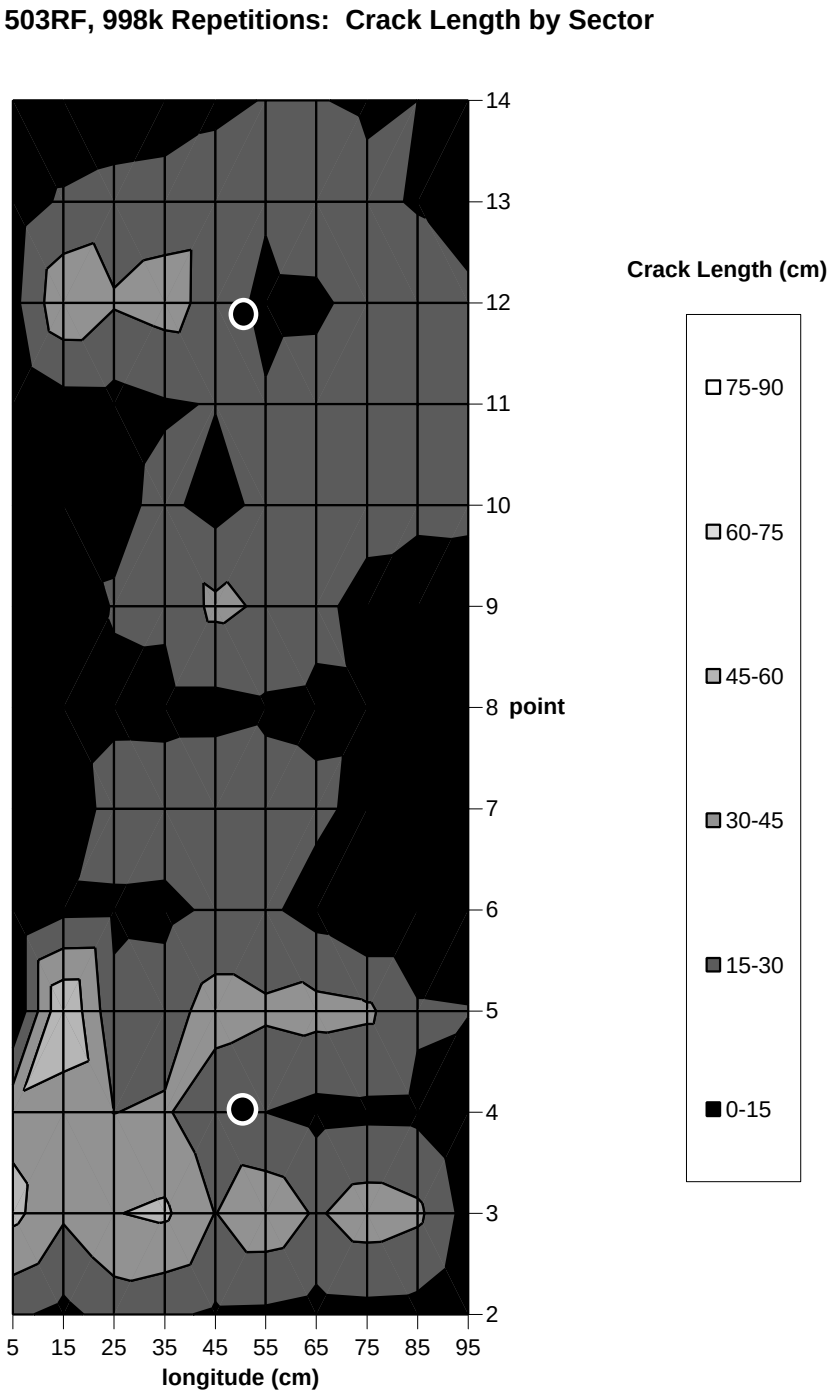

Figure 3.32 Crack length by sector at 998,000 repetitions

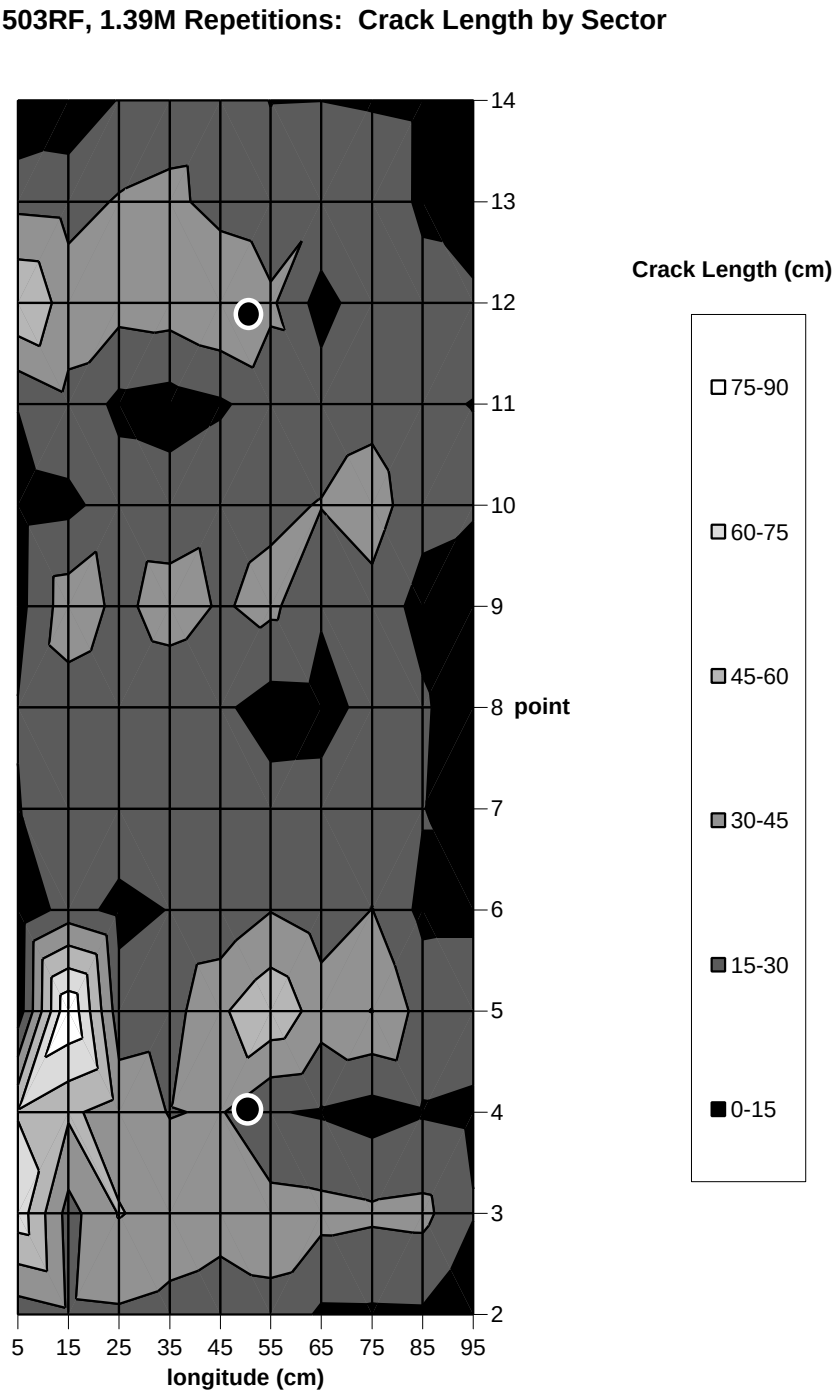

Figure 3.33 Crack length by sector at 1,390,000 repetitions

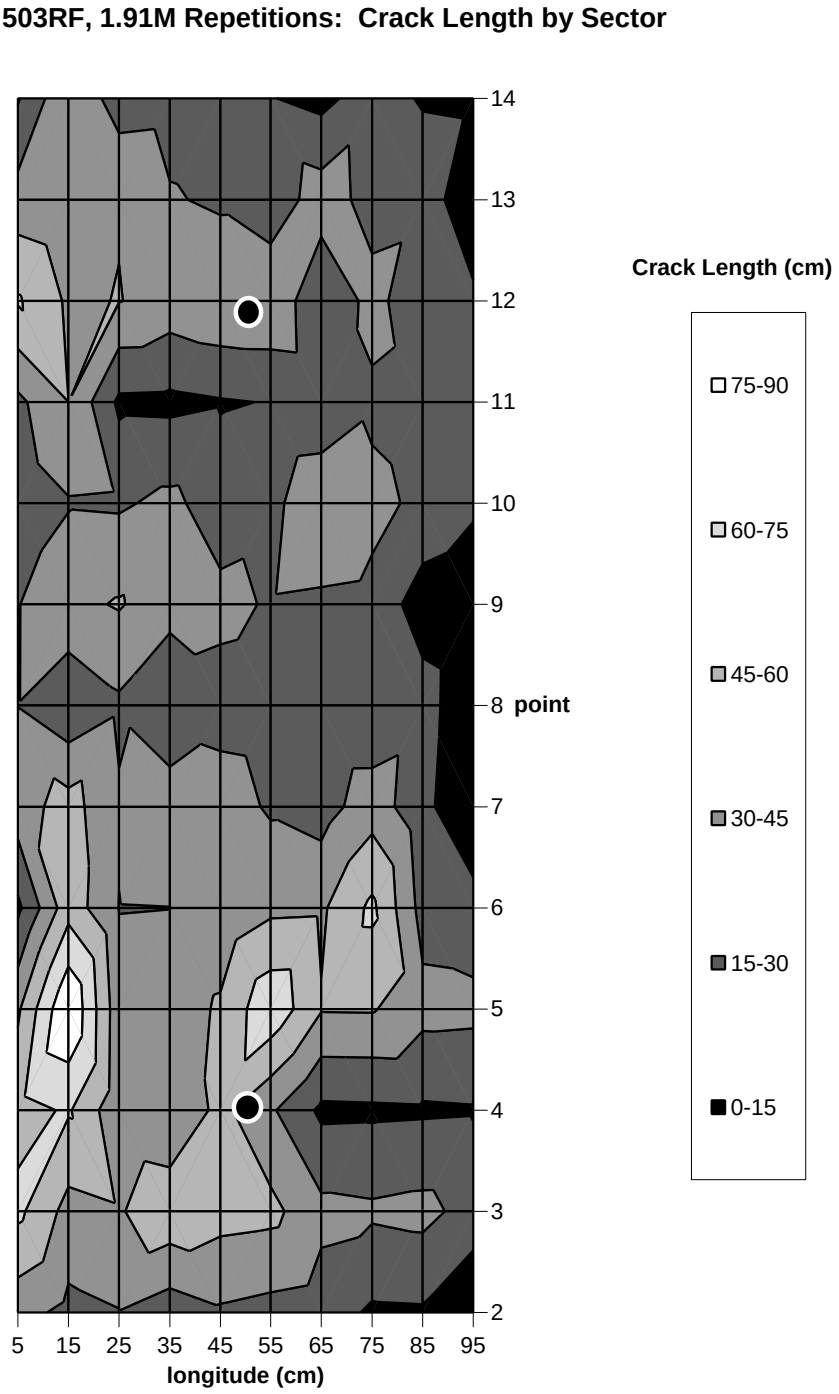

Figure 3.34 Crack length by sector at 1,910,000 repetitions

3.5.3 Cores from Section 503RF

Asphalt Concrete. It has been noted, from inspection of cores taken after construction for mix evaluation, that there appeared to be little or no bond between the two asphalt concrete lifts. No tack coat was placed between the lifts because it was not required by Caltrans specifications for the conditions experienced during construction, and therefore would not have been used in typical Caltrans practice. It is likely, however, that a tack coat would have contributed to an improved bond between the lifts.

After completion of the test, a few cores were taken from observed crack locations to determine whether both asphalt concrete lifts were cracked. It was evident that the cracks went completely through the top lift and there was no evidence of cracking in the bottom asphalt concrete lift. More cores will be necessary to fully assess the cracking condition of the pavement. However, further investigative coring is not possible until Goal 3 testing is completed.

As will be seen in Chapter 4, the absence of a tack coat and resultant weak bond between the two asphalt concrete lifts resulted in the critical horizontal tensile strain occurring at the bottom of the top asphalt concrete lift. As a result, crack formation probably started in this location rather than on the underside of the bottom asphalt concrete layer.

The fatigue resistance of the asphalt concrete is dependent, *inter alia*, on the air-voids content of the layer after construction. Determinations of these air-voids contents showed that the bottom lift had an average air-voids content of 6 percent while the top lift had an average air-void content of 7.7 percent. The improved compaction of the bottom lift resulted in that layer being more resistant to crack development than the top lift, where the cracks actually developed. In addition, since cracks developed in the top layer, the time necessary for

propagation to the surface was shorter than had cracks developed in the bottom layer; this would necessarily result in fewer repetitions associated with crack propagation.

Aggregate Base. It was observed that cores of the aggregate base taken outside the trafficked area at Point 5, Figure 3.12 in Section 503RF exhibited some degree of cementation. The cementation was sufficient to permit extracting a complete core from the aggregate base outside the test section using a wet coring drill. However, the two cores extracted from within the section did not exhibit cementation. The extent and influence of cementation, on Section 503RF can only be determined after Goal 3 testing is complete and a test pit is dug.

3.5.4 Comparison of Cracking for Sections 501RF and 503RF

Cracking initiated at approximately 550,000 repetitions for Section 501RF and at approximately 400,000 repetitions for Section 503RF. The crack lengths at the end of tests 501RF and 503RF were approximately 5600 cm and 3900 cm respectively, as shown on Figure 3.35. Section 503RF contained a thicker subbase; hence, the amount of fatigue cracking that developed throughout the test is less than for the thinner section, Section 501RF. The initial identification of cracking is fairly subjective, so cracks may go unnoticed when they first appear. This may explain why the cracks on Section 503RF were first observed sooner than these on Section 501RF, especially since the operators had more experience at the time of testing Section 503RF than at the time of testing Section 501RF.

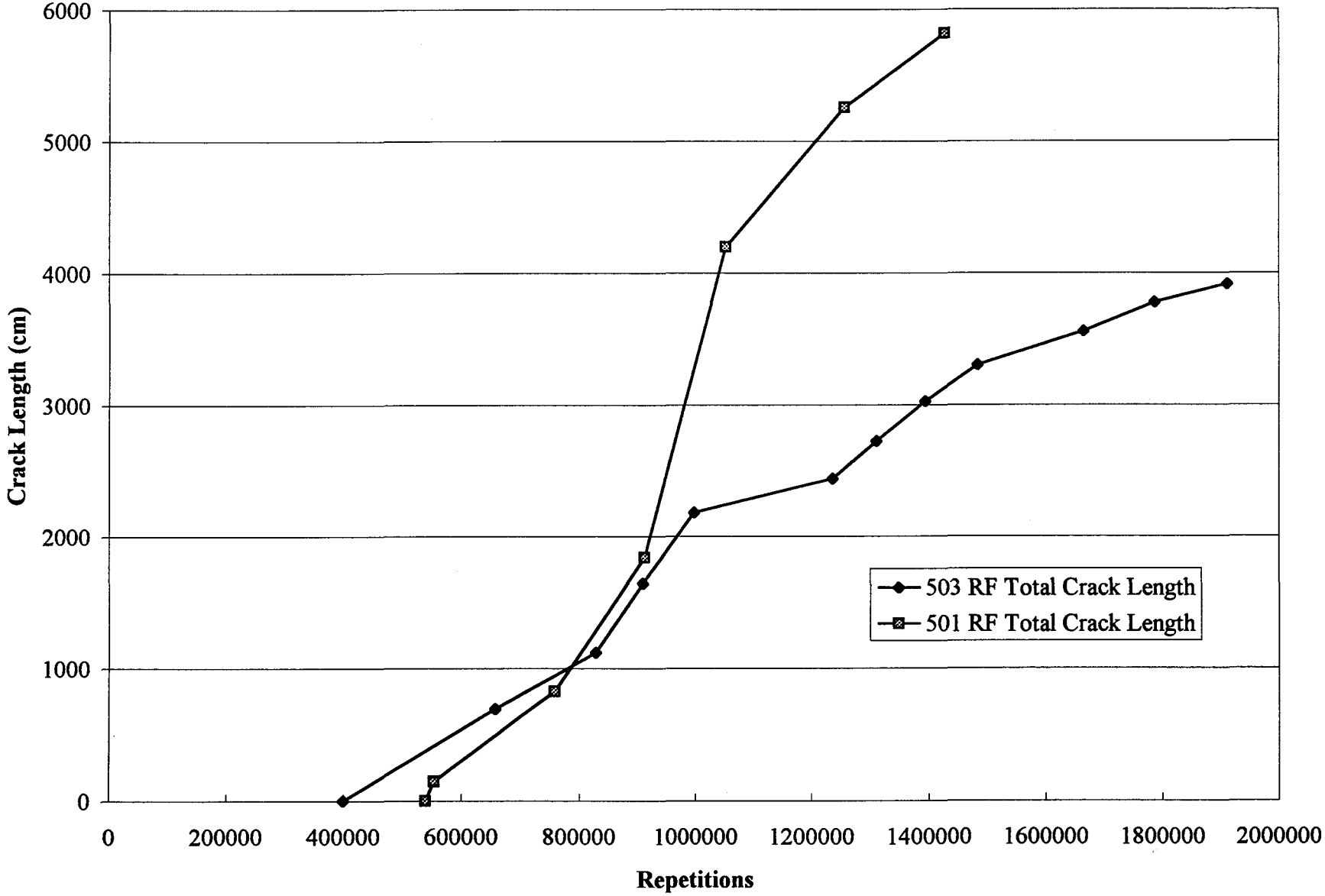

Figure 3.5 Comparison of initiation and development of cracks for Sections 501RF and 503RF

CHAPTER 4

SECTION 503RF PERFORMANCE EVALUATION

At the end of the accelerated pavement testing using the Heavy Vehicle Simulator (HVS), Section 503RF had been subjected to 150,000 applications of 40 kN loading, 50,000 applications of 80 kN loading, and 1,708,480 applications of 100 kN loading. Using an exponent of 4.2 in calculating load equivalency factors according to the Caltrans procedure[2], Section 503RF experienced approximately 81,000,000 ESALs during its useful life, much greater than its design life of approximately 1,000,000 ESALs. The primary purpose of this chapter is to investigate this large difference between the predicted Caltrans design loading and the performance of the test section.

As stated in the report of the test of Section 500RF *(3)*, the Caltrans flexible pavement design procedure does not identify and distinguish among various modes of pavement distress and does not enable detailed examination of many of the factors that can affect pavement performance. As a result, the methodology described for Section 500RF will be used to analyze Section 503RF since the predominant distress mode was surface cracking due to fatigue. The surface cracking was visible throughout the test section, averaging 6.5 m in length for each square meter of area.

Some surface rutting was also observed in Section 503RF. The average rut depth at the surface was approximately 7.9 mm. MDD measurements indicated that the asphalt concrete surface layers contributed approximately 48 percent to this average followed by 33 percent for the aggregate base, 17 percent for the subbase, and 2 percent for the subgrade. As was done for Sections 500RF and 501RF, an examination of rutting, as controlled by the elastic strain at

---

[2] Load equivalency factor = (wheel load in kN/40)$^{4.2}$.

the surface of the subgrade, has been made using the Asphalt Institute's subgrade strain criteria *(10)*.

4.1 FATIGUE ANALYSIS AND DESIGN SYSTEM

The fatigue analysis and design system used herein is the same as that used to analyze Sections 500RF *(3)* and 501RF *(4)*, and illustrated in Figure 4.1. It considers not only fundamental mix properties but also the level of design traffic, the temperature environment at the site, the pavement structural section, laboratory testing and construction variabilities, and the acceptable level of risk. It has the requisite capabilities for assessing the impact of the structural section on pavement performance in fatigue.

4.1.1 System Description

The fatigue analysis and design system is used herein to estimate the number of ESALs that can be sustained either in a design setting or in the HVS enclosure at the Richmond Field Station. The parameters used to determine ESALs have already been described *(3,9)*. The critical strain, determined using CIRCLY *(12)*, permitted determination of the shift factor, *SF*, according to the equation (Figure 4.1).

$$SF = 3.1833 \times 10^{-5}\varepsilon^{-1.3759}$$

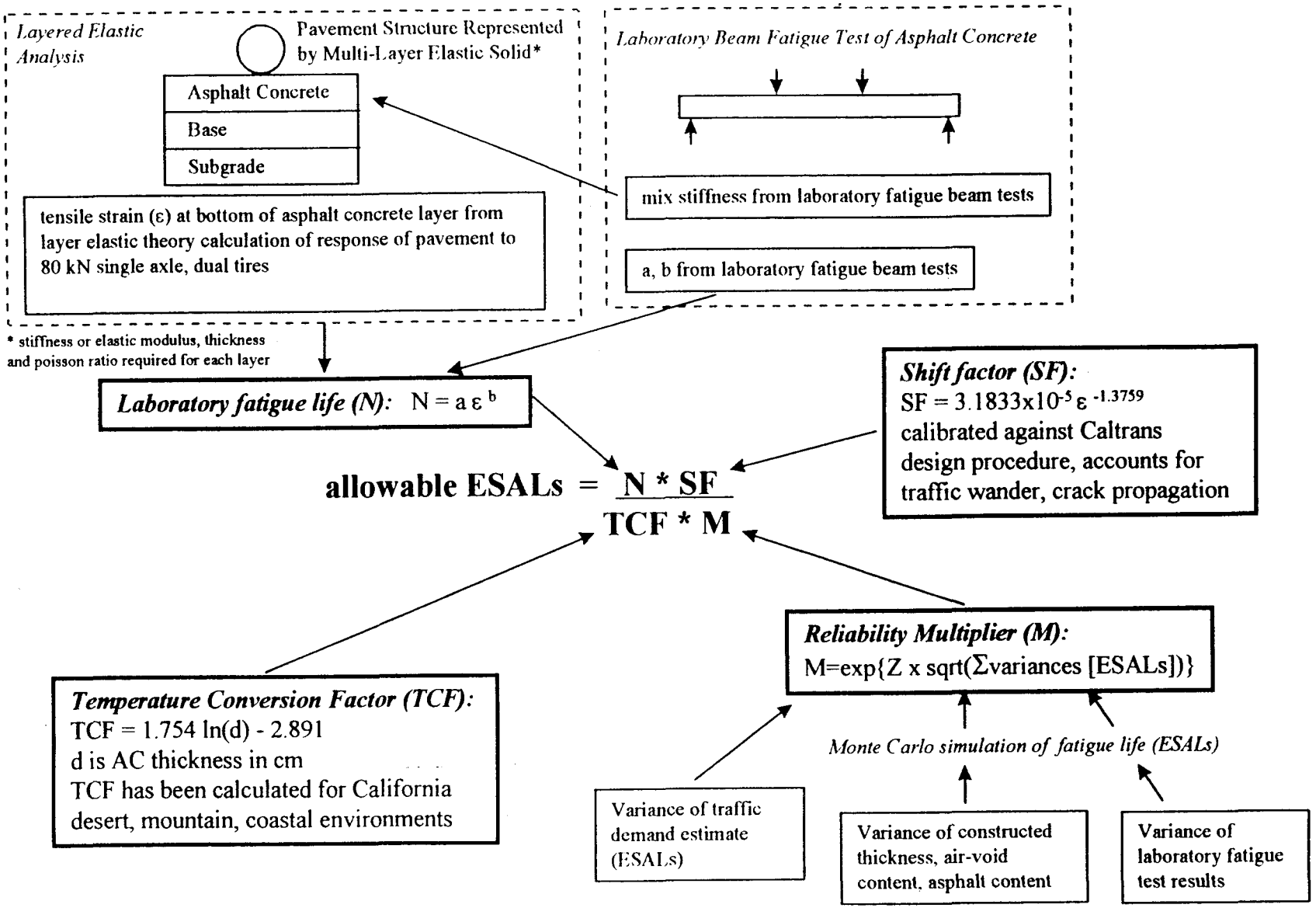

Figure 4.1 Methodology followed in the fatigue analysis system to determine ESALs

The temperature conversion factor, *TCF*, used for in-situ performance simulations is that derived earlier for a California coastal environment *(9)* (Figure 4.1):

$$TCF = 1.754\ln(d) - 2891$$

The reliability multiplier, *M*, is determined from the expression (Figure 4.1):

$$M = e^{z\sqrt{var(lnN) + var(lnESALs)}}$$

In this expression, the factor *Z* varies from 0 at a design reliability of 50 percent to 2.05 at a design reliability of 98 percent *(9)*.

The variance in the logarithm of the laboratory fatigue life, var(ln N), has been calculated using a Monte Carlo simulation procedure. This procedure accounts for the inherent variability in fatigue measurements; the nature of the laboratory testing program (principally the number of test specimens and the strain levels); the extent of extrapolation necessary for estimating fatigue life at the design, in-situ strain level; mix variability due to construction (namely asphalt and air-void contents); and structural variability due to construction (namely thickness of the asphalt concrete surface and the equivalent stiffness or modulus of supporting layers). Variances for these parameters considered representative of prevailing California construction practice have been used herein *(13)*. A var(ln ESALs) of 0.3, the variance associated with uncertainty in the traffic estimate, has also been used in the calculations.

4.1.2 Important Differences Between Pavement Design and HVS Testing

As with Sections 500RF and 501RF, some of the important factors that help to explain the difference between the Caltrans design estimate of approximately 1,000,000 ESALs and the HVS measurement of approximately 81,000,000 ESALs are considered in this analysis. The unknown error that results from assuming that the Caltrans design estimate is dictated

primarily by the prevention of premature fatigue cracking and not other distress modes is recognized at the outset.

One fundamental difference between a pavement design estimate and the corresponding test measurement is that the design must accommodate a range of mixes of varying performance characteristics and must incorporate a safety factor to prevent premature failure as a result of testing, construction, and traffic variability. A direct measurement in the HVS test, on the other hand, reflects the performance characteristics of a specific mix; is independent of laboratory testing and traffic variability; and, because the test section is limited to a relatively small area, 1 m×8 m in plan, the influence of construction variability is minimal. The design estimate is always expected to be much smaller in magnitude than the test measurement, with the difference between the two increasing as the design reliability increases. The fatigue design and analysis system has the ability to distinguish between design estimates and test measurements and to assess the impact of reliability on design estimates. No reliability factor is associated with simulations of HVS test ESALs for the reasons described above.

The next type of difference between design and testing relates primarily to pavement structural effects. In the current case, four notable differences distinguished Section 503RF from its design scenario including (1) a top asphalt concrete lift thickness of 74 mm instead of 61 mm, (2) a bottom asphalt concrete lift thickness of 88 mm instead of 76 mm, (3) a thickness of subbase of 305 mm instead of 229 mm, and (4) a largely unbonded interface between the lifts instead of a fully bonded one *(2)*.

Important differences are also found between the standard mix used for calibrating the fatigue analysis and design system and that used in HVS Section 501RF. Asphalt and air-void contents for the standard mix were set at 5 and 8 percent, respectively representing the approximate asphalt content found from the Caltrans mix design procedure and relative

compaction relative to laboratory test maximum density (LTMD) of about 95.8 percent. The asphalt content for the mix used in Section 501RF averaged 4.8 percent, also based on the Caltrans procedure. Air-void contents averaged 4.8 percent in the upper lift and 4.4 percent in the lower lift corresponding to about 99.2 percent and 99.6 percent relative compaction respectively for mix.

In addition to differences in degree of compaction, there were other differences between the standard mix and the mix used in the HVS test section. that is:

1. The aggregates for the two mixes came from different sources and did not have the exactly same gradations, although both constructed gradations met Caltrans' standard specifications for 19 mm coarse Type A mixes;
2. The asphalt binders in both mixes were identified as being from California Valley sources and exhibited similar rheological and aging behavior in laboratory tests performed at TransLab *(14)*; however, the binders were produced 6 years apart and not necessarily at the same refinery or using the same processes; and
3. Laboratory test results for the mix from the HVS test were obtained from beams cut from the test pavement soon after construction, while laboratory test results for the standard mix were obtained from laboratory mixed and compacted specimens.

In all likelihood, however, specimen compaction is not a source of the differences; an earlier comparison of laboratory test results on beams sawed from the test pavement and obtained by laboratory rolling wheel compaction exhibited little difference in stiffness and fatigue properties *(2)*. Moreover large differences in mix properties caused by laboratory mixing and short-term oven aging (STOA) versus plant mixing are also considered unlikely at

this time although they have only been evaluated in terms of mix and binder stiffness and not in terms of fatigue properties. More data will be obtained from future CAL/APT test pavements as well as from other studies such as WesTrack *(11)* to compare differences in fatigue properties between laboratory mixed and plant–mixed, laboratory compacted specimens.

As reported elsewhere *(3)*, laboratory testing of the standard mix yielded the following expressions:

$$\ln N = -22.0012 - 0.164566AV + 0.575199AC - 3.71763 \ln \varepsilon$$

and

$$\ln S = 10.282 - 0.076AV - 0.172AC$$

where N = laboratory fatigue life in a third-point loading controlled-strain flexural test,

AV = air-void content in percent,

AC = asphalt content in percent,

ε = tensile strain, and

S = laboratory flexural stiffness in MPa.

For the HVS mix *(2)*, the following expressions were obtained at the 4.8 percent asphalt content:

$$\ln N = -21.9252 - 0.106663AV - 4.14248 \ln \varepsilon$$

and

$$\ln S = 9.5603 - 0.084914AV$$

where S is again expressed in MPa.

Based on these results, the laboratory determined fatigue life of the HVS mix is two to eight times that of the standard mix, depending on strain level, while its stiffness is only 1 to

8 percent larger. Thus, the HVS mix is expected to exhibit improved performance over the standard mix.

These results emphasize the importance of laboratory fatigue testing to assess fatigue performance to insure a realistic estimate of pavement performance and in particular, in insuring proper interpretation of the HVS test results.

Environmental differences also distinguish the HVS test conditions from specific field pavement sites. These include the effects of temperature and moisture differences.

In the 500RF report *(3)*, for example, it was demonstrated that during the period of the test (May to November 1995), the temperature environment of the HVS was slightly more severe than the coastal environment, i.e. the predicted ESALs for the HVS site were about 85 percent of the number that could be sustained in situ.

The second major environmental difference is due to the effects of moisture. The protected HVS environment limits the amount of moisture in the pavement and practically eliminates cyclic wetting and drying. The net effect is expected to be beneficial. Moisture effects are simulated in this analysis by assuming that effective moduli of all supporting layers (aggregate base, aggregate subbase, and subgrade) under in-service conditions are 80 percent of those in Section 501RF. It must be emphasized, as stated in the earlier reports, that the 80 percent is an assumed quantity.

Quantification of the effects of these differences, using the fatigue analysis and design system, is described in the next section.

4.1.3 General Performance Analysis

For this analysis, the computer code, CIRCLY, was used in computing critical strain levels. The applied load consisted of a 40-kN (9,000-pound) wheel load distributed on dual

tires (305 mm [12.0 inches] center-to-center) with a contact pressure of 690 kPa (100 psi). A distinction was made between Section 503RF *design conditions* and the as-built and as-tested *HVS conditions* with respect to layer thicknesses and environmental influences. Quantitatively the differences are as follows, Table 4.1.

Table 4.1 Comparison of Section 501RF design conditions and HVS conditions

	Design conditions	HVS conditions
Thickness of upper asphalt concrete lift (mm)	61	74
Thickness of lower asphalt concrete lift (mm)	76	88
Thickness of aggregate subbase (mm)	229	305
Moduli of supporting layers (MPa) Aggregate Base Aggregate Subbase Subgrade	 240 120 56	 300 150 70

Further distinction was made between a *standard mix* and the *HVS mix*. The standard mix was that used in calibrating the fatigue analysis and design system. Components included a Watsonville granite and an AR-4000, apparently from California Valley sources. Asphalt and air-voids contents were assumed to be 5 and 8 percent respectively. The HVS test utilized a different aggregate but the grading was similar to that of the standard mix; both gradings conformed to the Caltrans specifications for the Type A, 19-mm-maximum size, coarse gradation. The asphalt was an AR-4000 from California Valley sources, and the asphalt content of the mix was 4.8 percent. Air-voids contents averaged 4.8 percent in the upper lift and 4.4 percent in the lower lift.

For the General Performance Analysis, a constant temperature of 20°C was assumed for both design conditions and HVS conditions. This assumption results in a TCF of 1.00 because the laboratory test temperature is 20°C. A preliminary comparison of the temperature

environments at the HVS site and for the California Coastal environment is included in this chapter.

Five different cases, defined as follows, were analyzed as shown in Table 4.2:

Table 4.2 Definition of five cases

Case	Description	Critical strain location
1	Design conditions with standard mix (8% air-voids content and 5% asphalt content); full friction interface	Bottom of lower lift
2	HVS conditions with standard mix (8% air-voids content and 5% asphalt content); full friction interface	Bottom of lower lift
3	HVS conditions with standard mix (4.4% air-voids content bottom lift, 4.8% air-voids content top lift and 5% asphalt content); full friction interface	Bottom of lower lift
4	HVS conditions with HVS mix (4.4% air-voids content bottom lift, 4.8% air-voids content top lift and 4.8% asphalt content); full friction interface	Bottom of lower lift
5	HVS conditions with HVS mix (4.4% air-voids content bottom lift, 4.8% air-voids content top lift and 4.8% asphalt content); frictionless interface	Bottom of upper lift

Elastic parameters used in the CIRCLY computations are identified in Table 4.3. These represent the best estimates of the stiffnesses of the pavement components based on laboratory determined and in-situ measured response characteristics, the latter having been computed from FWD measurements *(2)*.

Table 4.3 Elastic parameters for CIRCLY analyses

Layer	Case				
	1	2	3	4	5
Modulus (MPa)					
Upper Asphalt Concrete lift	6,729	6,729	8,575	9,440	9,440
Lower Asphalt Concrete lift	6,729	6,729	8,839	9,766	9,766
Aggregate Base	240	300	300	300	300
Aggregate Subbase	120	150	150	150	150
Subgrade	56	70	70	70	70
Poisson's ratio					
Upper Asphalt Concrete lift	0.35	0.35	0.35	0.35	0.35
Lower Asphalt Concrete lift	0.35	0.35	0.35	0.35	0.35
Aggregate Base	0.35	0.35	0.35	0.35	0.35
Aggregate Subbase	0.35	0.35	0.35	0.35	0.35
Subgrade	0.45	0.45	0.45	0.45	0.45
Thickness (mm)					
Upper Asphalt Concrete lift	61	74	74	74	74
Lower Asphalt Concrete lift	76	88	88	88	88
Aggregate Base	274	274	274	274	274
Aggregate Subbase	229	305	305	305	305
Subgrade	Semi-infinite	Semi-infinite	Semi-infinite	Semi-infinite	Semi-infinite

The first matter to be addressed includes both the effect of reliability on estimates of design ESALs as well as the fundamental difference between design ESALs (whether from the Caltrans or the UCB procedures described in Reference *13*),and HVS ESALs (whether measured under HVS loading or simulated using the UCB system). In computing HVS

ESALs, variances of the several parameters (asphalt content, air-void content, asphalt concrete thickness, foundation support, and traffic) were assumed to be negligible. Computations using the UCB system for Case 1 conditions yielded the following ESAL estimates:

Table 4.4 Simulated HVS ESALs for Case 1

Simulated HVS ESALs	UCB Design ESALs for reliability of:			
	80%	90%	95%	98%
2,446,000	1,030,000	656,000	453,000	297,000

This table shows the influence of reliability on design ESALs; the 2,446,000 simulated HVS ESALs is considerably greater than any of the design ESALs. For a design reliability level of 90 percent, the computed ratio of simulated HVS ESALs to UCB design ESALs is approximately 3.7.

The 90 percent design reliability estimate, assuming a constant 20°C asphalt concrete temperature, is 656,000 ESALs, less than the Caltrans design estimate of 1,000,000 ESALs. The UCB fatigue analysis and design system estimate of 1,030,000 ESALs at 80 percent reliability is nearly the same as the Caltrans design estimate, again assuming a 20°C asphalt concrete temperature. The preliminary UCB design estimates for the California coastal environment are presented later in this chapter.

Next, in order to demonstrate the significant difference between as-built and as-tested HVS conditions and the assumed Caltrans design conditions, the simulated HVS ESALs estimate for Case 2 was compared with that for Case 1. Results are in Table 4.5:

Table 4.5 Comparison of simulated HVS ESALs—Case 1 to Case 2

Simulated HVS ESALs for:	
Case 1	Case 2
Design conditions with standard mix (8% air-voids content and 5% asphalt content): full friction interface	HVS conditions with standard mix (8% air-voids content and 5% asphalt content): full friction interface
2,446,000	8,627,000

The ratio of HVS ESALs for HVS conditions to that for design conditions is approximately 3.5. The enhanced simulated performance for the HVS environment stems from a combination of thickness differences and the effect of moisture.

To demonstrate the effect of the excellent mix compaction achieved in the construction of Section 503RF, the simulated HVS ESALs estimate for Case 3 was compared with that for Case 2, Table 4.6:

Table 4.6 Comparison of simulated HVS ESALs—Case 2 to Case 3

Simulated HVS ESALs for:	
Case 2	Case 3
HVS conditions with standard mix (8% air-voids content and 5% asphalt content): full friction interface	HVS conditions with standard mix (4.4% air-voids content bottom lift, 4.8% air-voids content top lift and 5% asphalt content): full friction interface
8,627,000	39,193,000

The very significant effect of air-voids content is illustrated by a ratio of approximately 4.2 in the HVS ESALs estimate for an air-voids content of 4.4 percent in the bottom lift and 4.8 percent in the top lift compared an 8-percent air-voids content in both lifts. This finding further emphasizes the importance of good construction practice and the potential impact of improved compaction above that required in current Caltrans specifications, as stated in earlier Goal 1 reports *(9,13)*.

To demonstrate the effect of the superior fatigue performance of the HVS mix compared to the standard mix, the simulated HVS ESALs estimate for Case 4 was compared with that for Case 3. Results are in Table 4.7:

Table 4.7 Comparison of simulated HVS ESALs—Case 3 to Case 4

Simulated HVS ESALs for:	
Case 3	Case 4
HVS conditions with standard mix (4.4% air-voids content bottom lift, 4.8% air-voids content top lift and 5% asphalt content): full friction interface	HVS conditions with HVS mix (4.4% air-voids content bottom lift, 4.8% air-voids content top lift and 4.8% asphalt content): full friction interface
36,193,000	216,329,000

The ratio of simulated HVS ESALs for these two conditions is approximately 6.0. This large difference is not clearly attributable to any one particular component of the two mixes, and is likely due to a combination of potential differences in components including asphalt production and aggregate type and gradation.

It should be noted that the simulated HVS ESALs for Case 4 (216,329,000) exceeds the measured number of 81,000,000 HVS ESALs (assuming a 4.2 exponent for load equivalency). A part of this difference may well be due to imprecision of the fatigue analysis and design system, to inappropriate assumptions made for this analysis, and/or to important factors not yet identified and accounted for.

One such factor relates to the lack of bonding at the interface between upper and lower asphalt concrete lifts. CIRCLY allows an examination of the interface condition but, unfortunately, only at the two extremes, full-friction and frictionless interfaces. The interface condition of Section 503RF is likely somewhere between these two extremes: the interface is rough (but unbounded) and the weight of the upper layer combined with vertical compressive

stress beneath the load should allow some transfer of stress across the surface. Even though partial friction conditions cannot be modeled with available techniques, the notable effect of interface condition can be demonstrated by comparing the HVS ESALs estimate for Case 5 with that for Case 4. Results are shown in Table 4.8:

Table 4.8 Comparison of simulated HVS ESALs—Case 4 to Case 5

Simulated HVS ESALs for:	
Case 4	Case 5
HVS conditions with HVS mix (4.4% air-voids content bottom lift, 4.8% air-voids content top lift, and 4.8% asphalt content): full friction interface	HVS conditions with HVS mix (4.4% air-voids content bottom lift, 4.8% air-voids content top lift, and 4.8% asphalt content): frictionless interface
216,329,000	17,134,000

This remarkably large effect is due to two factors, one of which is the nature of friction at the interface between lifts. The other results from a shift in the critical strain location from the bottom of the lower lift for the full friction interface to the bottom of the upper lift for the frictionless interface. In the upper lift, the load repetitions necessary to propagate cracks to the top surface are expected to be smaller because of the reduced thickness through which the cracks must propogate. The combined effect of a somewhat larger air-voids content and a reduced thickness results in a significant decrease in simulated fatigue life.

Although this analysis is not definitive because the interface condition cannot be accurately modeled, the measurement of 60,000,000 ESALs under HVS loading is between the 17,134,000 ESALs determined for Case 5 (no friction) and the 216,329,000 ESALs for Case 4 (full friction). That cracking would occur in the upper lift before it occurred in the lower lift for the frictionless interface condition corroborates the cracking observations from the Section 503RF cores. Thus, analysis reported herein is of significant help in reconciling the

difference between the Caltrans design estimate of 1,000,000 ESALs and the HVS test measurement of 81,000,000 ESALs. As with Sections 500RF and 501RF, the analysis has highlighted the effects of air-void content and interface condition on pavement performance.

4.1.4 Preliminary Estimate of Design ESALs for California Coastal Environment

In the 500RF report *(3)* pavement performance in the HVS test was observed during the period May to November 1995. By comparing the performance with that for comparable periods of time in three regions of California for which Temperature Conversion Factors (TCF) had been determined *(9)*, it was demonstrated that the test conducted at the HVS site was more damaging than for comparable traffic conditions at the three in-service sites.

For this report, it was decided to examine an alternative approach and compare, across the entire year, the performance of the pavement at a constant temperature of 20°C at the HVS site with the variable temperature regime for the California Coastal environment. For Case 1 of the General Performance Analysis (standard mix, design conditions, 8 percent air-voids content, 5 percent asphalt content) the TCF computed for the California Coastal environment is 1.702. Assuming that the mix used to develop temperature conversion factors *(8,9)* has a temperature susceptibility similar to that of the standard mix, application of the 503RF TCF to Case 1 of the General Performance Analysis results in the following estimates shown in Table 4.9.

Table 4.9 Estimates of design ESALs applying 503RF TCF to Case 1

Simulated HVS ESALs	UCB Design ESALs for reliabilities of:			
	80%	90%	95%	98%
1,437,000	605,386	386,000	266,000	175,000

It can be seen for this assumption that the estimated fatigue life for the 90 percent reliability is considerably less than the Caltrans design estimate of 1,000,000 ESALs. The estimated reliability of the Case 1 pavement is 64 percent, indicating a 36 percent probability that the pavement would fail in fatigue cracking before carrying 1,000,000 ESALs. These are the same results obtained for Section 501RF which had the same design structure for Case 1. The same analysis applied to Section 500RF indicated a higher level of reliability, i.e. about 90 percent for 1,000,000 ESALs.

4.2 RUTTING CONSIDERATIONS

The Caltrans pavement design procedure is intended to prevent premature failure from rutting due to permanent deformation in the unbound materials as well as fatigue cracking. The average rut depth at the surface of Section 503RF at the termination of HVS trafficking was approximately 7.9 mm. MDD measurements indicated that about 50 percent, or 4.0 mm, occurred in the base and subbase layers, and about 2 percent, or 0.2 mm, occurred in the subgrade. A comprehensive procedure for evaluating the potential for rutting in the underlying layers including reliability (like that for fatigue) has not been developed as yet. However, an evaluation of the Section 503RF pavement with respect to rutting in the underlying layers was performed by determining the vertical compressive strain at the surface of the subgrade and comparing the computed value with Asphalt Institute criteria *(10)*. This rutting evaluation was performed for the five cases of mix type, site conditions, and construction included in the fatigue evaluation.

4.2.1 Subgrade Strain Criteria

The Asphalt Institute criterion for subgrade strain is *(10)*:

$$N = 1.05 \bullet 10^{-9} \varepsilon_c^{-4.484}$$

where N = number of load applications, and

ε_c = vertical compressive strain at subgrade surface.

This equation resulted from a series of analyses of pavements designed according to the Caltrans design procedure *(15)*. It has been stated that by using this subgrade strain relation: "*if good compaction of the pavement components is obtained and the asphalt mix is well designed, rutting should not exceed about 12.7 mm (0.5 in.) at the surface for the design traffic, N*" *(10)*. The statement implies some conservatism in the criteria; however it does not include an explicit factor of safety or reliability estimate.

4.2.2 Performance Analyses Considering Subgrade Strain

The vertical compressive strain at the top of the subgrade was calculated using the program CIRCLY, for the 40 kN (9,000 lb) dual tire wheel load (305 mm [12.0 in.] center-to-center) and 690 kPa (100 psi) contact pressure, and the pavement structures shown earlier. The difference in thermal environment between the design conditions and HVS conditions was not addressed in this study. The asphalt concrete stiffness at 20°C was used for the subgrade strain computations since this was about the temperature maintained at the surface of the Section 503RF pavement. A temperature sensitivity study of the type used to estimate the effects on fatigue life of in-situ temperatures for typical California environments has not been performed using the subgrade strain criteria.

The permissible ESALs for the calculated subgrade strain for each of the five cases are compared with the simulated HVS ESALs to fatigue failure in Table 4.10.

Table 4.10 Comparison of permissible ESALs for subgrade strain to simulate HVS ESALs to fatigue failure for five cases

Case	Permissible ESALs by Asphalt Institute Subgrade Strain Criteria	Simulated HVS ESALs to Fatigue Failure
Design conditions with standard mix (8% air-voids content and 5% asphalt content), full friction interface (Case 1)	14,614,000	2,446,000
HVS conditions with standard mix (8% air-voids content and 5% asphalt content), full friction interface (Case 2)	107,568,000	8,627,000
HVS conditions with standard mix (4.4% air-voids content bottom lift, 4.8% air-voids content top lift and 5% asphalt content), full friction interface (Case 3)	146,129,000	36,193,000
HVS conditions with HVS mix (4.4% air-voids content bottom lift, 4.8% air-voids content top lift and 5% asphalt content), full friction interface (Case 4)	165,990,000	216,329,000
HVS conditions with HVS mix (4.4% air-voids content bottom lift, 4.8% air-voids content top lift and 5% asphalt content), frictionless interface (Case 5)	28,698,000	17,134,000

The permissible ESALs based on subgrade strain for Case 1 are almost six times greater than the simulated HVS ESALs to fatigue cracking for the same case. This indicates that fatigue cracking is probably the dominant failure mode for Section 503RF for the design conditions and standard mix, the most critical case when a full friction interface between the asphalt concrete layers is assumed.

Comparison of the permissible ESALS for Cases 1 and 2 indicates that the HVS conditions were less critical than the design conditions considering subgrade strain. The differences between the HVS and design conditions for the subgrade strain criteria evaluation consisted of the thicker asphalt concrete layer, thicker aggregate subbase layer, and increased base, subbase and subgrade moduli of the HVS conditions. As for Case 1, fatigue appears to be the dominant failure mode for Case 2, since the permissible ESALs for subgrade strain are approximately 12.5 times greater than the simulated HVS ESALs to fatigue failure.

The beneficial effect of increased compaction of the asphalt concrete on subgrade strain can be seen from comparison of the results for Case 3 versus Case 2. Reduction of the air-voids content in the standard mix from 8 percent to the air-voids contents obtained in the Section 503RF pavement increases the permissible ESALs for the subgrade strain condition by about 36 percent. The increase is the result of the greater protection provided to the subgrade by the increased stiffness of the asphalt concrete at the smaller air-voids contents.

Comparison of Case 4 with Case 3 shows that substitution of the HVS mix for the standard mix results in a further 14 percent increase in permissible ESALs based on subgrade strain, due to the larger stiffness of the HVS mix. Despite this increase in permissible ESALs, the ESALs associated with fatigue cracking exceed those defined by subgrade strain due to the large difference in fatigue resistance between the HVS mix and the standard mix.

Simulation of a frictionless interface between the two asphalt concrete layers results in a significant reduction in the estimate of permissible ESALs based on subgrade strain, as can be seen from comparison of Case 5 with Case 4. The permissible ESALs for the frictionless interface condition are about 5.8 times less than for the full friction condition. The difference is due to reduction of the ability of the pavement to distribute stresses within the asphalt concrete layer because of the frictionless interface, resulting in increased vertical compressive strain in all underlying layers. The actual interface condition likely lies in between the simulated full friction and frictionless cases; however, the estimates of permissible ESALs indicate that a reduction in the bonding between the asphalt concrete layers results in increased compressive strains in the underlying layers (and thus potential for increased rutting), as well as reduced asphalt concrete fatigue life.

For all cases except Case 4, the simulated HVS ESALs for fatigue failure are less than the permissible ESALs based on the Asphalt Institute criteria for subgrade strain. This

suggests that fatigue should be the dominant distress mode for Section 503RF. This is supported by the fact that the section carried 81,000,000 HVS ESALs with an average rut depth in the combined base, subbase and subgrade layers of only 4.1 mm (0.16 in.), and an average maximum rut depth in the combined untreated layers of 5.6 mm (0.22 in.). The remainder of the rutting in Section 503RF occurred in the asphalt concrete layers (about 50 percent).

Like the fatigue analyses, these results emphasize that air-voids content of the asphalt concrete surface and the interface condition between asphalt concrete layers can significantly impact surface rutting resulting from permanent deformations in the unbound portions of the pavement.

4.3 PERFORMANCE ANALYSIS COMPARISON WITH SECTION 501RF

The pavement structures and materials of Section 501RF and 503RF were the same except for differences in the thicknesses and degrees of compaction of the asphalt concrete layers and subbase thicknesses. The performance of the two sections differed, despite identical HVS traffic loading and nearly identical pavement temperatures (Table 3.3). The independent effects on simulated performance in fatigue and rutting resulting from differences in asphalt concrete thickness and degree of compaction and subbase thickness were evaluated to provide a relative indication of the importance of these variables in obtaining improved pavement performance.

4.3.1 Summary of 501RF and 503RF Performance and Structural Differences

4.3.1.1 Structural Differences. Subgrade moduli back-calculated from Falling Weight Deflectometer (FWD) deflections indicated that the subgrade stiffness in Sections

501RF and 503RF were similar, although the south end of Section 503RF may have been somewhat stiffer than the rest of that section and most of Section 501RF (Figure 4.21 of Reference *2*). The back-calculated moduli for the combined base/subbase layers for both sections were nearly identical (Figure 4.20 of Reference *2*). The pavement structural models for Sections 503RF and 501RF used the same stiffnesses for the subgrade, base and subbase layers, based on the back-calculated moduli and triaxial resilient modulus tests performed on the three materials *(2,3)*.

The back-calculated moduli for the asphalt concrete were considerably smaller for Section 501RF than for 503RF (Figure 4.19 of Reference *2*). The differences in asphalt concrete modulus may be a result of the lower air-voids contents measured on cores from Section 503RF, and show a similar trend regarding the effects of compaction on the asphalt concrete stiffness measured in the laboratory flexural beam test. Stiffnesses calculated using the expression for the HVS mix developed from the flexural beam test, presented previously, measured air-voids contents from the two sections, and asphalt concrete and subbase thicknesses for the two sections are shown in Table 4.11.

Table 4.11 Summary of structural differences between Sections 501RF and 503RF

	Section 501RF	**Section 503RF**
Asphalt concrete top lift thickness (mm)	63	74
Asphalt concrete bottom lift thickness (mm)	84	88
Asphalt concrete top lift air-voids	7.2	4.8
Asphalt concrete bottom lift air-voids	5.6	4.4
Asphalt concrete top lift stiffness (MPa)	7,700	9,440
Asphalt concrete bottom lift stiffness (MPa)	8,820	9,766
Subbase thickness (mm)	215	305

4.3.1.2 Performance Differences. Sections 501RF and 503RF exhibited similar patterns of fatigue crack development and rutting under the same HVS loading programs. Temperature control on the two sections was nearly identical. The repetitions at which HVS trafficking was terminated, and measured distresses on the two sections are summarized in Table 4.12.

Table 4.12 Comparison of fatigue and unbound layers rutting performance for Sections 501RF and 503RF

	Section 501RF	Section 503RF
HVS repetitions at test completion	1,426,467	1,911,823
ESALs at test completion (millions)	59	81
Cracking first observed (repetitions)	550,000	400,000
Crack density at test completion (m/m^2)	9.6	6.5
Repetitions to 2,000 cm of crack length	935,000	971,000
Repetitions to 3,500 cm of crack length	1,000,000	1,618,000
Rut depth in unbound layers at test completion (mm)	5.1	5.7
Percent of total rutting in unbound layers at test completion	48	52
Percent of total rutting in subgrade at test completion	11	2

Section 501RF had a greater rate of crack development, and continued to a greater amount of cracking than did Section 503RF, although cracking was observed earlier on Section 503RF. Cores from both sections showed that cracking only occurred in the top asphalt concrete lift. The unbound layers rutting performance of both sections is very similar, except that Section 501RF exhibited a somewhat greater proportion of rutting in the subgrade whereas Section 503RF had a greater proportion in the base and subbase layers.

4.3.2 Effects of Asphalt Concrete Thickness, Asphalt Concrete Compaction, and Asphalt Subbase Thickness on Predicted Performance

Simulated HVS ESALs were calculated for Cases 4 and 5 (HVS conditions, HVS mix, as-built air-voids contents; full friction and no friction between asphalt concrete lifts, respectively) for Section 501RF, for the following sub-cases:

A. Section 501RF as-built,

B. Section 501RF with asphalt concrete air-voids contents of Section 503RF,

C. Section 501RF with asphalt concrete thicknesses of Section 503RF,

D. Section 501RF with aggregate subbase thickness of Section 503RF, and

E. Section 501RF with asphalt concrete air-voids contents and thicknesses of Section 503RF.

Simulated HVS ESALs to fatigue failure for the as-built 503RF structure is larger than for the as-built 501RF structure, as can be seen in Table 4.13. The relative better predicted fatigue performance of Section 503RF corresponds with the smaller amount of cracking on Section 503RF. Permissible ESALs by the Asphalt Institute subgrade strain criteria are also larger for Section 503RF than for Section 501RF, as can be seen in Table 4.14.

Table 4.13 Effects of air-voids content, asphalt concrete thickness, and asphalt subbase thickness on predicted fatigue life

	Case 4 (full friction)	Case 5 (no friction)
501RF as-built	66,013,000	6,416,000
503RF as-built	216,329,000	17,134,000
501RF with 503RF air-voids content	109,687,000	15,219,000
501RF with 503RF asphalt concrete thicknesses	118,956,000	6,491,000
501RF with 503RF air-voids content and asphalt concrete thicknesses	203,248,000	15,967,000
501RF with 503RF subbase thickness	70,106,000	6,671,000

Table 4.14 Effects of air-voids content, asphalt concrete thickness, and asphalt subbase thickness on allowable ESALs considering subgrade strain

	Case 4 (full friction)	Case 5 (no friction)
501RF as-built	45,764,000	8,351,000
503RF as-built	165,990,000	28,698,000
501RF with 503RF air-voids content	56,478,000	9,340,000
501RF with 503RF asphalt concrete thicknesses	70,247,000	10,582,000
501RF with 503RF air-voids content and asphalt concrete thicknesses	88,591,000	12,074,000
501RF with 503RF subbase thickness	90,756,000	19,313,000

For Case 5 (no friction, cracking occurring in top lift only), it can be seen that the smaller air-void contents and thicker asphalt concrete thickness of Section 503RF each independently accounted for about a third of the difference in predicted fatigue life between Section 501RF and 503RF. The difference in air-voids contents, 4.4 and 4.8 percent versus 5.6 and 7.2 percent, increased predicted fatigue life by 137 percent, and the difference in asphalt concrete thickness, 15 mm, increased predicted fatigue life by only one percent. If the two

lifts had been bonded (Case 4, cracking starting in bottom lift), the difference would have been 80 percent. When combined, the reduced air-voids contents and 50 mm of extra asphalt concrete thickness increased predicted fatigue life by 149 percent. For Case 4, the difference would have been 207 percent. In contrast, the increased subbase thickness of Section 503RF resulted in an increase of predicted fatigue life of 4 percent for no bonding and 228 percent for full bonding. While the difference in observed performance is not as great, with a difference of 62 percent in the number of HVS ESALs to a crack length of 3,500 cm, these calculations and HVS results indicate the importance of increased asphalt concrete compaction and asphalt concrete thickness to improved fatigue life, as opposed to increased thicknesses of unbound granular materials.

For Case 4 (full friction), the lower air-voids contents and increased asphalt concrete thickness of Section 503RF did not independently affect the difference in performance based on subgrade strain between Sections 501RF and 503RF, as they did for fatigue life. The difference in air-void contents increased the ESALs based on subgrade strain by 23 percent, while the difference in asphalt concrete thickness increased the ESALs by 54 percent. When combined, the reduced air-voids contents and 15 mm of extra asphalt concrete thickness increased computed ESALs based on subgrade strain criteria by 94 percent. The increased subbase thickness of Section 503RF resulted in a 98 percent increase in ESALs relative to Section 501RF. Together, all three variables resulted in a 263 percent increase in pavement life based on subgrade strain.

Comparison of the results of the HVS tests do not indicate much difference in the rutting of the combined unbound layers, although there was less rutting of the subgrade in Section 503RF. Results of HVS tests and calculations of allowable subgrade strain indicate that increased thickness of unbound granular material does decrease the likelihood reduced

rutting of the test sections. Increased asphalt thicknesses and better compaction also appear to have contributed somewhat to the reduced permanent deformations in the unbound layers. It should be remembered that the Asphalt Institute subgrade strain criteria are related to permissible ESALs to a 12.7 mm rut at the surface, while the rut depths on Sections 501RF and 503RF were only 8.4 and 7.9 mm, respectively. Thus, the subgrade strain criteria were never checked against limiting rut depths associated with the criteria in the test sections as were the criteria for fatigue cracking of the upper asphalt concrete lift.

4.4 FINDINGS

In general, the analyses reported herein found a rather good correspondence between the Caltrans design estimate of approximately 1,000,000 ESALs and the HVS test measurement of approximately 81,000,000 ESALs. As for Sections 500RF and 501RF, the major impediment to reconciling these two estimates seems to be the inability to accurately quantify effects of the layer interface condition. The following findings of this aspect of the study are considered to have been reasonably well demonstrated and to represent appropriate hypotheses for future inquiry and validation:

1. Fatigue life measurements under full-scale accelerated loading are typically expected to exceed design estimates because design estimates must incorporate a safety factor to minimize the risk of premature failure while accommodating, at the same time, expected variability in testing, in construction, in traffic, and in mix design. For a design reliability level of 90 percent, the computed ratio of simulated HVS ESALs to design ESALs estimated using the fatigue analysis and design system was approximately 3.7.

2. The mix fatigue analysis and design system proved to be an effective tool for explaining fatigue performance of the HVS pavement. The relatively good agreement between

the simulation estimate and actual HVS measurement suggests that the analysis and design system may prove useful for structural design as well as for mix design.

3. According to the Asphalt Institute's subgrade strain criteria, severe rutting associated with permanent deformations in the unbound layers in the HVS pavement would not be expected. Testing of HVS Section 503RF generally confirmed this.

4. The analyses reported herein corroborate prior work showing the importance of good compaction of the asphalt concrete surface for superior fatigue performance. Good compaction of the mix also reduces the amount of rutting contributed by the unbound pavement layers.

5. The improved fatigue performance of Section 503RF as compared to that of Section 501RF was primarily due to the increased thickness and higher degree of compaction of the asphalt concrete in Section 503RF.

6. Loss of bond at the interface between asphalt-concrete lifts can cause a significant reduction in fatigue life and an increase in rutting resulting from increased stresses in the unbound layers.

7. Different mixes, even with similar binders, can result in significantly different fatigue performance. The importance and effectiveness of laboratory fatigue testing and simulation to quantitatively estimate differences in fatigue performance in situ were demonstrated by the analyses presented in this chapter.

CHAPTER 5

SUMMARY AND CONCLUSIONS

5.1 SUMMARY

This report, the third in a series detailing the results of the CAL/APT program being performed jointly by UCB and Caltrans, describes the results of the fourth HVS test conducted by the UCB staff on the second of four pavement test sections—503RF, an asphalt concrete section containing only the aggregate base. Also included are: initial analyses of the test section; analyses of the performance of the test section; preliminary comparison of its performance relative to the performance of comparable pavements in the coastal climatic region of California; evaluation of the effect of air-voids content on its performance, and implications of these results relative to current Caltrans pavement construction requirements since the test pavements were constructed according to Caltrans's specifications.

HVS trafficking of Section 503RF commenced in March 1996 and was completed in September 1996. A total of 1.91×10^6 load repetitions were applied during this period consisting of 150,000 repetitions of a 40 kN (9,000 lb) half axle load, 50,000 repetitions of an 80 kN (18,000 lb) load, and the remainder with a 100 kN (22,500 lb) load.

The first load-associated (fatigue) cracks were observed at approximately 400,000 load repetitions. At 1.91×10^6 load repetitions cracking had reached a level which, according to Caltrans pavement management criteria, resembled a newer pavement that had failed by alligator cracking. The average maximum vertical rut depth at the centerline of the test section at this time was 10.8 mm, a significant rut but less than the Caltrans failure criteria of 12.5 mm. It was noted that the cracks were hairline (less than 1/32 inch) and pumping was not observed in contrast to typical field sections.

Thicknesses for the pavement sections were selected on the basis of a Traffic Index of 9 (800,000 to 1,200,000 ESALs) and a design "R" value for the subgrade of 10 (measured range—4 to 30) *(2)*. The number of ESALs actually carried according to the Caltrans conversion [(actual axle load/18000)$^{4.2}$] is 81 million, which corresponds to a Traffic Index of 15.2.

When the construction of the test pavements had been completed (April 1995), cores and slabs of the asphalt concrete were taken from the pavement for testing. As with Sections 500RF and 501RF, weakness in the bond (and even a lack thereof) between the two asphalt concrete lifts was observed. At the conclusion of the loading on the test section, a number of cores were taken to check changes in densities of the lifts. When these cores were removed it was noted the two lifts were unbonded and that there was evidence of movement between the lifts resulting from the deflection of the pavement under load. Also, it was observed that the cracking observed at the surface existed only in the top lift; the lower lift was uncracked.

Measurements of densities on cores from the trafficked portion of the pavement indicated that traffic compaction probably did not occur in the upper lift of the asphalt concrete. In the lower lift, the air-voids content was reduced by about 1.0 percent (from about 4.4 percent to 3.4 percent). This indicates that nearly all rutting in the asphalt concrete layer was due to shear deformation, not densification.

5.2 CONCLUSIONS

From the results of tests on Section 503RF and associated analyses, the following conclusions appear warranted.

1. The fatigue analysis and design system developed during the SHRP program and refined within the CAL/APT program has been used to explain the difference between the

design estimate for Section 503RF of approximately 1×10^6 ESALs and the HVS measurement of approximately 81×10^6 ESALs. Although some of the discrepancy remains unaccounted for (possibly as a result of difficulties in modeling the bonding between the two lifts of asphalt concrete), the overall agreement helps to validate the analysis and design system as a mechanism for structural design and provides some indication of the limits of validity of the current Caltrans design methodology.

2. As with Sections 500RF and 501RF, results of this HVS test suggest that the Asphalt Institute's subgrade strain criteria to control rutting resulting from permanent deformations in the unbound layers is a reasonable design parameter. Accordingly, these criteria are suitable for use in mechanistic/empirical analyses of rutting to supplement routine Caltrans design procedures in special investigations.

3. Results of the 503RF test suggest that the Caltrans structural design procedure may not be sufficiently conservative for pavements with aggregate base, typical compaction, and certain asphalt concrete mixes. The analysis and design system used herein and being refined, in part, through the CAL/APT program, should provide an improved methodology for structural pavement design permitting a higher level of reliability to be obtained for pavements of this type. The results indicate that thicker asphalt concrete layers and better asphalt concrete compaction can significantly improve pavement performance.

4. The recommendations regarding mix compaction and tack coat application resulting from the Sections 500RF and 501RF tests are supported by the results obtained for Section 503RF.

REFERENCES

1. California Department of Transportation, *CAL/APT Strategic Plan (July 1995-July 1997)*, adopted by the CAL/APT Steering Committee, May 18, 1995.

2. Harvey, J., L. Du Plessis, F. Long, S. Shatnawi, C. Scheffy, B-W. Tsai, I. Guada, D. Hung, N. Coetzee, M. Riemer, and C. Monismith, *Initial CAL/APT Program: Site Information, Test Pavements Construction, Pavement Materials Characteristics, Initial CAL/HVS Test Results, and Performance Estimates*, Interim Report No. RTA–65W4845–1 for the California Department of Transportation, Institute of Transportation Studies, University of California, Berkeley, April 1996.

3. Harvey, J., L. du Plessis, F. Long, J. Deacon, I. Guada, D. Hung, and C. Scheffy, *CAL/APT Program: Test Results from Accelerated Pavement Test on Pavement Structure Containing Asphalt Treated Permeable Base (ATPB)—Section 500RF*, Report No. RTA–65W4845–3 for the California Department of Transportation, Institute of Transportation Studies, University of California, Berkeley, June 1997.

4. Harvey, J.T., L. duPlessis, F. Long, I. Guada, D. Hung, and C. Scheffy, *CAL/APT Program: Test Results from Accelerated Pavement Test on Pavement Structure Containing Untreated Base—Section 501RF*, Report No. RTA-65W4845-3 for the California Department of Transportation, Institute of Transportation Studies, University of California, Berkeley, September 1997.

5. Harvey, J., B. Tsai, F. Long, D. Hung, and C. Monismith, *CAL/APT PROGRAM—Asphalt Treated Permeable Base (ATPB), Laboratory Testing, Performance, Predictions, and Evaluation of the Experience of Caltrans and Other Agencies,* Draft Report for the California Department of Transportation, Institute of Transportation Studies, University of California, Berkeley, June 1997.

6. California Department of Transportation, *Highway Design Manual*, Section 600, Sacramento, 1991.

7. Sousa, J.B., J. Deacon, S. Weissman, J. Harvey, C. Monismith, R. Leahy, G. Paulsen, and J. Coplantz, *Permanent Deformation Response of Asphalt-Aggregate Mixes*, Strategic Highway Research Program Report No. A–414, National Research Council, Washington, D.C., 1994.

8. Deacon, J., J. Coplantz, A. Tayebali, and C. Monismith, "Temperature Considerations in the Asphalt-Aggregate Mixture Analysis and Design," *Transportation Research Record 1454*, Transportation Research Board, 1994, pp. 97-112.

9. Harvey, J., J. Deacon, B. Tsai, and C. Monismith, *Fatigue Performance of Asphalt Concrete Mixes and Its Relationship to Asphalt Concrete Pavement Performance in California,* Report No. RTA-65W485-2 for the California Department of

Transportation, Institute of Transportation Studies, University of California, Berkeley, January 1996.

10. Shook, J.F., F.N. Finn, M.W. Witczak, and C.L. Monismith, "Thickness Design of Asphalt Pavements—The Asphalt Institute Method," *Proceedings*, Fifth International Conference on the Structural Design of Asphalt Pavements, University of Michigan, August 1982, pp. 17–44.

11. Epps, J.A., et al, "WesTrack Full-Scale Test Track: Interim Findings," *Proceedings, Volume 3*, Eighth International Conference on Asphalt Pavements, Seattle, WA, August 1997.

12. Wardle, L.J., *Program CIRCLY, User's Manual, Revision 1*, Geomechanics Computer Program No. 2, Division of Applied Geomechanics, Commonwealth Scientific and Industrial Research Organization, Melbourne, Australia, 1976.

13. Harvey, J.T., J.A. Deacon, A.A. Tayebali, R.B. Leahy, and C.L. Monismith, "A Reliability-Based Mix Design and Analysis System for Mitigating Fatigue Distress," *Proceedings, Volume 1*, 8th International Conference on Asphalt Pavements, Seattle, Washington, August 1997, pp. 301-323.

14. Reese, R., Faxed results of comparison of Valley binders aging properties with CAL/APT Goal 1 asphalt-concrete properties. Caltrans Engineering Service Center, Sacramento, October 6, 1995.

15. Santucci, L.E., "Thickness Design Procedure for Asphalt and Emulsified Asphalt Mixes," *Proceedings*, Fourth International Conference on the Structural Design of Asphalt Pavements, University of Michigan, August 1977, pp. 424-456.